Configurable and Up-Scalable Microfluidic Life Science Platform for Cell Based Assays by Gravity Driven Sequential Perfusion and Diffusion

by

Ivan Krastev Dimov

B.Eng. (UTFSM) 2002
M.Sc. (UTFSM) 2004

A dissertation presented to the

School of Physical Sciences
Dublin City University

for the degree of

Doctor of Philosophy

Research Supervisors:

Professor Luke P. Lee
Professor Jens Ducrée

July 2009

Declaration

I hereby certify that this material, which I now submit for assessment on the programme of study leading to the award of Doctor of Philosophy is entirely my own work, that I have exercised reasonable care to ensure that the work is original, and does not to the best of my knowledge breach any law of copyright, and has not been taken from the work of others save and to the extent that such work has been cited and acknowledged within the text of my work.

Signed: _____ ID No.: 56124881

Date: _____

Acknowledgements

As I look back I realize that all this would not have been possible without the help, support and guidance of so many people. I feel very privileged and deeply grateful to everybody who has helped me along my journey, whether it may have been a laugh we spent together during a quick break or simply a discussion about work or life.

The work presented in this thesis has been carried out at the Microfluidic Platform Group, RP5 at the Biomedical Diagnostics Institute in Dublin City University, Ireland.

I would like to express my deep and sincere thanks to all the people that have made this possible, in particular:

I would like to express my gratitude to my supervisors Luke Lee and Jens Ducrée for always having an open door, giving me support, guidance and freedom to develop my own ideas, and not least for giving me the opportunity to work in this field.

The RP5 group, Asif, Jose, Gregor, Lourdes, Claus and Brian who helped me and supported me throughout my PhD work, our discussions and work together were very fruitful and rewarding.

My parents Elka and Maximo and my sister Manuela for their constant support and understanding, teaching me the important things in life and for the home where I am always welcome.

Finally, I wish to express my deepest thank you to my beloved, for giving me endless love and support.

"Thank You All So Much"

Abstract

Microfluidics has the potential to significantly change the way modern biology is performed, but for this potential to be realized several on-chip integration and operation challenges have to be addressed. Critical issues are addressed in this work by first demonstrating an integrated microfluidic tmRNA purification and real time nucleic acid sequence based amplification (NASBA) device. The device is manufactured using soft lithography and a unique silica bead immobilization method for the nucleic acid micro purification column. The integrated device produced a pathogen-specific response in < 3 min from the chip-purified RNA. Further enhancements in the device design and operation that allow the on-chip integration of mammalian cell handling and culturing produced a novel integrated NASBA array. This system demonstrated for the first time that it is possible to combine on a single micro-device cell culture and real time NASBA. In order to expand the cell based assay capabilities of the integrated NASBA array and simplify the device operation novel hydrodynamics and cell sedimentation within trench structures and gravity driven sequential perfusion and diffusion mechanisms were developed. These mechanisms were characterized and implemented within an iCell array device. iCell array can completely integrate cell based assays with bio-analytical read-out. The device is highly scalable and can enable the configurable on-chip integration of procedures such as adherent and non-adherent cell-culture, cell-stimulation, cell-lysis, cell-fixing, protein-immunoassays, bright field and fluorescent microscopic monitoring, and real time detection of nucleic acid amplification. The device uses on-board gravity driven flow control which makes it simple and economical to operate with dilute samples (down to 5 cells per reaction), low reagent volumes (50 nL per reaction), highly efficient cell capture (100% capture rates) and single cell protein and gene expression sensitivity. The key results from this work demonstrate a novel technology for versatile, fully integrated microfluidic array platforms. By multiplexing this integrated functionality, the device can be used from routine applications in a biology laboratory to high content screenings.

List of Publications and Patent Applications

1. A. Riaz, R.P. Gandhiraman, I.K. Dimov, L. Basabe-Desmonts, A.J. Ricco, J. Ducrée, S. Daniels, and L.P. Lee, "Thin Film Diffusion Barrier Formation in PDMS Microcavities" 15th International Conference on Solid-State Sensors, Actuators and Microsystems, 2009. Transducers 2009:1051-1054

2. I.K. Dimov, A. Riaz, J. Ducrée, and L.P. Lee, "Hybrid Integrated Platform of PDMS Microfluidics and Silica Capillary for Effective CE And ESI-MS Coupling." 15th International Conference on Solid-State Sensors, Actuators and Microsystems, 2009. Transducers 2009:1281-1284

3. Great Britain Patent Nº GB 0910626.1: Co-inventor of a Great Britain patent (pending), for a novel method of surface treating microfluidic devices for generating among others internal glass like surfaces using PE-CVD processes.

4. Great Britain Patent Nº GB 0818579.5: Co-inventor of a Great Britain patent (pending), for a novel microfluidic multiplexed cellular and molecular analysis device and method.

5. Garcia-Cordero, J.L., Dimov, I.K., O'Grady, J., Ducrée, J., Barry, T., Ricco, A.J., "Monolithic Centrifugal Microfluidic Platform for Bacteria Capture and Concentration, Lysis, Nucleic-Acid Amplification, and Real time Detection" Micro Electro Mechanical Systems, 2009. MEMS 2009:356 – 359

6. Ivan K. Dimov, Jose L. Garcia-Cordero, Justin O'Grady, Claus R. Poulsen, Caroline Viguier, Lorcan Kent, Paul Daly, Bryan Lincoln, Majella Maher, Richard O'Kennedy, Terry J. Smith, Antonio J. Ricco and Luke P. Lee, "Integrated microfluidic tmRNA purification and real-time NASBA device for molecular diagnostics" Lab Chip, 8, 2071–2078 (2008).

7. I. K. Dimov and L.P. Lee, "Integrated Nasba Array For Drug Screening And Expression Profiling", 12th International Conference on Miniaturized Systems for Chemistry and Life Sciences, μTAS 2008:640-642

8. A. Riaz, I.K. Dimov, L. Kent, C.R. Poulsen, S. O'Toole, M. Radomski, J. O'Leary, A.J. Ricco, and L.P. Lee, "Integrated Microfluidic Systems Biology Platform: Cell Culture, Drug Treatment, Lysis, Separation And Detection", 12th International Conference on Miniaturized Systems for Chemistry and Life Sciences, μTAS 2008:1193-1195

9. J.L. Garcia-Cordero, L. Kent, I.K. Dimov, C. Viguier, L.P. Lee, and A.J. Ricco, "Microfluidic CD-Based Somatic Cell Counter For The Early Detection Of Bovine Mastitis", 12th International Conference on Miniaturized Systems for Chemistry and Life Sciences, μTAS 2008:1762-1764

10. C.R. Poulsen, B. Lincoln, I. Dimov, J.L. Garcia-Cordero, S. O'Toole, M. Radomski, J. O'Leary, and L.P. Lee, "Apoptotic Response Of Ovarian Cancer Cells In Hypoxic Conditions", 12th International Conference on

Miniaturized Systems for Chemistry and Life Sciences, μTAS 2008:1864-1866

11. I. K. Dimov, A. Riaz, J. Ducrée, and L.P. Lee, “Hybridly Integrated Modular Platform Combining PDMS Microfluidics and Silica Capillary for CE”, Submitted to Electrophoresis 2009.

12. Ivan K. Dimov, Lourdes Basabe-Desmonts, Jose L. Garcia-Cordero, Jens Ducrée, Antonio J. Ricco and Luke P. Lee, “Self-powered Integrated Microfluidic Blood Analysis System (SIMBAS)”, 13th International Conference on Miniaturized Systems for Chemistry and Life Sciences, μTAS 2009, In press.

13. Gregor Kijanka, Ivan K. Dimov, Luke P. Lee and Jens Ducrée, “A Fully Integrated Cell-Based Cytotoxicity, Gene and Protein Expression Analysis Platform”, 13th International Conference on Miniaturized Systems for Chemistry and Life Sciences, μTAS 2009, In press.

14. Robert Burger, Ivan K. Dimov and Jens Ducrée, “Highly Efficient Single Cell Capturing Under Stagnant Flow Conditions on a Centrifugal Microfluidic Platform”, 13th International Conference on Miniaturized Systems for Chemistry and Life Sciences, μTAS 2009, In press.

15. G. Kijanka, I.K. Dimov, R. Burger and J. Ducrée, “Minimizing stress exposure to cells using novel microfluidic cell capture devices”, World Congress 2009 on Medical Physics and Biomedical Engineering, In press.

Further Publications to be submitted:

1. Ivan K. Dimov, Gregor Kijanka, Luke P. Lee, and Jens Ducrée, “Simple and Versatile Platform for Parallelized Capture, Treatment and Analysis of Cells Based on Gravity Induced Forces”, To be submitted to PNAS.

2. Ivan K. Dimov, Jens Ducrée and Luke P. Lee, “iNASBA - Integrated NASBA Array for Quantitative Nucleic Acid Testing”, To be submitted to Integrative Biology.

Contents

List of Abbreviations

µ-TAS	micro total analysis systems
AMV-RT	avian myeloblastosis virus reverse transcriptase
APC	antigen presenting cells
aRNA	antisense RNA
CA	calcine AM
CCD	charge coupled devices
cDNA	complementary DNA
CE	capillary electrophoresis
CFD	computational fluid dynamics
CFU	colony forming units
COC	cyclic olefin copolymer
dH_2O	deionised H_2O
DMEM	dulbecco modified eagle medium
DNA	deoxyribonucleic acid
dsDNA	double-stranded DNA
ESR1	estrogen receptor alpha
FBS	fetal bovine serum
FRET	fluorescence resonance energy transfer
GFP	green fluorescent protein
HPV	human papilloma virus
I/O	input output
iCell	integrated cell based assay
IF	immuno-fluorescent
iNASBA	integrated NASBA
IVT	invitro transcription
LOD	level of detection
LPS	lipopolysaccharides
MM	multiple myeloma
MMLV-RT	moloney murine leukemia virus reverse transcriptase
mRNA	messenger RNA
NA	nucleic acid
NAA	nucleic acid amplification
NASBA	nucleic acid sequence based amplification
PBS	phosphate buffer solution
PCR	polymerase chain reaction
PDMS	polydimethylsiloxane
PEG	polyethylene glycol
RCA	rolling-circle amplification
RCP	rolling-circle product
RNA	ribonucleic acid
RPC	RNA purification chamber
rRNA	ribosomal RNA
RPM	revolutions per minute
RT-PCR	reverse transcriptase PCR
SDA	strand displacement amplification
SIMPLE	semi-implicit pressure linked equation
SMD	single molecule detection
SNP	single nucleotide polymorphisms
ssDNA	single stranded DNA
TMA	transcription mediated amplification
tRNA	transfer RNA
tmRNA	transfer messenger RNA
TTP	time-to-positive
UV	ultraviolet
WO	waste output

Chapter 1: Introduction

1.1 Motivation

Living organisms are unimaginably complex creations; yet, no matter how complex, large or small, all living beings are assemblies of sub-units. The smallest living unit is the cell. Cell size can vary considerably, but most cells in mammals are in the range of tens of microns. To gain a better understanding of how cells function we have to be able to probe cells within their micron-scaled environment. Until recently, being able to access the micron-sized world of cells was complex and very limited. Since the development of the integrated circuit many micro-fabrication technologies have appeared. These technologies have provided the basic tools for constructing miniaturized systems that can operate at or below the cellular level. So far, biotechnology applications have benefited from using miniaturized systems [1] [2, 3]. The often-sited advantages of these miniaturized systems are that they allow scientists to study cells in a disaggregated form or at the single-cell level with a considerable reduction in reagent and sample volumes, increased sensitivities and higher process integration and automation. This, in turn, allows for parallelization and a drastic decrease in the experiment time making it feasible for scientists to explore the vast complexity of biological systems.

However, in general, the life science community and biologists have only moderately made use of these emerging miniaturized tools. This is partly because existing miniaturized tools are simply not yet versatile and flexible enough to carry out complex biological protocols. The present thesis is a contribution to the field of advanced fully-integrated micro-fluidic systems.

The rest of this chapter is structured as follows: Initially, a motivation for in-vitro RNA analysis is presented followed by a brief overview of the principles of nucleic acid-based diagnostics including NAA and NA extraction and purification. Microfluidic lab-on-a-chip technology for bioanalysis is presented next, specifically focusing on microfluidic cell

capturing and culture and lab-on-a-chip devices for nucleic acid analysis such as PCR and NASBA devices. A further discussion of the microfluidic nucleic acid amplification characteristics is provided. The discussion is focused on key aspects such as integration, low volume and high speed processing. The chapter is finalized with a description of what is missing, the aims of the research and the outline of the thesis.

1.2 Motivation for in-vitro RNA analysis

As a fundamental pillar in biology, genetic information stored in DNA is translated into protein through messenger RNA. In the past ten to twenty years, further evidence has accumulated suggesting that RNA molecules perform a wider range of functions within the living cell machinery; these functions include among others essential catalytic roles, providing structural support for molecular machines and gene silencing.

Generally the functions of RNA molecules in a cell are controlled through temporally and spatially dynamic processes of expression levels and stability. Thus determining the dynamics and location of RNA molecules in living cells is of substantial importance to molecular biology and medicine.

Several tools and technologies have been created for studying intracellular RNA biology. These technologies are mainly based on tagged full length RNAs or probes that target specific RNAs. The tags used in these techniques are generally fluorescent, radioactive, or in some cases magnetic. Tagged full-length RNAs have been used successfully to monitor the localization of a specific mRNA or nuclear RNA [4], [5], [6] in living cells (Figure 1.1). This approach is however limited because it cannot be used to measure RNAs produced within the living cell.

Probes that target specific RNAs enable the measurement of endogenous RNA. One such type of probe is the linear labelled oligonucleotides probe. Through in situ hybridization these probes directly label intracellular mRNA [7], but for the probes to be specific and function correctly several steps have to be performed. Initially cells have to

be fixed and permeabilized to increase the access to the target RNA and after hybridization unbound probes have to be washed away [8]. Signals can be further enhanced by designing multiple probes to target the same RNA [7]. Even though this type of labelling provides us with the localization information, it is quite limited. Fixing agents and other supporting chemicals can have considerable effect on the signal [9] and they can also degrade the integrity of certain intra cellular structures such as mitochondria. Fixing cells with cross-linking or denaturing agents and permeabilizing them with proteases may distort the localization of intracellular mRNA. Further more in situ hybridization requires that cells be fixed and thus killed so most of the dynamics on gene expression in the cell are lost.

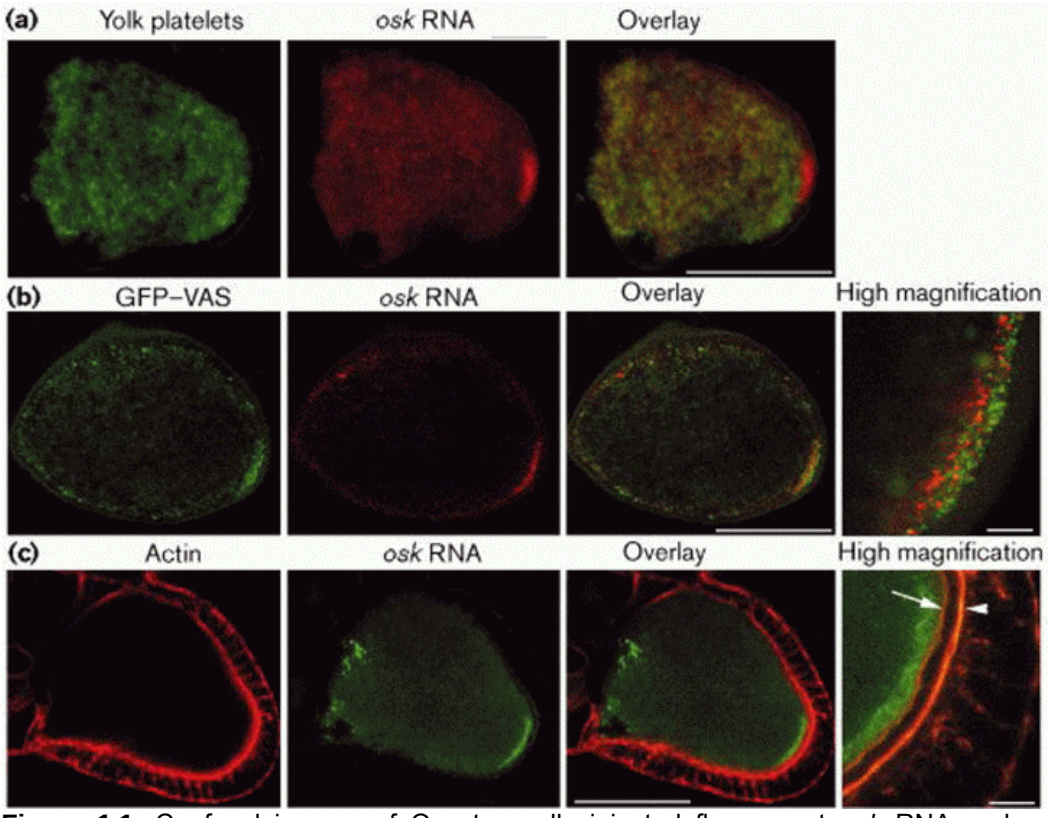

Figure 1.1. Confocal images of Oocytes cells injected fluorescent *osk* RNA probes which accumulate in the pole plasm. The injected probes were rhodamine-labelled (a, b) or fluorescein-labelled (c) *osk* RNA (3′ UTR) at the anterior. Scale bars: 100*μ*m; 10 *μ*m in images at high magnification. Reproduced from REF [4].

Tagged RNA-binding proteins are an alternative to oligonucleotide probes. Proteins such as GFP tags have been used to detect mRNA in live cells [10]. A major limitation though,

is that a protein has to be identified that specifically binds to the mRNA of interest. To resolve this challenge, a method that implants a transgene into an organism has been developed. The transgene generates a binding site for the phage MS2 protein [11]. Tagging this protein with GFP in Drosophila eggs enabled nanos mRNA to be specifically labelled in a living egg system. Single molecule sensitivity has also been demonstrated with the GFP-MS2 approach while being used to dynamically track and localize RNA in living cells [12]. However, generating transgenes that can fulfil the same functionality and behaviour as endogenous mRNA is still significantly challenging so the applications of this technique are limited.

In order to be able to truly detect and track in-vivo endogenous mRNA, probes must satisfy a number of criteria:

1. Probes should be able to convert target recognition directly into a measurable signal (transduction) to differentiate between background, true and false-positive signals.
2. Probes should be highly sensitive for quantifying low gene expression levels.
3. Probes should have fast kinetics for tracking changes in gene expression in real time.

Linear labelled oligonucleotides are the simplest type of probes used in living cells for RNA tracking and localization studies [13] [14] [15], but these probes cause significant problems in distinguishing the true signal from the background. This is because they lack any signal transduction mechanism. To address this issue FRET based mechanisms have been used with linear labelled oligonucleotide probes. Signal transduction is done by using two linear probes labelled with a pair of donor and acceptor fluorophores, when the probes hybridize with their target the donor and acceptor fluorophores are in close proximity (within 10 nm) and a change in the emission spectrum occurs [15]. A limitation of this technique is that there is still a considerable amount of background signal and also linear probes are not sensitive to single base

differences (single nucleotide polymorphisms - SNPs) in the target which limits their application in disease studies (such as cancer detection).

Hairpin nucleic acid probes try to resolve most of the deficiencies of the linear labelled oligonucleotide probes. One type of hairpin nucleic acid probes are the molecular beacons. They consists of an oligonucleotide sequence that is designed in its native state (in the absence of a complementary target) to form a stem-loop structure. At one end the molecular beacon oligonucleotide is labelled with a fluorophore and on the other end it is labelled with a quencher [16]. Upon hybridization with a target nucleic acid the molecular beacon opens and the fluorophore and quencher are physically separated, this allows the fluorophore to emit a fluorescence signal when excited. In ideal conditions, upon binding with a target the molecular beacon fluorescence intensity can increase over 200-fold with respect to its native state [16]. This makes the molecular

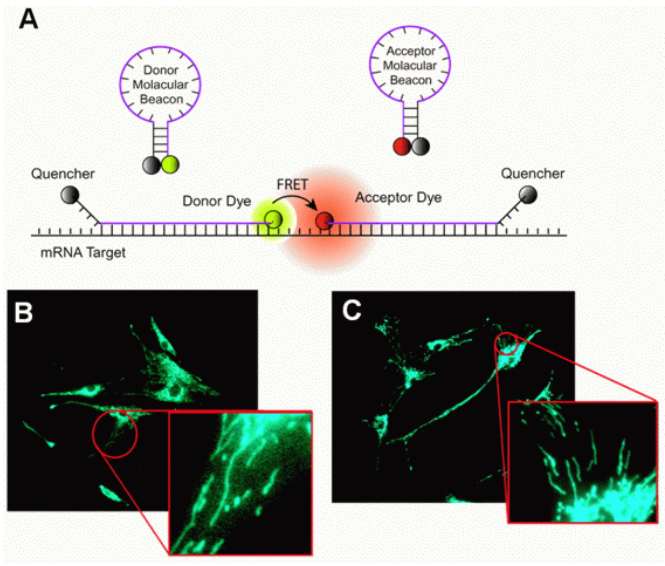

Figure 1.2 (A) Diagram showing the concept of dual FRET molecular beacons. Hybridization of donor and acceptor molecular beacons to adjacent regions on the same mRNA target results in FRET between donor and acceptor fluorophores upon donor excitation. By detecting the FRET signal, fluorescence signals due to probe/target binding can be readily distinguished from that due to molecular beacon degradation and non-specific interactions. **(B-C)** mRNA localization in HDF cells. Fluorescence images of K-ras mRNA in stimulated HDF cells. Note the filamentous K-ras mRNA localization pattern. Adapted from REF [17].

beacon a sensitive probe with a high signal-to-background ratio. Furthermore the stem-loop structure provides a means to adjust the energy state of the molecule such that the stem-loop opens and hybridizes with the target when there is a perfect match. This enables molecular beacons to be highly specific. These transduction and high specificity abilities of the molecular beacon probes have made them widely used in biology and medicine, in applications including multiple analyte detection, real time enzymatic cleavage assaying, cancer cell detection, protein–DNA interactions, real time monitoring of PCR, gene typing and mutation detection, and mRNA detection in living cells. For further signal-to-background enhancement (Figure 1.2) dual molecular beacon probes have been used with FRET detection techniques [17].

1.3 Principles of nucleic acid-based diagnostics

In 1953, Watson and Crick [18] were able describe the structure and role of DNA molecules. A DNA molecule is composed of four repeating nucleotides (also known as nucleotide bases or simply bases): adenine, guanine, cytosine, and thymine. These bases form two polymeric structures or strands that coil to form a double helix (doublestranded DNA [dsDNA]). The attachment of the two strands is based on hydrogen bonds between the bases. These reversible bonds can be disrupted by heat or pH to form single strands of DNA (ssDNA). These single strands are relatively stable until the heat source or high pH is removed after which the DNA molecule reanneals (re-forms) into the doublestranded configuration. Hybridization occurs when ssDNAs from different sources anneal or bind to each other. The binding process between two strands of DNA is quite specific; hydrogen bonds form only between complementary bases; adenine pairs with thymine, and cytosine pairs with guanine. This is one of the key aspects that allows DNA to carry information. RNA differs from DNA in that the nucleotide base thymine is replaced by uracil and specifically pairs with adenine. The hybridization strength and stability between two nucleic acid strands (DNA or RNA) depends on their base sequences. In a perfect base complementary match a very stable dsDNA is produced, however if there are one or more base mismatches there is an increased instability and a weaker hybridization strength between the two strands.

A DNA or RNA probe is a single-stranded nucleic acid that can hybridize in a specific way to the target nucleic acid that is of concern. Due to their stability in general DNA probes, are more common than RNA probes [19]. Probes are generally composed of a short sequence of nucleotide bases (approximately 10 - 40 bases) [20] but probes as long as 10,000 bases or more (molecular weight of 3,300,000) [21] [22] [23] can also be found. A successful probe has to be able to specifically bind to a precise site of an organism's genome, since for example in a simple organism such as Escherichia coli, the DNA chromosome is composed of about 4.2×10^6 bp, a minimum of 20 nucleotide bases is usually required for statistical uniqueness [24]. Generally all the bases in a probe form part of the combination site, and are thus the critical factors in determining an assay's specificity and sensitivity. Generally shorter probes tend to hybridize quicker (in the range of minutes) and are easier to prepare with synthetic methods, but are prone to more non-specific hybridizations and are thus limited in specificity. Furthermore in some cases they are more difficult to label without affecting the hybridization efficiency [20] [25]. On the other hand longer probes have longer reaction times, in the order of hours, to achieve a stable hybridization; generally they also have a lower stringency in the reaction conditions, meaning that they can hybridize in a greater range of temperatures and at lower salt concentrations. When designing a probe a few basic principles have to be followed, the probe must hybridize specifically to the target nucleic acids which should be unique and the probe must not hybridize to itself or to non-target nucleic acids present in the sample matrix (e.g. indigenous microbial DNA)[26].

Cellular DNA contains unique regions so targeting these regions in a nucleic-acid based diagnostics assay, results in high specificity. Nevertheless, RNA targets have the advantage of existing in much higher copy numbers compared to DNA, within a cell, resulting in higher assay sensitivity. There are two main types of RNA targets, mRNA and rRNA. mRNA is not a widely used target because of its function as a messenger molecule within cells, causing its copy numbers to greatly fluctuate depending on the state of the cell. However in certain applications it could be advantageous to target

mRNA as it can allow to distinguish different cell states (e.g. between dormant and actively growing cells, or live and dead cells) [27]. On the other hand rRNA is one of the most useful probe targets, the main reasons being that it contains the 16S and 23S ribosomal genes, these are highly conserved genes [28] [29] used for detecting taxonomic groups and classifying organisms. The other relevant advantage of rRNA is it exists in very high copy numbers in each cell. For example each *E.coli* in growth phase, contains approximately 10,000 ribosomes and in the best case four copies of genomic DNA so detecting ribosomal targets rather than DNA targets increases the sensitivity by at least three orders of magnitude [30]. Finally whether RNA or DNA, the targeted sequence of nucleotides must not be present in non-target cells.

Generally cellular materials of interest or infectious agents are sampled in very limited amounts so enrichment or culturing is required prior to detection. In some cases infectious agents cannot be enriched with culturing, while in general others require long periods of culturing time to be sufficiently enriched for detection. Furthermore extensive culturing has also produced highly resistant bacterial strains. So to avoid culture based sample enrichment other methods of enhancing the detection of nucleic acids samples are required.

1.3.1 Principle of Nucleic Acid Amplification

In 1983, Mullis [31] discovered a conceptually simple, single tube process for amplifying the number of specific nucleic acid fragments present in a sample. Later this process became know as PCR. PCR works by successively repeating three-steps:

1. *Dividing or denaturing dsDNA into single strands*
2. *Hybridizing or annealing specific primers to the single strands of DNA.*
3. *Enzymatically extending the primers to form a single strand of DNA that is complementary to the template strand.*

During the extension phase nucleotides present in the solution in excess are enzymatically attached to the annealed primer to form the complementary DNA strand

(cDNA). During the subsequent cycles, not only is the original DNA segment used as a template but also the newly generated cDNAs. Thus during each cycle the amount of specific DNA is doubled resulting in exponential growth of the number of specific DNA sequences. Therefore generally an amplification of 20 to 40 cycles results in a 10^6-fold increase of the sample DNA sequence [32].

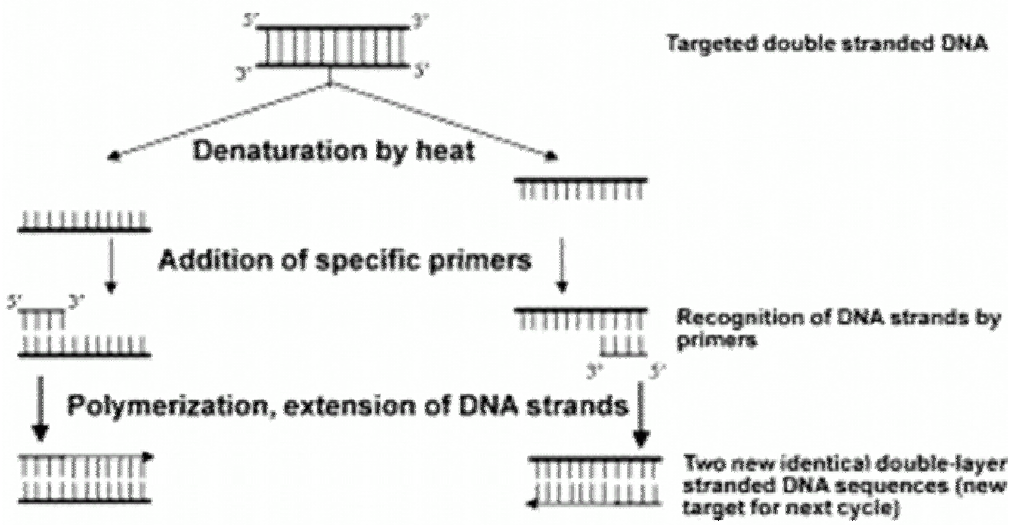

Figure 1.3 Principal mechanism of PCR DNA amplification. Reproduced from REF [33].

The virtually unlimited amplification potential of PCR, increases diagnostic sensitivity to such an extent that false positives due to contamination with extraneous DNA fragments are a significant issue. DNA contamination can be introduced from other sources or carried over from previous amplifications, these problems are usually solved with careful laboratory procedures, such as rigid quality control of enzyme preparations and the use of dedicated pipettes and pre-aliquoted reagents.

There are various types of PCR methods [33]; reverse transcriptase PCR (RT-PCR), that translates an RNA strand into DNA and amplifies it; Real time PCR in which by using special probes, such as molecular beacons, that fluoresce only when the correct hybridization occurs result in a fluorescent signal proportional to the number of target

sequences and thus show the amplification process in real time; and multiplex PCR that allows for a simultaneous amplification of different targets.

Close to the same time that PCR was invented various similar isothermal amplification techniques were also developed, namely Nucleic acid sequence-based amplification (NASBA), transcription-mediated amplification (TMA) and strand displacement amplification (SDA) [34]. The interesting thing about these techniques is that they amplify DNA and RNA sequences without the need for thermal cycling though an initial thermal step is still required. Just like PCR, amplification with isothermal techniques is exponential but in the case of TMA it is faster than PCR because in each amplification cycle 100 to 1000 copies are created as compared with only two for PCR. This means TDA can produce a 10 billion-fold increase of copies within about 15–30 min. The fact that isothermal methods such as NASBA and TMA amplify RNA strands is an advantage when it comes to sample cross contamination because RNA strands are less stable molecules which makes them less prone to contaminate other samples. Another interesting isothermal amplification method is the rolling circle amplification. The main difference and advantage of this method is that during amplification a long single-stranded DNA of multiple repeats (as many as 10^{12} copies/hr) is produced. This makes this type of amplification very resistant to contamination and also permits to quantify the exact number of initial target DNAs present at the beginning of the amplification [35].

1.3.1.1 Principle of NASBA

Nucleic acid sequence based amplification is an isothermal method for amplifying single stranded nucleic acid sequences such as RNA sequences (Figure 1.4.) NASBA is a form of transcription based amplification that relies on the replication capabilities of T7 RNA polymerase. Transcription mediated amplification (TMA) is an almost identical amplification process to NASBA, the main difference between the two is that NASBA uses avian myeloblastosis virus reverse transcriptase (AMV-RT) while TMA uses Moloney murine leukemia virus reverse transcriptase (MMLV-RT). Besides performing reverse transcriptase MMLV-RT, also performs Rnase H type digestion, so the RnaseH

enzyme is omitted from the reaction mixture in the case of TMA [36]. The basis of this technique is the incorporation of a T7-promotor sequence during cDNA synthesis with the help of a reverse transcription reaction. This step is followed by an amplification of the cDNA product with T7 RNA polymerase, generating 10 to 1000 RNA copies of each cDNA product. The reaction follows an exponential accumulation of product because the newly synthesized cDNAs and RNAs serve as templates for a continuous series of reverse transcription and direct T7 RNA polymerase synthesis reactions. Single-stranded RNA amplicons are produced by NASBA which can be used directly in subsequent rounds of amplification or probed for detection without the need for denaturation or strand separation.

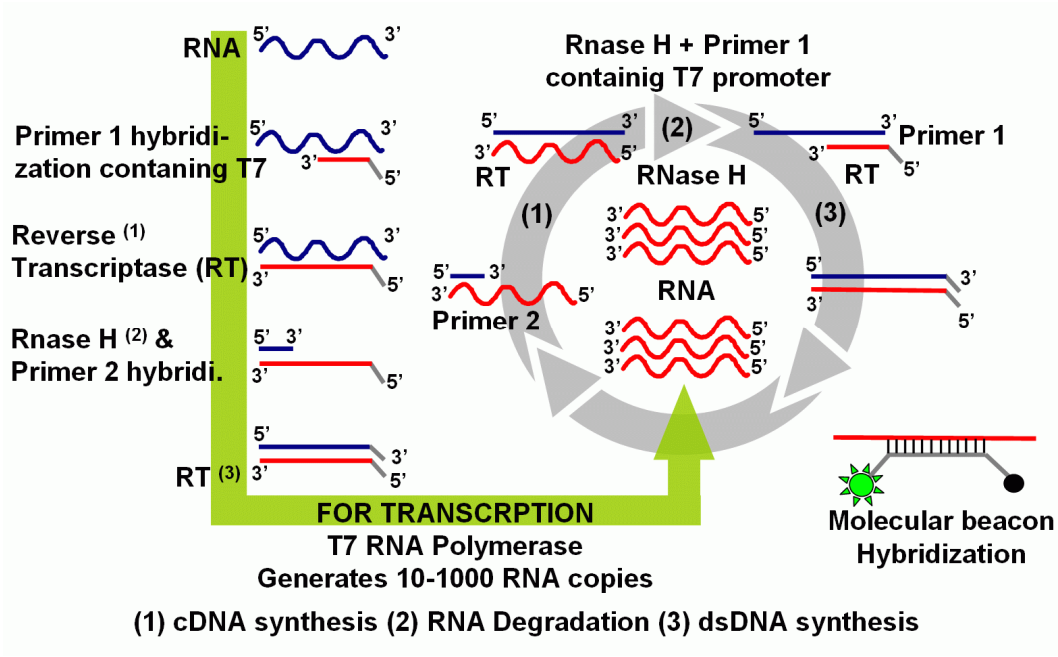

Figure 1.4. Nucleic Acid Sequence Based Amplification (NASBA) is an enzyme based technology used for the exponential amplification of nucleic acids, specially RNA, in a single mixture and at a constant temperature.

Initially developed by Compton in 1991 [37], NASBA is a 41 ºC isothermal process that can produce in 90 min more than 10^9 copies of each RNA target molecule that was initially present in the reaction. The isothermal nature of NASBA eliminates any thermo-cycling requirements during the procedure. Compared to other in-vitro amplification methods such polymerase chain reaction (PCR) [31], strand-displacement amplification

(SDA) [38] or rolling-circle amplification (RCA) [39]. NASBA also has the unique characteristic that it can, in a single assay step, amplify RNA sequences.

Several nucleic acid types, including mRNA, rRNA, tmRNA, and ssDNA, as well as nucleic acids from virus particles, can be analysed with NASBA, enabling a range of diagnostics, along with gene expression and cell viability measurements [40]. In some cases the one step NASBA protocol can achieve levels of detection of extracted RNA a 100 times lower [41] compared to the three step RT-PCR protocol. Further advantages of NASBA over other methods such as reverse transcriptase PCR include faster amplification kinetics and selective amplification of RNA in a background of comparable DNA sequences [42] which reduces the sample purification requirements. The initial NASBA methods relied on liquid or gel-based probe-hybridisation for post-amplification detection of products. More recently, real time procedures incorporating molecular beacons within the amplification reaction have enabled detection in a single step. Real time NASBA has become a sensitive and specific method for detection, quantification and differentiation of RNA and DNA targets.

1.3.2 Principles of nucleic acid extraction

To obtain successful results with in-vitro nucleic acid-based diagnostic assays the target nucleic acid molecules have to be accessible to the probes, primers and rest of the agents involved in the assay. In some cases the target nucleic acid molecules are shielded within cells and other complex sample matrices, moreover sample matrices can include assay inhibitory elements that can disrupt the successful completion of the diagnostic assay. Therefore in certain cases nucleic acid isolation or purification steps are required before the sample can be diagnosed. In certain cases when the target nucleic acid code is located within cells, a cell lysis or disruption procedure must be performed. The objective of this procedure is to release all the intracellular components such as DNA, RNA, proteins, etc. for the downstream analysis. The different techniques available for release of intracellular products include mechanical, physical, chemical, enzymatic and combined methods. The effectiveness of the various methods differs

depending on the sample matrix. In general, mechanical methods are non-specific, but their efficiency (between 80% and 99.9%) is higher and application broader in comparison to any of the other methods. For a review of the different lysis methods see [43].

In some cases after cell disruption, nucleic acids have to be purified from the rest of the lysate. This is usually required if the cell lysate contains amplification or hybridization inhibitors or non-specific binding promoters. Nucleic acid purification techniques are mainly based on two fundamental principles, differential phase solubility and specific solid-phase adsorption. Differential phase solubility based purification techniques generate conditions such that the target nucleic acid would specifically migrate to a separate aqueous or solid phase due to a change in the solubility of their environment. Then the phase containing purified nucleic acids is physically separated from the rest of the solution. While solid-phase adsorption techniques rely on specific adsorption properties that nucleic acid molecules have to certain solid phase materials. These methods usually generate the necessary conditions that promote the specific adsorption of the nucleic acid molecule to the solid phase, after which washing steps maintain the adsorption but remove the rest of the mixture. Finally the purified nucleic acids are eluted from the solid phase by removing the adsorption conditions.

1.3.3 Nucleic acid purification

The principal nucleic acid purification methods are:

Nucleic Acid purification by silica adsorption

Described by Boom et al. [44], this method uses the nucleic acids property of adsorption to silica matrices in the presence of chaotropic salts and alcohol [45]. The term "chaotropic salt" refers to the division (Hofmeister series [46, 47]) of salts into two subsets, chaotropic and kosmotropic salts. Chaotropic agents are salts which disrupt the three dimensional structure in macromolecules such as proteins, DNA, or RNA and denature them while kosmotropic salts have the opposite effect. According to the current

knowledge, guanidine thiocyanate salt is one of the most powerful chaotropes which is why it is commonly used in Boom based methods. Furthermore Guanidine thiocyanate is also characterized with having RNase-inactivating and lysing properties for viral particles and cellular structures [48, 49] and promotes binding of nucleic acids to silica surfaces [50].

The basic steps involved in this type of purification process are:

1. First the sample is mixed with a strong Chaotropic agent and incubated with a solid phase silica element.
2. NA bind to the silica surface and all other molecules remain in buffer solution.
3. The remaining buffer is washed off the silica surface.
4. An elution buffer removes NA from silica surfaces and NAs are collected in a pure solution ready for further processing.

Commercially available kits commonly implement the Boom method in conjunction with spin columns. More recent improvements make the method more amenable to automation such as the use of magnetic beads that bind the nucleic acids to their silica surface and transfer the nucleic acids through the various steps of the extraction process [51] [52]. Recently also other nucleic acid binding properties or conditioning methods have been discovered, and based on them similar purification methods have been developed [53, 54].

Alcohol Precipitation

This is a differential phase solubility technique that changes the solubility properties of the nucleic acid containing sample, making the nucleic acids insoluble and causing them to precipitated into solid phase particles [55, 56] that can be separated with centrifugation. The technique works by adding monovalent cations (K+, Na+, NH4+) to the nucleic acid solution that form salts with the negatively charged nucleic acids. After which alcohol (ethanol or isopropanol) is added and causes the nucleic acids to

precipitate. Precipitations are typically performed at -20°C. However, it was found that ammonium acetate precipitation may be carried out at room temperature [57].

Phenol-Chloroform Extraction

This very popular method was developed by P. Chomczynski & N. Sacchi in 1987 [58] to rapidly deliver high yields of RNA from multiple samples retrieving small and large, low-abundance and high-abundance RNA isoforms. The method is based on the discovery that mostly total RNA free from DNA and proteins coming from cells or tissue samples remained soluble in the acidic aqueous upper phase after centrifugation of a mixture containing the sample and water-saturated phenol, chloroform and a chaotropic denaturing solution such as guanidinium thiocyanate [59]. After which the RNA is recovered from the aqueous phase by alcohol precipitation. DNA can also be recovered in the aqueous phase if the chaotropic denaturing agent is left out of the initial mixture. Thus this technique can also be used for DNA purification.

1.4 Microfluidic lab-on-a-chip technology for bioanalysis

Micro total analysis systems (μ-TAS), also known as lab-on-a-chip devices, promise to integrate entire analytical processes on a single microfluidic platform [60-62]. Much of the research effort focused during the 1990s on developing a range of analytical micro-components, and recent activity has increasingly tackled the problem of integrating multiple components to achieve complex processes. Compared to conventional macro-scale laboratory methods, integrated μ-TAS platforms offer potential advantages of lower cost, higher speed, smaller sample and reagent volumes, and automation of all processes from sample preparation to analytical result: the “sample to answer” concept. For some bioanalytical measurements, however, the most important consequences of successfully implementing μ-TAS will be enhanced assay reproducibility and more quantitative results [63] relative to classical analytical procedures.

1.4.1 Lab-on-a-chip devices for cell capturing and culture

Cell culture and cell based assays are fundamental tools in biology and the life sciences. Microfluidic systems provide new opportunities for the development of cell based assays. Some of the advantages of microfluidic cell based systems are the ability of very precise spatial and temporal control of cell growth and stimuli. This can be realized by combining surfaces that mimic complex biochemistries and geometries of the extracellular matrix with microfluidic channels that regulate transport of fluids and soluble factors. Furthermore microfluidics allows the integration of bio-analytic functionality together with cell handling and assaying which results in multifunctional platforms for basic biological insights into cells and tissues, as well as for cell-based sensors with biochemical, biomedical and environmental functions. These highly integrated microfluidic devices are especially promising for basic biomedical and pharmaceutical research, and can provide robust and portable point-of-care systems that would be of great use in clinical settings, both in the developed and the developing world.

One of the basic requirements of any cell based microfluidic system is the ability to handle and capture cells within particular regions of a micro-system for the further stimulation and analysis. Several mechanical principles have been developed to capture and handle cells for microfluidic cell based analysis. Mechanical methods have the advantage of not requiring any special biochemical processing and can handle any cell type whether adherent or non adherent. Mechanical methods can be classified into hydrodynamic, capillary and gravitational based mechanisms.

Hydrodynamic mechanisms are some of the most popular methods for capturing cells. Di Carlo et al. [64] reported a microfluidic device composed of arrays of physical C-shaped hydrodynamic trapping structures that can trap single cells and dynamically culture them (Figure 1.5). Each trapping structure is designed and dimensioned to capture only a single HeLa cell. While Ryley and Pereira-Smith [65] developed a

trapping system composed of micro-pillar chamber structures (resembling yeast jails) that allowed to physically capture single yeast cells and over time monitor their gene expression. By also using pillars and flow conditions Valero et al. [66] presented a silicon-glass microfluidic device capable of real time analysis of apoptotic cell death dynamics. In the case of Yang et al. [67] a popular dam like structure was used to capture cells for on-chip monitoring of cellular reactions. In this case the dam structure was in parallel to the fluid flow allowing the user to dock the cells of interest in precise locations within the device, furthermore this strategy also allowed the control of the number of cells retained. A common shortcoming of hydrodynamic capture mechanisms is that it is based on the exertion of mechanical stress on the captured or flowing cells, which could cause cell deformation and shear-induced changes in cell behaviour. Therefore to address this issue channel design and flow control must be carefully considered.

Another astute way of trapping cells with a minimum exertion of hydrodynamic stress is a capillary based technique presented by Park et al. [68], where cells are captured within predefined micro-wells, driven by a receding meniscus formed upon natural evaporation of the medium solution. Cells were spontaneously inserted into the centre of micro-wells in order to minimize the lateral capillary force created at the bottom of the receding meniscus. It was demonstrated that the microwells can either be constructed with soft lithographic capillary moulding of UV curable PUA resin onto glass or directly with replica moulding of PDMS. An advantage of this technique is that capillary force is a well known microfluidic flow propulsion mechanism that can be naturally coupled with this technique to produce a pumpless loading mechanism. However a complication that naturally arises from using the natural evaporation of the medium solution is that cell viability might be compromised due to the exposure of the cells to air during the loading period.

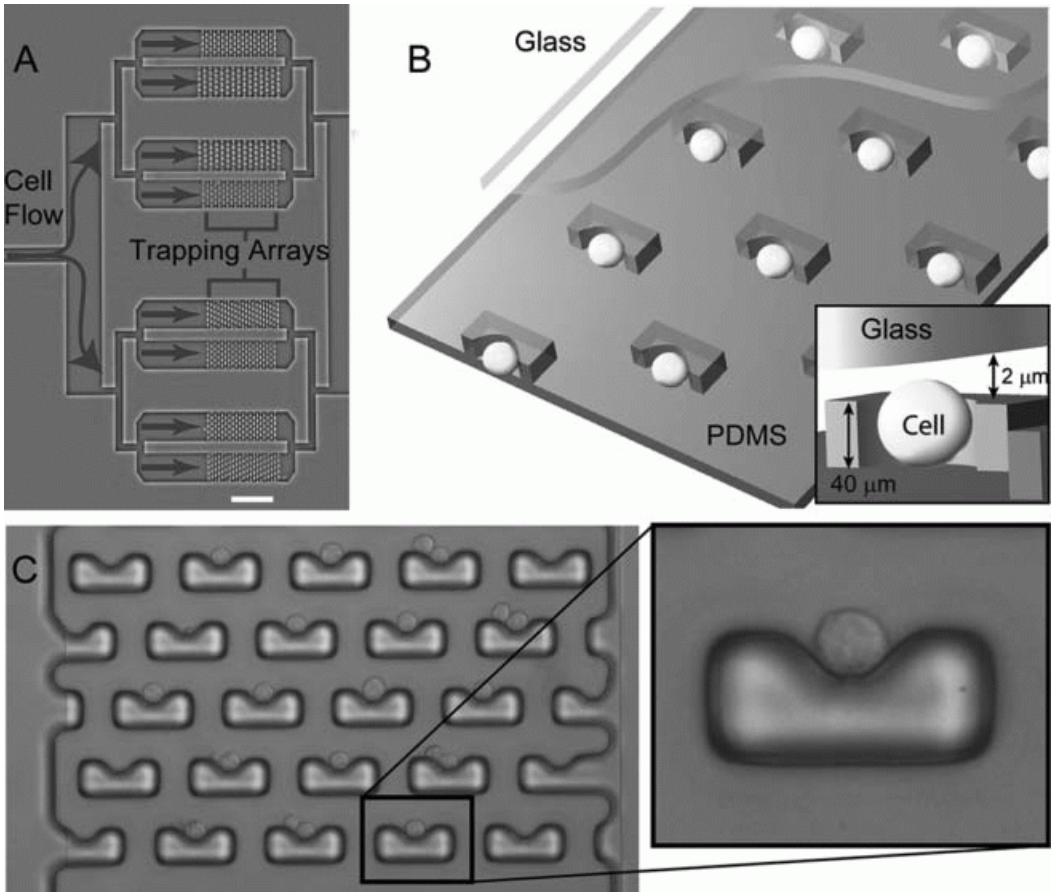

Figure 1.5. Single cell trapping arrays. **(A)** A photograph of the cell trapping. The scale bar is 500 μm. **(B)** A diagram of the device and mechanism of trapping is presented. Trap size biases trapping to predominantly one or two cells. An inset shows the geometry of an individual trap. **(C)** A high resolution brightfield micrograph of the trapping array with trapped cells is shown. In most cases cells rest at the identical potential minimum of the trap. Reproduced from REF [64].

Sedimentation based on gravitational force is well known by most biologists and is the most direct and simple and low-expertise means for manipulating cells within solutions whether they be in microfluidic channels or not. The simplest way of capturing cells within particular regions of a micro-device whether it be for high-throughput screening or cell to cell signal interactions for biological research or tissue engineering is based on cell sedimentation and adherence to pre-coated adhesive ligands [69]. This simple approach generally exposes the cells to the direct flow within the micro-device and is thus prone to shear driven modifications in cell behaviour. To overcome this limitation, special microfluidic designs involving micro-wells and grooves have been developed to capture and localize cells exploiting gravitational force but also shielding them from shear stress. Khademhosseini et al. [70] introduced a simple soft lithographic technique

to fabricate PEG microstructures within microfluidic channels that can immobilize cells within specific locations despite shear flow in the channel. This technique was further advanced to produce multi-cell patterning with multi-cell condition testing [71]. The core advancement was the use of reversible sealing of a multi-channel microfluidic lid that is used to load each row of micro-wells with a different cell type after which the multi-channel lid is removed and orthogonally placed over the loaded micro-wells so that each column of the micro-wells is subjected to a different test condition. By using open high density micro-well arrays Rettig and Folch [72] presented a method for generating and trapping high-density single cell arrays. With optimization more than 18 000 single cells per image (4× objective) can be analyzed and their cellular response detected. The cells can be adherent or non-adherent. Deutsch et al.[73] improved this concept of high-density single cell arrays by fabricating a densely packed 2-D arrangement of hexagonal pico-litre wells directly in glass and placing them into a microfluidic channel that allows the dynamic flow medium and stimulants. Love et al. [74] astutely applied high-density single cell arrays made from PDMS micro-wells to the detection of hybridoma cells producing antigen-specific antibodies. This reduced the minimum time for a screening from 30 days to just 2 days. The array of micro-wells was filled with hybridoma cells and sealed with an antigen coated glass slide. After incubation the glass slide was detached and the antigen-antibody protein array analyzed through immuno-staining. This allowed the analysis of over 100 000 cells per assay.

Although sedimentation provides a simple, low-expertise route to docking and capturing cells into micro wells or hollow structures, its efficiency is relatively low (between 30%-50%) with poor reproducibility. Due to the local dispersion of cells in the solution as well as flow conditions cells are usually deposited non-uniformly over an area leaving many empty sites. An improved design or experimental set up effectively harnessing hydrodynamics can further enhance the efficiency and reproducibility of sedimentation based cell capture methods.

Furthermore microfluidic cell culture is very effective in terms of achieving high throughput parallel analysis with various culture conditions (i.e. different concentration or different stimuli) or various target cells. A range of concentrations can be readily established on the chip through the use of microfluidic gradient generators, which has motivated the construction of systems for the investigation of the cellular response to different reagent concentrations [75-79]. Multiple reagent concentrations have also been combined with multiple cell types on a single device to form two-dimensional cell culture arrays for combinatorial analysis [71, 80, 81]. Additionally 2-dimensional cell culture arrays with different stimuli [82] and with different reporter cells [83] have also been demonstrated.

1.4.2 Lab-on-a-Chip devices for nucleic acid analysis

The ideal microfluidic nucleic acid amplification device should be able to perform in small volumes, rapid nucleic acid amplification, with full integration of pre-amplification steps such as sample preparation and post amplification steps and perform all this in a highly parallelized platform. However, after a careful literature review, to date, such a device has yet to be developed. This sub-section starts by presenting the different types of in-vitro amplifications techniques that have been microfluidically implemented and finalizes by examining the key characteristics of microfluidic nucleic acid amplification.

1.4.2.1 Microfluidic devices for nucleic acid amplification

1.4.2.1.1 PCR microfluidic devices

Conventional PCR as is done in bench-top thermo-cyclers has principally two limitations, the first one is that the reaction volumes require relatively large amounts of reagents which increases the cost per reaction and secondly there is a large thermal mass which limits the thermo-cycling rate and slows down the reaction. Microfluidic PCR devices precisely try to address these issues. Since the mid 90's a lot of work has been published on the construction of microfluidic devices [84] [85] [86] [87].

Initially the simplest approach to microfluidic PCR [88] [89] [90] was to miniaturize the classical PCR thermo-cycler (Figure 1.6) and thus reduce both the reagent consumption and the thermal mass of the system. A further innovation to this basic approach was to develop a flow-based system.

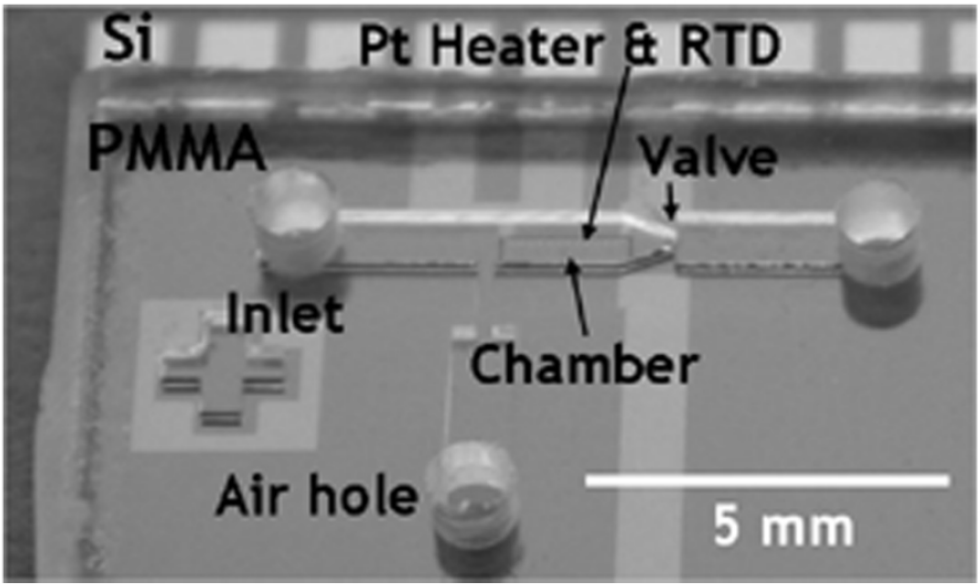

Figure 1.6 Miniaturization of a classical PCR thermo-cycler. PCR mixture is injected into the miniature reaction chamber and sealed with mineral oil. On-chip Pt heaters cycle the temperature during the amplification reaction. Reproduced from REF [90].

This brought a change of paradigm in PCR thermo-cycling, instead of having a static reaction vessel that is thermally cycled one can inject a reaction plug into a stream that flows across the various static temperature regimes [91] [92] [93] [94]. The flow velocity of the reaction plug determines the residence time at each thermal step as compared to conventional reactors. This resolves the thermal mass limitations and allows for PCR to be done in much faster rates and in a continuous reaction. The main limitations to the cycling rate in this type of PCR reaction are the intrinsic biochemical kinetics within the PCR reaction itself.

Furthermore, within continuous flow PCR, reaction volumes can be miniaturized by encapsulating them in droplets separated by an immiscible fluid (Figure 1.7) [95] [96] [97] [98]. Due to the continuous flow, fast cycling and extremely low reaction volume

capabilities of this type of microfluidic PCR systems have a great potential for high throughput applications where rates of 30-50,000 reactions per day or more are feasible.

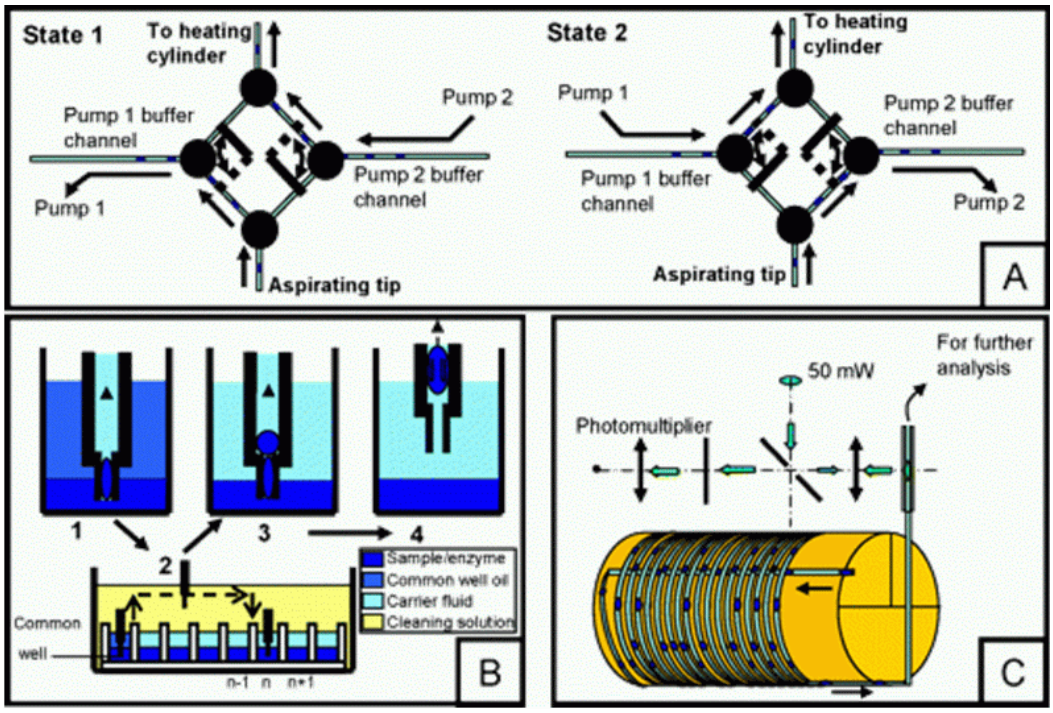

Figure 1.7 Setup for droplet based continuous flow PCR. **(A)** Three-way pinch valve 2 state loop for sequential injection with continuous flow **(B)** 4 step injection and droplet generation process using a dual diameter aspirating tip. **(C)** Capillary wrapped 35 times around a three-zone heating cylinder for PCR thermocycling and endpoint LIF detection. Reproduced from REF [98].

Recently there has also been a great interest in developing more robust and portable PCR systems for low resourced field point-of-care and pathogen detection applications. Unfortunately the microfluidic devices cited above still mostly relay on external mechanisms to actuate fluids and perform detections so essentially that approach makes them dedicated laboratory apparatuses. A promising approach to making devices more portable is natural convection-based flow PCR [99] [100] [101] [102] [103] [104] [105] [106]. The classical approach to convection-based flow PCR is the Rayleigh–Benard (RB) convection cell (Figure 1.8) [99] [100]. The RB convection cell is characterized by

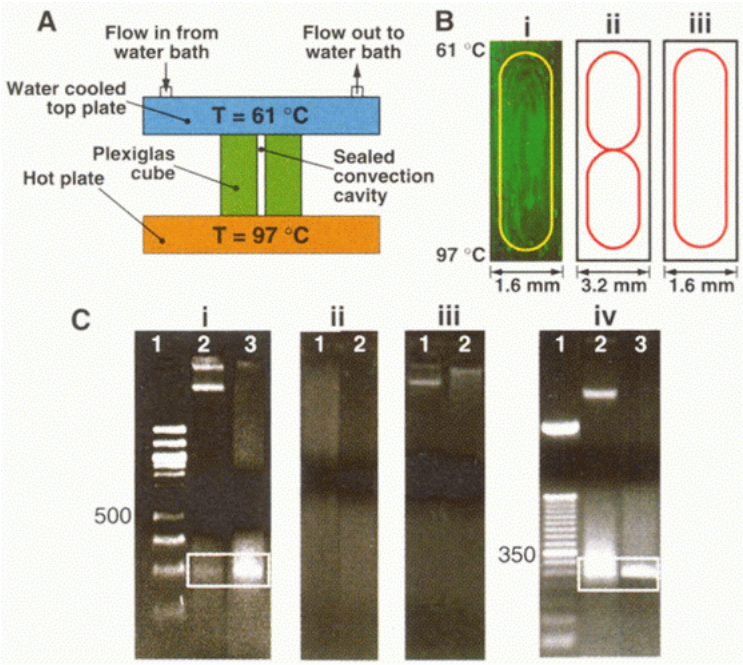

Figure 1.8. Rayleigh-Benard (RB) convection based PCR cycling cell **(A)** RB-PCR cell schematic. **(B)** Influence of geometry on Rayleigh-Benard convection **(C)** DNA amplification in RB-PCR cell. (i) Amplification with 0.1 U/idl Ampli-Taq Polymerase. Lane 1, 100-bp ladder; lane 2, RB-PCR product; lane 3, PCR product generated in a thermo-cycler. (ii) Negative control with no template. (iii) Negative control with no enzyme. (iv) Amplification with 0.15 U/[LL AmpliTaq Polymerase. Lane 1, 50-bp ladder; lane 2, RB-PCR product; lane 3, thermo-cycler product. Reproduced from REF [99].

having two heated plates one on the top and the other on the bottom of the cell the PCR cocktail is contained between these two heated plates. The lower plate is held at the denaturation temperature (approx. 98 °C) and the upper plate held at the annealing temperature (approx. 61 °C). This generates a convection flow because the hot fluid on the bottom is less dense than that above, and rises due to buoyancy. As the less dense hot fluid reaches the top of the device, it cools and then begins to flow back towards the bottom. The suspended DNA and nucleotides are naturally flowed across the temperature gradient and thermo-cycled between the denaturing and annealing temperatures, crossing through the extension temperature during their transit. Advancements on natural convection PCR have demonstrated some potentially very simple, robust and portable systems that would be suitable for developing world applications, including an immersion heated system [104] and a device that runs on two AA batteries [106].

One of the key factors controlling the efficiency of natural convection PCR is the geometry of the microreactors. In an effort to better control the residence time of the DNA in each temperature zone a number of groups [102] [100] [103] [105] [106] have moved from simple flow cells to looped geometries.

1.4.2.1.2 NASBA microfluidic devices

The first successful microfluidic NASBA reactions were demonstrated by Gulliksen et al. (2004) [107] in 10 nL silicon-glass reaction chambers (Figure 1.9). To enable the 10 nL real time NASBA reaction, yeast tRNA was added to the standard reagent mixture. To obtain amplification in the silicon-glass micro-chambers SigmaCote surface passivation was required plus the addition of small quantities of carrier molecules. Due to the manufacturing complexity a limited number of devices were fabricated.

An improvement to this initial design was shown by Gulliksen et al. (2005) [108]. The new design was injection moulded in COC polymer and it contained 10 parallel 80 nL reaction channels. Based on this design microfluidic real time NASBA was well characterized and shown to perform as well as conventional off chip real time NASBA. Off chip handling of nucleic acids especially RNA is very prone to degradation, causing quality and reproducibility problems. The integration of sample preparation steps with RNA amplification and detection all on a single microfluidic device would be very beneficial in decreasing the reproducibility problems.

In this direction Yobas et al. [109] demonstrated all the steps required in a fully integrated diagnostic assay for nucleic-acid-based detection of viral particles in whole blood. These steps include separation of viral particles from blood cells followed by extraction, purification, amplification, and detection of viral nucleic acids. Unfortunately each step was shown to function in a separate independent microfluidic chip. In the RNA amplification chip, NASBA was used to amplify cDNA transcripts of the viral RNA and amplicons were detected on the same chip using a colorimetry assay based on DNA probes conjugated with horse radish peroxide (HRP).

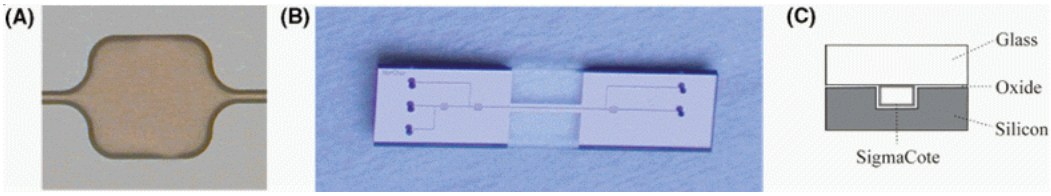

Figure 1.9. The first successful microfluidic NASBA reactions were demonstrated by Gulliksen et al. (2004) [107] in 10nL silicon-glass reaction chambers. (A) 10 nL chamber, (B) Complete device. (C) Cross sectional sketch. Reproduced from REF [107].

Recently Furuberg et al. [110] demonstrated a semi-integrated spatially multiplexed NASBA based diagnostic chip. The complete diagnostic assay is done on two separate disposable polymer chips. The two-chip system is designed to diagnose a group of viruses known to cause cervical cancer. The first chip is designed to perform nucleic acid extraction from patient epithelial cervical cells, while the second chip performs NASBA based mRNA amplification and fluorescent detection. The purified sample is inserted into the second chip and splits into ten smaller chambers for simultaneous amplification and detection of ten viruses. Each chamber contains a separated set of lyophilized reagents that are re-hydrated (within 11 min.) before the reaction starts. A positive amplification of HPV type 16 viruses is shown.

1.4.2.1.3 Other types of nucleic acid amplification devices

Microfluidic devices based on rolling-circle amplification (RCA) have been shown capable of single-molecule detections (SMD). Specifically RCA provides the capability of transforming specific molecular recognition events at nanometre dimensions to micrometer-sized DNA molecules [111] which allows single-molecule enumeration. The specific molecular recognition event can be used to detect nucleic acids through hybridization reactions or low copy protein molecules through target-specific padlock probe ligation, followed by rolling circle amplification (RCA) [112]. RCA provides a means of generating a confined amplification micron-sized product that can later be enumerated. During RCA a circularized DNA molecule is specifically copied by a DNA polymerase, generating a long DNA strand composed of tandem repeats of complements of the circular DNA strand. The rolling circle products (RCPs) form individual random-coil DNA molecules and thus no physical barriers are needed to confine the amplification products from individual molecules in one spot. By using

fluorescent probes each random-coil DNA molecule can be labelled with hundreds of fluorophores making then directly visible to standard fluorescent microscopy. The RCA principle was first applied for biotechnological purposes by Fire [39] and Kool [113], and later the discrete nature of the amplification products was established by Lizardi et al. [114]. RPCs generated in solution can be quantified by pumping them through a microfluidic channel and observing the flow under a fluorescence microscope.

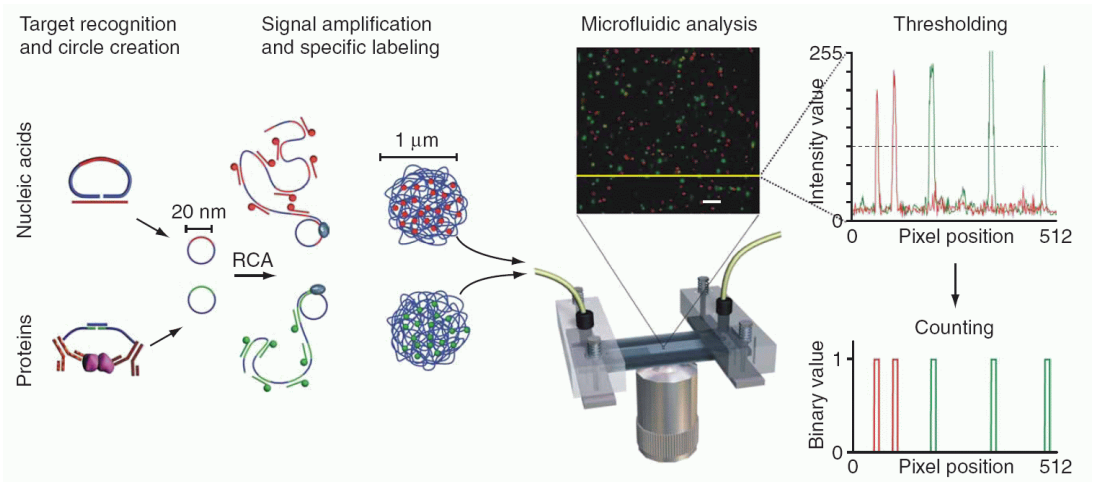

Figure 1.10. Molecular recognition of DNA or protein targets through padlock probe ligation or proximity ligation results in the formation of a unique circular DNA molecule with a diameter of approximately 20 nm. The circular molecule acts as an endless template for a rolling-circle-replication reaction. This produces a long single-stranded concatemer DNA molecule complementary in sequence to the DNA circle, repeated approximately 1,000 times, which spontaneously collapses into a random coil of DNA. Fluorescent molecule–tagged probes are hybridized to the repeated sequence, resulting in a confined cluster of up to 1,000 fluorophores, visible in a fluorescence microscope as a bright object with a diameter of approximately 1 µm. Individual DNA molecules are detected and quantified by pumping a sample through a thermoplastic microchannel mounted in a standard confocal fluorescence microscope operating in line-scan mode. Various circles can be formed corresponding to unique analyte entities and amplified in the same reaction. Hybridization of detection probes of distinct colours allows multiplexed signal readout (as shown in the fluorescence image inset; scale bar, 20 µm). Reproduced from REF [116].

A confocal volume based technique can achieve high-precision measurements (Figure 1.10) in the microfluidic quantification (C. V. ~3%) of RPCs [115] [116]. A further benefit of miniaturizing RCA was demonstrated by Hutchison et al. [117]. The principal difficulty with amplification of small amounts of template by RCA using φ29 DNA polymerase is “background” DNA synthesis that usually occurs when the target DNA is omitted, or present at low concentrations. By exploiting the capabilities of microfluidics the reaction

volume can be reduced while keeping the amount of targets fixed which in turn increases the template concentration, resulting in a suppression of background synthesis. Cloning of single circular molecules with φ29 DNA polymerase was achieved in 600 nL volume RCA reactions.

Microfluidic based invitro transcription (IVT) of cDNA sequences from single-cell quantities of mRNA immobilized on packed beads has also been demonstrated [118]. IVT is a linear amplification mechanism that uses T7 RNA polymerase to transcribe double-stranded cDNA (ds cDNA) into antisense-RNA (aRNA). It is the most commonly used RNA amplification method for microarray analysis because it amplifies all fragments at an equal rate and thus there is no significant biasing of the gene expression levels during the amplification [119].

1.4.2.2 Microfluidic nucleic acid amplification characteristics

1.4.2.2.1 Integration

Many argue that one of the most fundamental advantages of microfluidics is the ability to integrate several functions or steps on a single device. The full integration of all the steps required by a complete assay is key in being able realize the full potential of micro total analysis systems. In the case of NAA devices many research groups have developed devices that accommodate all or several of the necessary fluid, thermal and detection functions on a common device. The first attempt was to integrate PCR with a post amplification step such as CE for product analysis as reported by Woolley et al. in 1996 [120].

After about ten years of research in the field of full integration and there are still very few devices that can demonstrate full assay capabilities, some of the best examples are [121] [122]. These devices integrate all the necessary steps common to diagnostic and pathogen detection assays and achieve sample in and answer out capabilities. Even though these devices demonstrate important steps in the right direction, they are still

quite limited in terms of their levels of detection, ability to handle complex sample matrixes and restricted to a defined set of protocols.

Most of the work on integration has concentrated on partial component integration. This partial integration of procedures with NAA on a single device can be classified into main two fields, pre-NAA function integration and post-NAA function integration.

Post-NAA function integration includes nucleic amplification analysis steps which can be classified as hybridization based (Microarray, Figure 1.11) [123], real time fluorescent based [124], electrophoresis based [61], electrochemical based [125] or immuno-staining based [126]. Post-NAA function integration is singularly the most developed area within PCR integration in a single microdevice. This is most likely due to the higher complexities associated with sample handling during pre-NAA treatment.

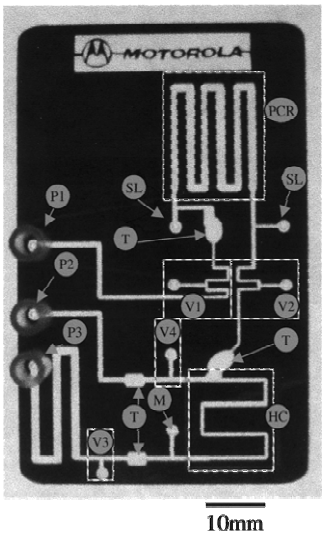

Figure 1.11. Monolithic integrated polycarbonate DNA assay device. Serpentine PCR channel (PCR), hybridization channel (HC), Pluronics valves (V1−V4), Pluronic traps (T), hydrophobic air-permeable membrane (M), PCR reagent loading holes (SL), sample driving syringe pump (P1), waste-withdrawing syringe pump (P2), and wash syringe pump (P3). Reproduced from REF [123]

Generally the aim of integrated NAA devices is to analyze, within the confines of a usually portable miniaturised platform, real biological samples with complex matrices, so pre-NAA function integration involves sample purification and pre-concentration.

Authors	Woolley, A.T., et al.	Waters, L.C., et al.	Wilding, P., et al.	Christel, L.A., et al.	Yuen, P.K., et al.	Liu, Y., et al.	Lee, T.M. et al.	Liu, R.H., et al.	Cady, N.C., et al.	Easley, C.J., et al.	Wang, J., et al.	Lee, J.-G., et al.
Integration of Pre- NAA steps												
Microfluidic Filtering			✓		✓							
Immunomagnetic Separation								✓				
Silica based Nucleic Acid Purification				✓					✓	✓		
Sample Desalting				✓								
Thermal Lysis		✓	✓		✓			✓				✓
Integration of Post-NAA steps												
Electrochemical Based Detection							✓					
Immunostaining based Detection											✓	
Microarray Hybridization Detection						✓		✓				
Real Time Fluorescent Detection									✓			✓
Electrophoresis Based Detection	✓	✓								✓		
Amplification Method	PCR	PCR	PCR	PCR	PCR	PCR	PCR	PCR	PCR	PCR	PCR	PCR
Year	1996	1998	1998	1999	2001	2002	2003	2004	2005	2006	2006	2006
Reference	[120]	[61]	[127]	[130]	[128]	[123]	[125]	[121]	[124]	[122]	[126]	[129]

Table 1.1 Microfluidic integration achievements over the last decade.

Sample purification is often done in two stages. First there is a cell filtration stage where the target cells are filtered out from the rest of the sample (examples of these are white blood cell separators based on microfluidic filtering [127] [128] and immunomagnetic bead-based separation from whole blood [121]). After the target cells are separated usually their DNA is extracted through lysis [129] and pre-concentration steps. The pre-concentration is usually based on standard purification by silica adsorption [130] [124]. Other sample conditioning steps such as sample desalting have also been demonstrated [130]. Table 1.1 summarizes the microfluidic integration achievements over the last decade. For a comprehensive review of integration with PCR please refer to [131].

1.4.2.2.2 Low-volume

With microfabricated devices comes the ability to react extremely small volumes of solution. The smallest nucleic acid amplification (NAA) reaction volume reported to date is found in the work by Beer et al. [132]. Their device is based on a shearing T-junction made in a silicon substrate to generate a stream of aqueous monodisperse picolitre droplets in an oil-phase carrier (Figure 1.12). Once the droplets were generated, they were statically kept inside the microfluidic channel and thermally cycled on a peltier based system and fluorescently interrogated during each thermal-cycle. With this system, a 10 pL droplet, encapsulating less than one copy of viral genomic DNA (verified through Poisson statistics), showed real time PCR amplification curves with a cycle positive threshold of ~18. This is approximately 20 cycles earlier than what is common in conventional instruments. Since the entire micro-device is heated the thermal cycling rates are quite slow, requiring 108 min. for 40 amplification cycles.

Another very low volume NAA device was demonstrated by Nagai et al. [133] who fabricated an array of 86 pL microchambers on silicon substrates with silicon oxide on the inner walls. Smaller chamber size was explored but no detectable amplification was observed. The device did not exploit the small volumes for a fast thermal cycling. Instead the complete device was placed onto a conventional thermo-cycler requiring 2 hrs to complete 40 cycles. PCR end product was fluorescently detected with real time

Taqman probe with a fluorophore and a quencher. The amplification was observed in real time by a CCD camera through a microscope.

In a more operational attempt Liu et al. [134] reported the use of hydraulic valves and pneumatic pumps to perform PCR in 3 nL reaction volumes. Even though this system has a considerably higher reaction volume it has the advantage that it can very efficiently load 400 distinct parallel reaction chambers. Through a valve multiplexing system the device can load an N x N matrix of reaction centres with just 2N + 1 pipetting steps compared to the conventional $3N^2$ steps. As in the previous cases this work does not focus on the thermal cycling speed so the entire device was placed on a conventional thermo-cycler tacking 1 hr to complete the amplification of a 294-bp fragment of the human β-actin cDNA fragment.

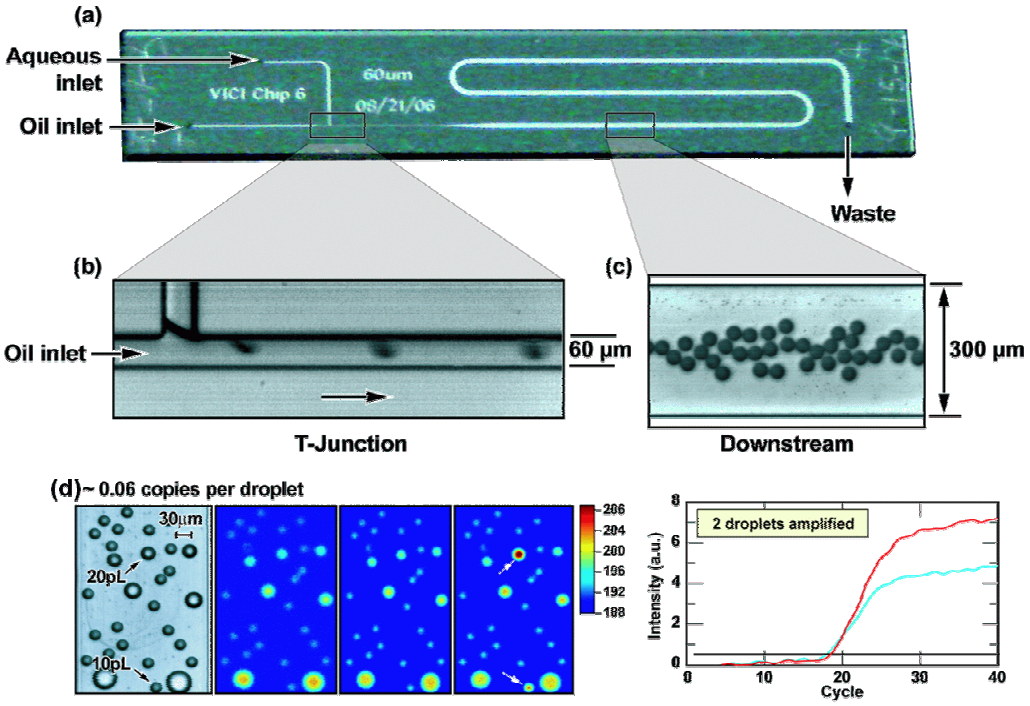

Figure 1.12. Images of the low volume PCR chip showing (**a**) the overall channel and flow configuration, (**b**) droplet generation at the T-junction, and (**c**) monodisperse droplets in the downstream channel. Real time PCR data from picolitre droplets at an estimated (**d**) 0.06 copies of genomic DNA per singlet droplet. Droplets were identified from the bright-field image and then monitored at each cycle to generate real time fluorescence curves. Adapted from REF [132].

The lowest volume non-PCR NAA device was reported by Gulliksen et al. (2004) [107] with a 10 nL real time NASBA reaction in silicon-glass reaction chamber. Since NASBA in an isothermal reaction no cycling is required and the whole chip was incubated at 41 °C. The real time NASBA reaction was shown to generate a positive signal distinguishable over the background noise in approximately 20 mins.

Small volume NAA is advantageous in reducing the cost of reagents used for the amplification. In case of nucleic acid amplification reactions that also require thermal cycling such as PCR the reduced volume should also allow for more rapid thermo-cycling. However, as described previously, the use of small-volume thermal cycling chambers does not necessarily coincide with reduced amplification times if the mode of heating does not exploit the advantages of low-volume design. This is generally the case when the entire device is thermo-cycled. In order to avoid the complications and thermal optimizations required in PCR based reactions other isothermal forms of nucleic acid amplification may be used. Furthermore these forms of amplification can be biochemically optimized to produce extremely fast amplifications. For example in NASBA each cycle produces 10-1000 copies of the template compared to just a doubling in PCR reactions.

1.4.2.2.3 High-speed

Commonly in case the of NAA reaction that require thermal cycling such as PCR reducing the thermal mass of the system can increase the heating and cooling rates during temperature cycling. This has the advantage that it can speed up the amplification reaction, this is important in applications where high throughput processing is critical. The fastest reported NAA reactions to date are performed with a flow-through PCR device where the only thermal mass was the solution and not the micro-device. Hashimoto et al. [135] is one such case with the flow-through device, they achieved amplification of a 500-bp region of λ-phage DNA in only 1.7 min and a 997-bp fragment took 3.2 min. In case of flow though devices, since the thermal mass is so small, the factor that limits the speed of the reaction is the kinetic limit of nucleotide incorporation

by Taq polymerase and not the thermal cycling. This was the case with Hashimoto et al. [135] where the temperature transition is faster than the kinetic limit of nucleotide incorporation thus the system is limited only by the properties of the enzyme. This means that as one increases the thermal cycling speed to over a certain threshold the amplification efficiency is reduced This results in very poor levels of detection (Hashimoto et al. reported an LOD of 1 x 10^7 copies). Another flow-through PCR device capable of either PCR or reverse-transcriptase PCR (RT-PCR) developed by Obeid et al. [136] improved the LOD to 6.25 x 10^6 copies within 6 min. The PCR and RT-PCR reactions were performed with volumes ranging from 10 µL to 700 nL.

Another way of increasing the thermo-cycling speed but also maintaining a low reaction volume was pioneered by Landers and co-workers [89] that use infrared-mediated heating for performing the thermal cycling. Infrared-mediated heating has the advantage that it can focus all the thermal heating only on the solution in the PCR chamber. This is further optimized by completely etching away as much of the glass near the PCR reactor and so minimize heating of the surrounding area. In demonstrations IR-mediated PCR has been performed in just 4 min, resulting in one of the fastest cycling times using a non-flow-through system. However, the use of IR-mediated heating requires an IR-source, and it is not easily integrated into a portable system.

An elegant system that can combine both high speed cycling and very low reaction volumes was recently demonstrated by Rothberg et al. [137]. Roughly millions of real time PCR reactions were done in uniform, monodisperse droplets of 65 pL. The droplets were generated via flow-focusing where the PCR mix was infused with two perpendicular channels flowing immiscible oil. Thermal cycling was achieved by flowing the droplets though distinct thermal zones resulting in a rapid (55-s cycles) and efficient PCR amplification. An 18 cycle amplification time would take 16.5 min. The droplets were shown to be able to perform single molecule PCR. The device was used for limiting dilution PCR (also known as digital PCR) very useful in high precision detection and quantification of the number of initial templates.

1.4.3 What is missing and aim of this research

Recent advances in NAA micro-devices most notably in PCR based-devices have produced high-throughput, sensitive, and rapid systems. Most of these systems effectively integrate amplification and post-amplification functionality. The few systems that do integrate pre-amplification functionality are exclusively designed for diagnostics and pathogen identification. Even though nucleic acid amplification is a ubiquitous technique used throughout the life sciences and has revolutionized the way information is extracted from biological samples, it has yet to be developed and integrated into microfluidic systems for total cell based analysis. Furthermore since the invention of PCR other amplification techniques have also been developed, NASBA is one such technique that poses advantages over PCR such as isothermal amplification, lower non-specific detection and direct amplification of RNA (critical in gene expression analysis, bacterial and viral diagnostics, cell viability analysis, etc.). Yet microfluidic systems that exploit the advantages of NASBA have been very limited, and there have been no previous reports or demonstrations of integrated microfluidic NASBA devices with pre-amplification functionality. Moreover despite all the advantages of microfluidics current integrated and multiplexed systems require expensive and complex fluidic setups to be operated, this has contributed to the slow up-take, deployment and use of the microfluidic tools and systems by the general community. There is an evident lack of simple and robust microfluidic systems that can be easily adopted and used by a non-specialized community of microfluidic users.

Microfluidics has demonstrated important advantages over its conventional counterpart technology. These often cited advantages are decreased reagent and sample consumption and waste, faster analyses, more controllable process parameters and higher parallelism. To date, however, most of the microsystems developed do not take advantage of the potential of a fully integrated functionality offered by the miniaturized nature of the systems. The goal of the work presented in this thesis is to develop the necessary components and integration mechanisms that can enable high-throughput and fully-integrated systems with sample or experiment-in and answer-out capabilities.

1.5 Outline of the thesis

Chapter 2 outlines the principal theoretical models and calculations related to the novel microfluidic technologies and techniques propose in this thesis. Firstly the behaviour of flow in microfluidic devices is briefly discussed. This is based on the Navier-Stokes model in the region of laminar flow and low Reynolds numbers (Re<10). Secondly the convection-diffusion equation is presented as a dynamic model for species mixing in a flow field. Thirdly a basic cell sedimentation model is described for the calculation of the cell trajectories and capture efficiencies. Finally a hydrostatic pressure model is presented as a means for generating flow within microfluidic devices.

Chapter 3 presents all the experimental details associated with the results shown in the following chapters. The chapter is divided into three main sections; each section focuses on one of the principal micro-device designs. The three designs are the RNA Extraction & Real Time NASBA device, iNASBA array device and the iCell array device. Each section shows the device design, device operation, all the fabrication procedures required for implementation and the materials and methods associated with the characterization of the device.

Chapter 4 presents the characterization results of the RNA Extraction & Real Time NASBA device incorporating real time detection. The real time amplification and detection step produces a pathogen-specific response in less than 3 min from the chip-purified RNA of 100 lysed bacteria. On-chip RNA purification uses a novel silica bead immobilization method. On-chip amplification uses custom-designed high-selectivity primers and real time detection uses molecular beacon fluorescent probe technology; both are integrated on-chip with NASBA.

Chapter 5 presents the characterization results of the iNASBA array. The iNASBA array for the first time demonstrates that microfluidic dynamic cell culture, cell stimulation, cell

labelling, lysis, and real time NASBA based RNA analysis can de done a on a single chip.

Chapter 6 presents the characterization results of the novel micro-fluidic technology, iCell array that can perform completely integrated cell based assays with bio-analytical read-out protocols such as immuno-fluorescent imaging or real time NASBA based nucleic acid amplification. The iCell array permits the parallel and configurable on-chip integration of complex procedures such as adherent and non adherent cell culture, cell stimulation, cell lysis, cell fixing, protein immunoassays, bright field and fluorescent microscopic monitoring, and real time detection of nucleic acid amplification. With onboard gravity driven flow control the device is simple and economical to operate, very low reagent volumes (50 nL per reaction or less) are required for the device to function, and it does not use any external macro-scale power sources. This enables the iCell array to be directly used with existing laboratory infrastructure such as multichannel pipettes and/or robot fluid handling systems, incubation or environmental control chambers and microscope systems. iCell array can process up to 512, 10 nL reactions in a single chip and up to 64 different user selected integrated assays can be done simultaneously.

Finally, chapter 7 discusses the prospects and possible future applications of the devices and technologies developed in this thesis and concludes with a summary of the research results.

1.6 References

1. Brody, J.P., et al., *Biotechnology at low Reynolds numbers.* Biophysical Journal, 1996. **71**(6): p. 3430-3441.
2. Voldman, J., M.L. Gray, and M.A. Schmidt, *Microfabrication in biology and medicine.* Annual Review of Biomedical Engineering, 1999. **1**: p. 401-425.
3. Beebe, D.J., G.A. Mensing, and G.M. Walker, *Physics and applications of microfluidics in biology.* Annual Review of Biomedical Engineering, 2002. **4**: p. 261-286.
4. Glotzer, J.B., et al., *Cytoplasmic flows localize injected oskar RNA in Drosophila oocytes.* Current Biology, 1997. **7**(5): p. 326-337.
5. Huang, Q. and T. Pederson, *A human U2 RNA mutant stalled in 3' end processing is impaired in nuclear import.* Nucl. Acids Res., 1999. **27**(4): p. 1025-1031.
6. Jacobson, M.R. and T. Pederson, *Localization of signal recognition particle RNA in the nucleolus of mammalian cells.* Proceedings of the National Academy of Sciences of the United States of America, 1998. **95**(14): p. 7981-7986.
7. Bassell, G.J., et al., *Single mRNAs visualized by ultrastructural in situ hybridization are principally localized at actin filament intersections in fibroblasts.* J. Cell Biol., 1994. **126**(4): p. 863-876.
8. Buongior.M and F. Amaldi, *Autoradiographic Detection of Molecular Hybrids between Rrna and DNA in Tissue Sections.* Nature, 1970. **225**(5236): p. 946-&.
9. Behrens, S., et al., *Is the In Situ Accessibility of the 16S rRNA of Escherichia coli for Cy3-Labeled Oligonucleotide Probes Predicted by a Three-Dimensional Structure Model of the 30S Ribosomal Subunit?* Appl. Environ. Microbiol., 2003. **69**(8): p. 4935-4941.
10. Brodsky, A.S. and P.A. Silver, *Identifying proteins that affect mRNA localization in living cells.* Methods, 2002. **26**(2): p. 151-155.
11. Forrest, K.M. and E.R. Gavis, *Live Imaging of Endogenous RNA Reveals a Diffusion and Entrapment Mechanism for nanos mRNA Localization in Drosophila.* Current Biology, 2003. **13**(14): p. 1159-1168.
12. Shav-Tal, Y., et al., *Dynamics of single mRNPs in nuclei of living cells.* Science, 2004. **304**(5678): p. 1797-1800.
13. Molenaar, C., et al., *Poly(A)+ RNAs roam the cell nucleus and pass through speckle domains in transcriptionally active and inactive cells.* J. Cell Biol., 2004. **165**(2): p. 191-202.
14. Molenaar, C., et al., *Linear 2' O-Methyl RNA probes for the visualization of RNA in living cells.* Nucl. Acids Res., 2001. **29**(17): p. e89-.
15. Tsuji, A., et al., *Direct Observation of Specific Messenger RNA in a Single Living Cell under a Fluorescence Microscope.* Biophysical Journal, 2000. **78**(6): p. 3260-3274.
16. Tyagi, S. and F.R. Kramer, *Molecular beacons: Probes that fluoresce upon hybridization.* Nature Biotechnology, 1996. **14**(3): p. 303-308.
17. Santangelo, P.J., et al., *Dual FRET molecular beacons for mRNA detection in living cells.* Nucl. Acids Res., 2004. **32**(6): p. e57-.
18. Watson, J.D. and F.H.C. Crick, *Genetical implications of the structure of deoxyribonucleic acid.* Nature, 1953. **171**: p. 964-967.
19. Walker, J. and G. Dougan, *DNA probes: a new role in diagnostic microbiology.* J. Appl. Bacteriol. , 1989(67): p. 229-238.
20. Tenover, F.C., *Diagnostic deoxyribonucleic acid probes for infectious diseases.* Clin. Microbiol. Rev. , 1988(1): p. 82-101.
21. Gingeras, T.R., et al., *Methodologies for in vitro nucleic acid amplification and their applications.* Vet. Microbiol., 1990(24): p. 235-251.
22. Hilborne, L.H. and W.W. Grody, *Diagnostic applications of recombinant nucleic acid technology: basic techniques.* Lab. Med. , 1991. **22**(849-856).
23. Rubin, F.A. and D.J. Kopecko, *Nucleic acid probes for the detection of clinically significant bacteria.*, in *Nucleic acid and monoclonal antibody probes. Applications in diagnostic microbiology.*, Swaminathan and G. Prakash, Editors. 1989, Marcel Dekker, Inc.: New York. p. 185-219

24. Berry, A.J. and J.B. Peter, *DNA probes for infectious disease.* . Diagn. Med. , 1984(7): p. 62-72.
25. Bryan, R.N., et al., *Diagnosis of clinical samples with synthetic oligonucleotide hybridization probes.* L. Leive (ed.), Microbiology, American Society for Microbiology, 1986( ): p. 113-116.
26. Kohne, D., et al., *Novel approach to rapid and sensitive detection of microorganisms: DNA probes to rRNA.* Leive (ed.), Microbiology. American Society for Microbiology, Washington, D.C., 1986: p. 110-112.
27. Watson, J.D., et al., *Molecular biology of the gene*. 1987 Menlo Park, Calif.: The Benjamin/Cummings Publishing Co. Inc.
28. Kitchin, P.A., et al., *Avoidance of false positives.* . Nature, 1990: p. 344:201.
29. Knight, P., *Amplifying probe assays with Q-beta replicase.* Biotechnology 1989(7): p. 609-610.
30. Kohne, D.E., *Application of DNA probe tests to the diagnosis of infectious disease.* Am. Clin. Prod. Rev., 1986. **5**(11): p. 20-29.
31. Mullis, K.B., *The unusual origin of the polymerase chain reaction.* . Sci. Am., 1990(240): p. 56-65.
32. Brunt, J.V., *Amplifying genes: PCR and its alternatives.* Biotechnology, 1990(8): p. 291-293.
33. Lazcka, O., F.J.D. Campo, and F.X. Munoz, *Pathogen detection: A perspective of traditional methods and biosensors.* Biosensors and Bioelectronics, 2007. **22**(7): p. 1205-1217.
34. Mothershed, E.A. and A.M. Whitney, *Nucleic acid-based methods for the detection of bacterial pathogens: Present and future considerations for the clinical laboratory.* Clinica Chimica Acta, 2006. **363**(1-2): p. 206-220.
35. Demidov, V.V., *Rolling-circle amplification in DNA diagnostics: the power of simplicity.* Expert Review of Molecular Diagnostics, 2002. **2**(6): p. 542-548.
36. Langabeer, S.E., et al., *Transcription mediated amplification and hybridisation protection assay to determine BCR-ABL transcript levels in patients with chronic myeloid leukaemia.* Blood, 1999. **94**(10): p. 1267.
37. Compton, J., *Nucleic acid sequence-based amplification.* Nature, 1991. **350 (6313)**: p. 91-92.
38. Walker, G.T., et al., *Strand displacement amplification--an isothermal, in vitro DNA amplification technique.* Nucl. Acids Res., 1992. **20**(7): p. 1691-1696.
39. Fire, A. and S.-Q. Xu, *Rolling replication of short DNA circles.* Proc. Natl. Acad. Sci. U. S. A. , 1995(92): p. 4641–4645.
40. Leone, G., et al., *Molecular beacon probes combined with amplification by NASBA enable homogeneous, real-time detection of RNA.* Nucl. Acids Res., 1998. **26**(9): p. 2150-2155.
41. Wacharapluesadee, S. and T. Hemachudha, *Nucleic-acid sequence based amplification in the rapid diagnosis of rabies.* The Lancet 2001. **358**(9285): p. 892-893.
42. Deiman, B., P. van Aarle, and P. Sillekens, *Characteristics and applications of nucleic acid sequence-based amplification (NASBA).* Molecular Biotechnology, 2002. **20**(2): p. 163-179.
43. Geciova, J., D. Bury, and P. Jelen, *Methods for disruption of microbial cells for potential use in the dairy industry--a review.* International Dairy Journal, 2002. **12**(6): p. 541-553.
44. Boom, R., et al., *Rapid and simple method for purification of nucleic acids.* J. Clin. Microbiol., 1990. **28**(3): p. 495-503.
45. Vogelstein, B. and D. Gillespie, *Preparative and analytical purification of DNA from agarose.* Proceedings of the National Academy of Sciences of the United States of America, 1979. **76**(2): p. 615-619.
46. Cacace, M.G., E.M. Landau, and J.J. Ramsden, *The Hofmeister series: salt and solvent effects on interfacial phenomena.* . Q Rev Biophys, 1997(30): p. 241-277.
47. Hippel, P.v. and K.Y. Wong, *Neutral salts: the generality of their effects on the stability of macromolecular conformations.* . Science 1964(145): p. 577-580.
48. Castellino, F.J. and R. Barker, *The denaturing effectiveness of guanidinium, carbamoylguanidinium, and guanylguanidinium salts.* . Biochemistry, 1968(7): p. 4135-4138.

49. Chirgwin, J.M., et al., *Isolation of biologically active ribonucleic acid from sources enriched in ribonuclease.* . Biochemistry 1979(18): p. 5294-5299.
50. Melzak, K., et al., *Driving forces for DNA adsorption to silica in perchlorate solutions.* . J Colloid Interface Sci 1996(181): p. 635-644.
51. Bartl, K., P. Wenzig, and J. Kleiber, *Simple and broadly applicable sample preparation by use of magnetic glass particles.* . Clin Chem Lab Med 1998(36): p. 557-559.
52. Kessler, H., et al., *Fully automated nucleic acid extraction: MagNA Pure LC.* . Clin Chem 2001(47): p. 1124-1126.
53. Hourfar, M.K., et al., *High-Throughput Purification of Viral RNA Based on Novel Aqueous Chemistry for Nucleic Acid Isolation.* Clin Chem, 2005. **51**(7): p. 1217-1222.
54. Witek, M.A., et al., *Purification and preconcentration of genomic DNA from whole cell lysates using photoactivated polycarbonate (PPC) microfluidic chips.* Nucl. Acids Res., 2006. **34**(10): p. e74-.
55. Zeugin, J. and J. Hartley, *Ethanol Precipitation of DNA.* Focus 1985. **7** (4): p. 1–2.
56. Shapiro, D.J., *Quantitative Ethanol Precipitation of Nanogram Quantities of DNA and Rna.* Analytical Biochemistry, 1981. **110**(1): p. 229-231.
57. Crouse, J. and D. Amorese, *Ethanol Precipitation: Ammonium Acetate as an Alternative to Sodium Acetate.* Focus 1987. **9** (2): p. 3–5.
58. Chomczynski, P. and N. Sacchi, *Single-step method of RNA isolation by acid guanidinium thiocyanate-phenol-chloroform extraction.* . Anal. Biochem. , 1987(162): p. 156–159.
59. Chomczynski, P. and N. Sacchi, *The single-step method of RNA isolation by acid guanidinium thiocyanate-phenol-chloroform extraction: twenty-something years on.* Nat. Protocols, 2006. **1**(2): p. 581-585.
60. Dittrich, P.S., K. Tachikawa, and A. Manz, *Micro Total Analysis Systems. Latest Advancements and Trends.* Anal. Chem., 2006. **78**(12): p. 3887-3908.
61. Waters, L.C., et al., *Microchip Device for Cell Lysis, Multiplex PCR Amplification, and Electrophoretic Sizing.* Analytical Chemistry, 1998. **70**(1): p. 158-162.
62. Sia, S.K. and G.M. Whitesides, *Microfluidic devices fabricated in Poly(dimethylsiloxane) for biological studies.* ELECTROPHORESIS, 2003. **24**(21): p. 3563-3576.
63. Nagrath, S., et al., *Isolation of rare circulating tumour cells in cancer patients by microchip technology.* Nature, 2007. **450**(7173): p. 1235-1239.
64. Carlo, D.D., L.Y. Wu, and L.P. Lee, *Dynamic single cell culture array.* Lab on a Chip, 2006. **6**(11): p. 1445-1449.
65. Ryley, J. and O.M. Pereira-Smith, *Microfluidics device for single cell gene expression analysis in Saccharomyces cerevisiae.* Yeast, 2006. **23**(14-15): p. 1065-1073.
66. Valero, A., et al., *Apoptotic cell death dynamics of HL60 cells studied using a microfluidic cell trap device.* Lab on a Chip, 2005. **5**(1): p. 49-55.
67. Yang, M., C.-W. Li, and J. Yang, *Cell Docking and On-Chip Monitoring of Cellular Reactions with a Controlled Concentration Gradient on a Microfluidic Device.* Analytical Chemistry, 2002. **74**(16): p. 3991-4001.
68. Park, M.C., et al., *Pumpless, selective docking of yeast cells inside a microfluidic channel induced by receding meniscus.* Lab on a Chip, 2006. **6**(8): p. 988-994.
69. Khademhosseini, A., et al., *A Soft Lithographic Approach To Fabricate Patterned Microfluidic Channels.* Analytical Chemistry, 2004. **76**(13): p. 3675-3681.
70. Khademhosseini, A., et al., *Molded polyethylene glycol microstructures for capturing cells within microfluidic channels.* Lab on a Chip, 2004. **4**(5): p. 425-430.
71. Khademhosseini, A., et al., *Cell docking inside microwells within reversibly sealed microfluidic channels for fabricating multiphenotype cell arrays.* Lab on a Chip, 2005. **5**(12): p. 1380-1386.
72. Rettig, J.R. and A. Folch, *Large-Scale Single-Cell Trapping And Imaging Using Microwell Arrays.* Analytical Chemistry, 2005. **77**(17): p. 5628-5634.
73. Deutsch, M., et al., *A novel miniature cell retainer for correlative high-content analysis of individual untethered non-adherent cells.* Lab on a Chip, 2006. **6**(8): p. 995-1000.
74. Love, J.C., et al., *A microengraving method for rapid selection of single cells producing antigen-specific antibodies.* Nat Biotech, 2006. **24**(6): p. 703-707.
75. Chung, Y.-C., et al., *Microfluidic chip for high efficiency DNA extraction.* Lab on a Chip, 2004. **4**(2): p. 141-147.

76. Hong, J.W., et al., *Integration of gene amplification and capillary gel electrophoresis on a polydimethylsiloxane-glass hybrid microchip.* ELECTROPHORESIS, 2001. **22**(2): p. 328-333.
77. Li, C.-W., J. Yang, and M. Yang, *Dose-dependent cell-based assays in V-shaped microfluidic channels.* Lab on a Chip, 2006. **6**(7): p. 921-929.
78. Pihl, J., et al., *Microfluidic Gradient-Generating Device for Pharmacological Profiling.* Analytical Chemistry, 2005. **77**(13): p. 3897-3903.
79. Yamada, M. and M. Seki, *Microfluidic Particle Sorter Employing Flow Splitting and Recombining.* Analytical Chemistry, 2006. **78**(4): p. 1357-1362.
80. Wang, C., et al., *Rapid high-yield mRNA extraction for reverse-transcription PCR.* Journal of Biochemical and Biophysical Methods, 2007. **70**(3): p. 507-509.
81. Lee, P.J., et al., *Nanoliter scale microbioreactor array for quantitative cell biology.* Biotechnology and Bioengineering, 2006. **94**(1): p. 5-14.
82. Sugiura, S., et al., *Pressure-driven perfusion culture microchamber array for a parallel drug cytotoxicity assay.* Biotechnology and Bioengineering, 2008. **100**(6): p. 1156-1165.
83. Bruckner-Lea, C.J., et al., *Renewable microcolumns for automated DNA purification and flow-through amplification: from sediment samples through polymerase chain reaction.* Analytica Chimica Acta, 2002. **469**(1): p. 129-140.
84. Auroux, P.A., et al., *Miniaturised nucleic acid analysis.* Lab on a Chip, 2004. **4**(6): p. 534-546.
85. Roper, M.G., C.J. Easley, and J.P. Landers, *Advances in Polymerase Chain Reaction on Microfluidic Chips.* Analytical Chemistry, 2005. **77**(12): p. 3887-3894.
86. Zhang, C., et al., *PCR microfluidic devices for DNA amplification.* Biotechnology Advances, 2006(24): p. 243–284.
87. Zhang, C. and D. Xing, *Miniaturized PCR chips for nucleic acid amplification and analysis: latest advances and future trends.* Nucl. Acids Res., 2007. **35**(13): p. 4223-4237.
88. Wilding, P., M. Shoffner, and L. Kricka, *PCR in a silicon microstructure. .* Clin Chem, 1994(40): p. 1815–1818.
89. Giordano, B.C., et al., *Polymerase Chain Reaction in Polymeric Microchips: DNA Amplification in Less Than 240 Seconds.* Analytical Biochemistry, 2001. **291**(1): p. 124-132.
90. Lee, D.-S., et al., *Bulk-micromachined submicroliter-volume PCR chip with very rapid thermal response and low power consumption.* Lab on a Chip, 2004. **4**(4): p. 401-407.
91. Kopp, M.U., et al., *Chemical Amplification: Continuous-Flow PCR on a Chip.* Science, 1998. **280**(5366): p. 1046-1048.
92. Chiou, J., et al., *A Closed-Cycle Capillary Polymerase Chain Reaction Machine.* Analytical Chemistry, 2001. **73**(9): p. 2018-2021.
93. Liu, J., M. Enzelberger, and S. Quake, *A nanoliter rotary device for polymerase chain reaction.* ELECTROPHORESIS, 2002. **23**(10): p. 1531-1536.
94. Obeid, P.J. and T.K. Christopoulos, *Continuous-flow DNA and RNA amplification chip combined with laser-induced fluorescence detection.* Analytica Chimica Acta, 2003. **494**(1-2): p. 1-9.
95. Curcio, M. and J. Roeraade, *Continuous Segmented-Flow Polymerase Chain Reaction for High-Throughput Miniaturized DNA Amplification.* Analytical Chemistry, 2003. **75**(1): p. 1-7.
96. Park, N., S. Kim, and J.H. Hahn, *Cylindrical Compact Thermal-Cycling Device for Continuous-Flow Polymerase Chain Reaction.* Analytical Chemistry, 2003. **75**(21): p. 6029-6033.
97. Dorfman, K.D., et al., *Contamination-Free Continuous Flow Microfluidic Polymerase Chain Reaction for Quantitative and Clinical Applications.* Analytical Chemistry, 2005. **77**(11): p. 3700-3704.
98. Chabert, M., et al., *Automated Microdroplet Platform for Sample Manipulation and Polymerase Chain Reaction.* Analytical Chemistry, 2006. **78**(22): p. 7722-7728.
99. Krishnan, M., V.M. Ugaz, and M.A. Burns, *PCR in a Rayleigh-Benard Convection Cell.* Science, 2002. **298**(5594): p. 793-.
100. Krishnan, M., et al., *Reactions and Fluidics in Miniaturized Natural Convection Systems.* Analytical Chemistry, 2004. **76**(21): p. 6254-6265.
101. Braun, D., N.L. Goddard, and A. Libchaber, *Exponential DNA Replication by Laminar Convection.* Physical Review Letters, 2003. **91**(15): p. 158103.

102. Chen, Z., et al., *Thermosiphon-Based PCR Reactor: Experiment and Modeling.* Analytical Chemistry, 2004. **76**(13): p. 3707-3715.
103. Wheeler, E.K., et al., *Convectively Driven Polymerase Chain Reaction Thermal Cycler.* Analytical Chemistry, 2004. **76**(14): p. 4011-4016.
104. Hennig, M. and D. Braun, *Convective polymerase chain reaction around micro immersion heater.* Applied Physics Letters, 2005. **87**(18): p. 183901-3.
105. Agrawal, N. and V.M. Ugaz, *A Buoyancy-Driven Compact Thermocycler for Rapid PCR.* Clinics in Laboratory Medicine, 2007. **27**(1): p. 215-223.
106. Nitin Agrawal, Yassin A.H.Victor M.U., *A Pocket-Sized Convective PCR Thermocycler13.* Angewandte Chemie International Edition, 2007. **46**(23): p. 4316-4319.
107. Gulliksen, A., et al., *Real-Time Nucleic Acid Sequence-Based Amplification in Nanoliter Volumes.* Anal. Chem., 2004. **76**(1): p. 9-14.
108. Gulliksen, A., et al., *Parallel nanoliter detection of cancer markers using polymer microchips.* Lab on a Chip, 2005. **5**(4): p. 416-420.
109. Yobas, L., et al., *Microfluidic chips for viral RNA extraction & detection.* 2005 IEEE Sensors, Vols 1 and 2, 2005: p. 49-52.
110. Furuberg, L., et al., *RNA amplification chip with parallel microchannels and droplet positioning using capillary valves.* Microsystem Technologies, 2008. **14**(4): p. 673-681.
111. Melin, J., et al., *Ligation-based molecular tools for lab-on-a-chip devices.* New Biotechnology, 2008. **25**(1): p. 42-48.
112. Fredriksson, S., et al., *Protein detection using proximity-dependent DNA ligation assays.* Nat Biotech, 2002. **20**(5): p. 473-477.
113. Liu, D., et al., *Rolling Circle DNA Synthesis: Small Circular Oligonucleotides as Efficient Templates for DNA Polymerases.* Journal of the American Chemical Society, 1996. **118**(7): p. 1587-1594.
114. Lizardi, P.M., et al., *Mutation detection and single-molecule counting using isothermal rolling-circle amplification.* Nat Genet, 1998. **19**(3): p. 225-232.
115. Melin, J., et al., *Homogeneous amplified single-molecule detection: Characterization of key parameters.* Analytical Biochemistry, 2007. **368**(2): p. 230-238.
116. Jarvius, J., et al., *Digital quantification using amplified single-molecule detection.* Nat Meth, 2006. **3**(9): p. 725-727.
117. Hutchison, C.A., et al., *Cell-free cloning using Ï†29 DNA polymerase.* Proceedings of the National Academy of Sciences of the United States of America, 2005. **102**(48): p. 17332-17336.
118. Kralj, J.G., et al., *T7-based linear amplification of low concentration mRNA samples using beads and microfluidics for global gene expression measurements.* Lab on a Chip, 2009. **9**(7): p. 917-924.
119. Van Gelder, R.N., et al., *Amplified RNA synthesized from limited quantities of heterogeneous cDNA.* Proceedings of the National Academy of Sciences of the United States of America, 1990. **87**(5): p. 1663-1667.
120. Woolley, A.T., et al., *Functional Integration of PCR Amplification and Capillary Electrophoresis in a Microfabricated DNA Analysis Device.* Analytical Chemistry, 1996. **68**(23): p. 4081-4086.
121. Liu, R.H., et al., *Self-Contained, Fully Integrated Biochip for Sample Preparation, Polymerase Chain Reaction Amplification, and DNA Microarray Detection.* Analytical Chemistry, 2004. **76**(7): p. 1824-1831.
122. Easley, C.J., et al., *A fully integrated microfluidic genetic analysis system with sample-in-answer-out capability.* Proceedings of the National Academy of Sciences, 2006. **103**(51): p. 19272-19277.
123. Liu, Y., et al., *DNA Amplification and Hybridization Assays in Integrated Plastic Monolithic Devices.* Analytical Chemistry, 2002. **74**(13): p. 3063-3070.
124. Cady, N.C., et al., *Real-time PCR detection of Listeria monocytogenes using an integrated microfluidics platform.* Sensors and Actuators B: Chemical, 2005. **107**(1): p. 332-341.
125. Lee, T.M.-H., M.C. Carles, and I.M. Hsing, *Microfabricated PCR-electrochemical device for simultaneous DNA amplification and detection.* Lab on a Chip, 2003. **3**(2): p. 100-105.
126. Wang, J., et al., *A disposable microfluidic cassette for DNA amplification and detection.* Lab on a Chip, 2006. **6**(1): p. 46-53.

127. Wilding, P., et al., *Integrated Cell Isolation and Polymerase Chain Reaction Analysis Using Silicon Microfilter Chambers.* Analytical Biochemistry, 1998. **257**(2): p. 95-100.
128. Yuen, P.K., et al., *Microchip Module for Blood Sample Preparation and Nucleic Acid Amplification Reactions.* Genome Research, 2001. **11**(3): p. 405-412.
129. Lee, J.-G., et al., *Microchip-based one step DNA extraction and real-time PCR in one chamber for rapid pathogen identification.* Lab on a Chip, 2006. **6**(7): p. 886-895.
130. Christel, L.A., et al., *Rapid, Automated Nucleic Acid Probe Assays Using Silicon Microstructures for Nucleic Acid Concentration.* Journal of Biomechanical Engineering, 1999. **121**(1): p. 22-27.
131. Chen, L., A. Manz, and P.J.R. Day, *Total nucleic acid analysis integrated on microfluidic devices.* Lab on a Chip, 2007. **7**(11): p. 1413-1423.
132. Beer, N.R., et al., *On-Chip, Real-Time, Single-Copy Polymerase Chain Reaction in Picoliter Droplets.* Analytical Chemistry, 2007. **79**(22): p. 8471-8475.
133. Nagai, H., et al., *Development of A Microchamber Array for Picoliter PCR.* Analytical Chemistry, 2001. **73**(5): p. 1043-1047.
134. Liu, J., C. Hansen, and S.R. Quake, *Solving the "world-to-chip" interface problem with a microfluidic matrix.* Analytical Chemistry, 2003. **75**(18): p. 4718-4723.
135. Hashimoto, M., et al., *Rapid PCR in a continuous flow device.* Lab on a Chip, 2004. **4**(6): p. 638-645.
136. Obeid, P.J., et al., *Microfabricated Device for DNA and RNA Amplification by Continuous-Flow Polymerase Chain Reaction and Reverse Transcription-Polymerase Chain Reaction with Cycle Number Selection.* Analytical Chemistry, 2003. **75**(2): p. 288-295.
137. Kiss, M.M., et al., *High-Throughput Quantitative Polymerase Chain Reaction in Picoliter Droplets.* Analytical Chemistry, 2008. **80**(23): p. 8975-8981.

Chapter 2: Theory

This chapter outlines the principal theoretical models and calculations related to the novel microfluidic technologies and techniques proposed in this thesis. First, the behaviour of flow in microfluidic devices is briefly discussed. This is based on the Navier-Stokes model in the region of laminar flow and low Reynolds numbers (Re<10). Second, the convection-diffusion equation is presented as a dynamic model for species mixing in a flow field. Third, a basic cell sedimentation model is described for the calculation of the cell trajectories and capture efficiencies. Finally, a hydrostatic pressure model is presented as a means for generating flow within microfluidic devices.

2.1 Navier-Stokes model

As opposed to Lagrangian Modelling where dynamics is expressed in terms of a set of point vectors $\{\mathbf{r}_i\}$ that describe the position in time of every particle in the system Eulerian Modelling statistically summarizes the molecular level details in statistical quantities like temperature and pressure as function in space and time. This means that mechanical quantities such as mass m_i, velocity $\mathbf{v}_i$ and force $\mathbf{F}_i$ become a mass distribution $m(\mathbf{r})$, a velocity field $\mathbf{v}(\mathbf{r})$ and force field $\mathbf{F}(\mathbf{r})$. This greatly simplifies fluid analysis where modelling problems generally have to analyze the dynamics of more than 10^{23} particles (1 mole).

The Navier–Stokes equations for modelling fluid flow, in their general form are the expression of Newton's second law (the conservation of momentum) in a continuum form and written for an arbitrary control volume. This yields;

$$\rho \frac{D\mathbf{v}}{Dt} = \nabla \cdot \mathbf{S} - \nabla p + \mathbf{F} \qquad (2.1)$$

using the material derivative and $\mathbf{v}$ to represent flow velocity field the left side of the equation describes acceleration multiplied by ρ the fluid density, while the right side of

the equation describes the summation of body forces $\mathbf{F}$ (such as gravity) and divergence (∇ the del operator) of stress (p pressure and $\mathbf{S}$ is the stress tensor). If the material derivative is extended the Navier-Stokes equations assume the form:

$$\rho\left(\frac{\partial \mathbf{v}}{\partial t} + \mathbf{v}\cdot\nabla\mathbf{v}\right) = \nabla\cdot\mathbf{S} - \nabla p + \mathbf{F} \qquad (2.2)$$

2.1.1 Incompressible flow of Newtonian fluids

If the fluid is assumed incompressible $\rho(\mathbf{r}, t) = const.$ then mass continuity can be expressed as:

$$\nabla\cdot\mathbf{v} = \mathbf{0} \qquad (2.3)$$

Using these relations the Navier-Stokes equations can be rewritten as:

$$\rho\left(\frac{\partial \mathbf{v}}{\partial t} + \mathbf{v}\cdot\nabla\mathbf{v}\right) = \eta\nabla\mathbf{v} - \nabla p + \mathbf{F} \qquad (2.4)$$

The assumption of incompressibility means that effects such as shock or sound waves are disregarded from the model and are assumed to be non-important. Even though incompressibility is assumed the equations can be applied to liquids with small compressibilities (less than 10^{-9} Pa^{-1}) without significant error.

2.2 Laminar Flow Simplification

In the case of laminar flow the (2.4) can be further simplified. The key factors are that inertial effects are not present during laminar flow and the body forces such as gravity or centrifugal can also be neglected. Simplifying the convective (inertial) term $(\mathbf{v}\cdot\nabla)\mathbf{v} = \mathbf{0}$ and the body force term $\mathbf{F}$ from (2.4) the so called Stokes equation is obtained:

$$\rho \frac{\partial \mathbf{v}}{\partial t} = \eta \nabla^2 \mathbf{v} - \nabla p \qquad (2.5)$$

The key feature of this equation are that velocity field $\mathbf{v}$ is always linear and it expresses that the pressure force $-\nabla p$ is completely spent on overcoming the viscous losses expressed by the term $\eta \nabla^2 \mathbf{v}$. One way of further characterizing the type of flow is the so called Raynolds number.

2.2.1 Reynolds Number

Conceptually the Reynolds number (Re) is a dimensionless indicator that summarizes the dynamics of the Navier-Stokes momentum equation (2.4). The emergence of this indicator is apparent if the equation (2.4) is made independent of physical dimensions. This is done by applying the following substitutions to eq 2.4:

$$x \to \frac{x}{\bar{l}}, t \to \frac{\bar{\mathrm{v}} t}{\bar{l}}, \mathbf{v} \to \frac{\mathbf{v}}{\bar{\mathrm{v}}}, p \to \frac{p - \bar{p}}{\rho \bar{\mathrm{v}}^2} \qquad (2.6)$$

this results in:

$$\frac{\partial \mathbf{v}}{\partial t} + \mathbf{v} \cdot \nabla \mathbf{v} = \frac{\eta}{\rho \bar{\mathrm{v}} l} \nabla^2 \mathbf{v} - \nabla p + \frac{\bar{l}}{\bar{\mathrm{v}}^2} \mathbf{F} \qquad (2.7)$$

In the cases where the bodily forces such as gravity or centrifugal are not relevant then the $\mathbf{F}$ term can be discarded and simplified it to:

$$\frac{\partial \mathbf{v}}{\partial t} + \mathbf{v} \cdot \nabla \mathbf{v} = \frac{\eta}{\rho \bar{\mathrm{v}} l} \nabla^2 \mathbf{v} - \nabla p \qquad (2.8)$$

From 2.8 it can be seen that the dimensionless term $\frac{\eta}{\rho \bar{\mathrm{v}} l}$ completely characterise the dynamics of the equation. This is why the Reynolds number is defined as:

$$\frac{\eta}{\rho \bar{\mathrm{v}} l} = \frac{1}{\mathrm{Re}} \quad \Rightarrow \quad \mathrm{Re} = \frac{\rho \bar{\mathrm{v}} l}{\eta} = \frac{\text{inertial forces}}{\text{viscous forces}} \qquad (2.9)$$

Based on this concept the Reynolds number can be defined for a number of different situations and the definition should generally include the density and viscosity properties of the fluid, its characteristic velocity and a characteristic dimension or length of the boundary conditions. The term characteristic refers to a velocity and a length that is representative of the inertial forces in the system such as the dynamic pressure and the viscous forces due to the viscous stress. General definitions of characteristic dimensions include for example the diameter for spheres, circles or pipes. For non-spherical shapes an equivalent diameter is usually defined as a ratio between the cross sectional area and the perimeter.

2.2.2 Reynolds Number Values

Values of the Re are commonly between 0.001 and 100,000 [1]. It is generally cited that systems where the Re number is above 2300 [1] the flow is a fully developed and turbulent while Re numbers below this transition threshold are completely laminar. Generally microfluidic channels with cross sectional areas of 100μm x 100μm and lengths in the order centimetres supporting flow rates of micro-litres per minute have Re numbers in the range of 10 or less. This is much lower then the transition threshold of 2300. These low Reynolds number flows guarantee that for example in straight channel, every fluid particle moves with uniform velocity along straight streamlines or laminas.

2.2.3 Numerical Solution

Only few analytical solutions exist for the Navier-Stokes equations, the two main ones are the Hagen-Poiseuille flow [2] through a circular cross sectioned tube and Couette fluid [2] flow between two infinite parallel flat plates driven by the motion of one or more of the plates. However in most particle problems these simplified solutions are not sufficient to analyze and describe fluid dynamics in complex geometries, multi-phase fluid interactions, fixed or flexible solid boundary structures and interactions with

electrical, thermal, acoustic or optical phenomenon. To address these issues computational fluid dynamics (CFD) can be used to numerically solve these highly coupled and complex multi-physics problems [3].

2.3 Convection Diffusion

Another critical aspect of any microfluidic device is the phenomenon of chemical and biochemical species transport within the microfluidic system. Species transport can be modelled based two phenomenon convection and diffusion. The relation between these phenomenon and the fluid velocity field $\mathbf{v}$ and the concentration profile is given by the convection–diffusion equation:

$$\frac{\partial c}{\partial t} = -\nabla \cdot (\mathbf{v}c) + \nabla \cdot (D\nabla c) \tag{2.10}$$

This equation is composed of two terms. The first term is the convective term that expresses the effect of the inhomogeneous flow field on the concentration profile represented by the scalar field c. More precisely the advection term $\nabla \cdot \mathbf{v}$ is the calculation of the transport of a scalar (c) by vector field ($\mathbf{v}$). The second term of (2.10) models the diffusive transport due to the formation of a concentration gradient $\nabla \mathrm{c}$ as stated in Fick's law [4]. The convection-diffusion equation can also be viewed as an extension of the continuity equation (2.3) such that the principal of the conservation of mass is satisfied in conjunction with diffusive and advective transport.

2.3.1 Indicator for Mass Transport the Péclet Number

The Péclet number (Pe) is defined as the quotient between advective and diffusive mass transport.

$$\mathrm{Pe} = \frac{vl}{D} = \frac{\text{advective mass transport}}{\text{diffusive mass transport}} \tag{2.11}$$

where l represents the characteristic length, v the fluid velocity and D the diffusion coefficient. For diffusion coefficients ranging from 10^{-5} m^2s^{-1} to 10^{-11} m^2s^{-1} the Péclet number in a typical microfluidic device is usually 100 < Pe < 100,000 [5] which means that a advective transport of species dominates within microfluidic systems. That is why there has been a great effort in the community to develop strategies for purposefully enhancing species mixing within microfluidic systems.

2.4 Cell flow and sedimentation model

In order to model cell flow and sedimentation within fluid velocity field we have to account for the forces that are exerted onto a particle suspended within a fluid. These forces a depicted within Figure 2.1. The forces are the buoyancy-corrected gravitational sedimentation force $\mathrm{F_{gb}}$ and the fluid drag force $\mathrm{F_d}$.

$$\mathbf{F_{gb}} = \Delta m_p g \tag{2.12}$$

where Δm_p represents the difference in the masses of the particle and the displaced fluid volume. Thus particle trajectories can be calculated by solving the force balance equation for any given particle:

$$m_p \frac{d^2\mathbf{r}}{dt^2} = \mathbf{F_d}(t, \mathbf{r}, \frac{d\mathbf{r}}{dt}) + \mathbf{F_{gb}} \tag{2:13}$$

The fluid drag force $\mathrm{F_d} \propto \mathrm{v}$ is modelled by the Khan and Richardson force [6] which is an empirical estimation of the fluid drag force on spherical particles with radius that is valid for a wide range of Reynolds numbers, (including Re<1).

$$\left|\mathbf{F_d}\right| = \pi r_p{}^2 \rho(\mathbf{v} - \mathbf{v_p})^2 (1.84(\mathrm{Re}_p)^{-0.31} + 0.293\mathrm{Re}_p^{0.06})^{3.45}$$

.

$$\mathrm{Re}_p = \frac{(\left|\mathbf{v} - \mathbf{v_p}\right| 2 r_p \rho)}{\eta} \qquad (2.14)$$

Where the suspended spherical particle has a mass m_p and a radius r_p immersed in a fluid with a density ρ, dynamic viscosity η and velocity field $\mathbf{v}$.

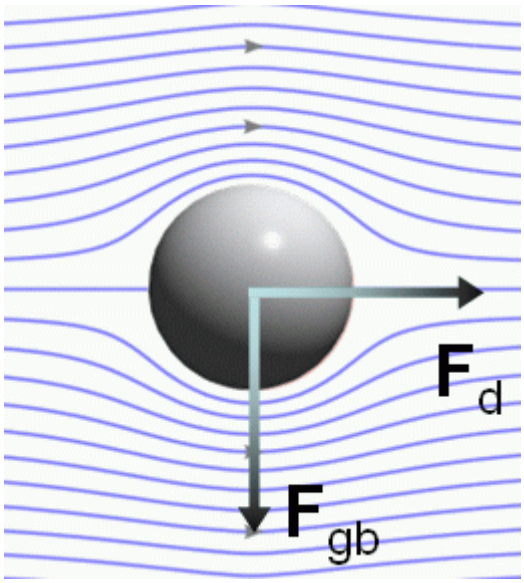

Figure 2.1. Particle suspended in a liquid volume under the impact of a gravity field and a fluid flow field. The motion of the particle follows the buoyancy corrected gravitation force $\mathbf{F}_{gb}$ which accounts for the mass difference Δm between the particle and the displaced liquid volume in combination with the fluid drag force $\mathbf{F}_d$.

2.5 Hydrostatic pressure model

This type of pressure arises from to the weight of a fluid column and can be described through the Bernoulli equation. The Bernoulli equation can be directly derived from the Navier-Stokes model by applying the following restrictions:

1. The fluid is assumed incompressible: $\rho(r,t) = const.$ (2.15)

2. The velocity field can be described as the gradient of a velocity field potential:

$$\mathbf{v} = -\nabla U \Rightarrow \nabla \times \mathbf{v} = 0 \tag{2.16}$$

3. The flow is assumed to be inviscid, that is to say the fluid has zero viscosity:

$$\eta = 0 \tag{2.17}$$

4. The body forces must be conservative and thus be generated from the field potential:

$$\mathbf{F} = -\nabla \Phi \tag{2.18}$$

If these restrictions are applied to eq.(2.4) and Φ is considered to be the gravitational potential we obtain the following:

$$0 = \frac{\partial}{\partial t}(-\nabla U) + \nabla U \cdot \nabla \nabla U + \nabla \Phi + \frac{1}{\rho}\nabla p \tag{2.19}$$

$$0 = \nabla\left[-\frac{\partial U}{\partial t} + \frac{\mathbf{v}^2}{2} + \Phi + \frac{p}{\rho}\right] \tag{2.20}$$

$$\frac{1}{2}\rho \mathrm{v}^2 + \rho g h + p = const. \tag{2.21}$$

Using Bernoulli's equation to model a microfluidic device coupled to a macro scale column of fluid as shown in Figure 2.2. The dynamic pressure component of the Bernoulli equation can be disregarded since the flow rates generated within the reservoir outlet (Figure 2.2 radius b) is 2 orders of magnitude smaller than the flow rate through the device making the dynamic pressure term 4 orders of magnitude smaller than the reservoir hydrostatic pressure. This means that the pressure generated at the inlet of the microfluidic device is mostly hydrostatic pressure directly proportional to the fluid column height.

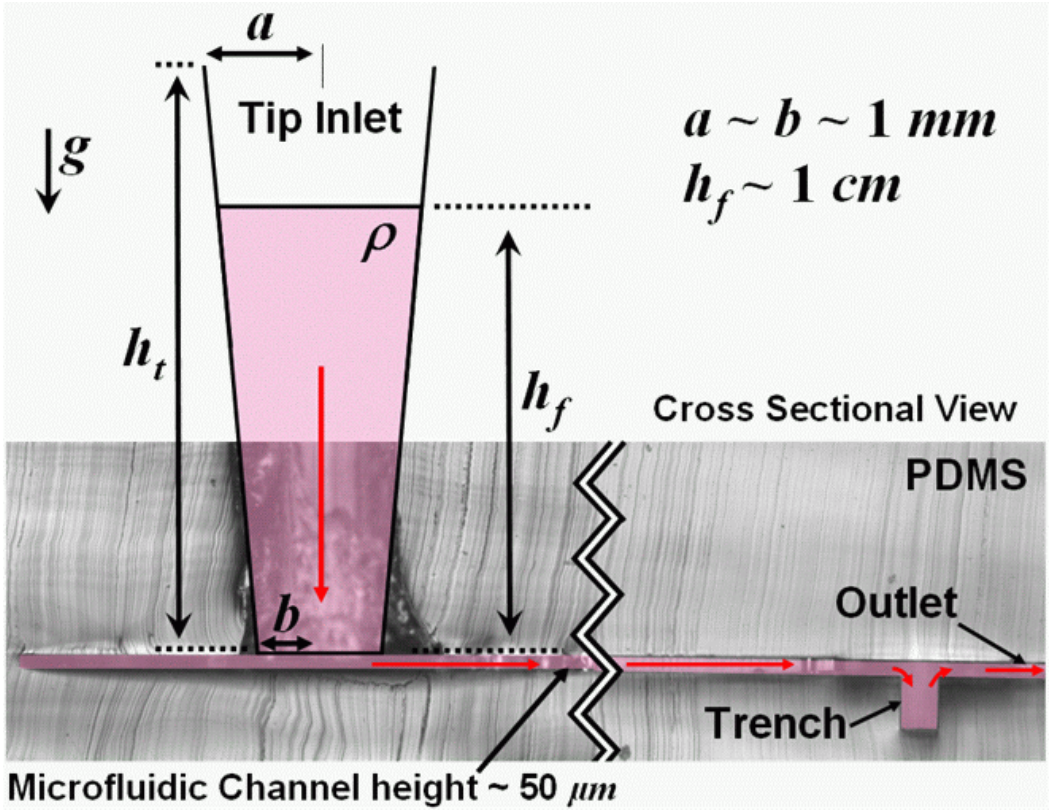

Figure 2.2. Microfluidic device coupled to a macro scale column of fluid with a density ρ. The maximum fluid column height is given by the container (eg. 1 *mL* Eppendorf pipette tip) height h_t. while the column width can be represented by the container inlet and outlet inner radius a, b respectively. h_t represents the fluid column height at any given point in time. The orders of magnitude of the variable dimensions are represented as well as the direction of the gravitational acceleration.

Furthermore the flow through the microfluidic system coupled to hydrostatic fluid column can be modelled as Puisille flow resulting in a linear relationship between the pressure gradient and the flow velocity through the microfluidic system. This linear relation is described by the hydraulic resistance of the device.

$$\Delta P = R_h \cdot Q \tag{2.22}$$

In case of a conical fluid column as shown in Figure 2.2 the column height as function of time can be estimated by applying the following differential model that relates the height variation with time:

$$\frac{dV}{dt} = -Q \tag{2.23}$$

$$\frac{dh_f}{dt} = \frac{3h_t \rho g h_f}{R_h \pi (a-b) h_f + 3R_h \pi b (a-b) h_c} \tag{2.24}$$

2.6 Summary

In this chapter, models for microfluidic operation were introduced: The Navier-Stokes equation and its simplification for microfluidic systems, which is directly applicable to microfluidic cell handling, the convection and diffusion model for species transport and distribution which is directly applicable to cell based assays and enzymatic reactions within microfluidic systems, the cell sedimentation model which is the key to microfluidic cell capture and finally a hydrostatic pressure model which is directly applicable to gravity drive flow within a microfluidic system.

2.7 References

1. Gravesen, P., J. Branebjerg, and O.S. Jensen, *Microfluidics-a review.* Journal of Micromechanics and Microengineering, 1993(4): p. 168.
2. Bruus, H., *Theoretical microfluidics*. illustarted ed. Vol. 18. 2008: Oxford University Press US. 346.
3. Peyret, R., *Handbook of computational fluid mechanics*. Illustrated reprint ed. 2000: Academic Press. 467.
4. Tabeling, P., *Introduction to microfluidics*. 2005: Oxford University Press. 301.
5. Nguyen, N.-T., *Micromixers: fundamentals, design and fabrication*. 2008: William Andrew.
6. Coulson, J.M. and J.F. Richardson, *Particle Technology and Separation Processes*. 5 ed. Vol. 2. 1991, Oxford: Pergamon

Chapter 3: Experimental Details

This chapter presents all the experimental details associated with the results shown in the following chapters. The chapter is divided into three main sections; each section focuses on one of the principal micro-device designs. The three designs are the RNA Extraction & Real Time NASBA device, the iNASBA array device and the iCell array device. Each section shows the device design, device operation, all the fabrication procedures required for implementation and the materials and methods associated with the characterization of the device.

3.1 RNA Extraction & Real Time NASBA device

In this sub section, a monolithic integration of a microfluidic sample-to-answer tmRNA analysis system that includes RNA capture and purification, NASBA, and real time detection is presented. A novel clog-free bead immobilisation method is used to construct the RNA capture and purification module. The device design also allows for future integration of cell lysis and automated fluid-control functions.

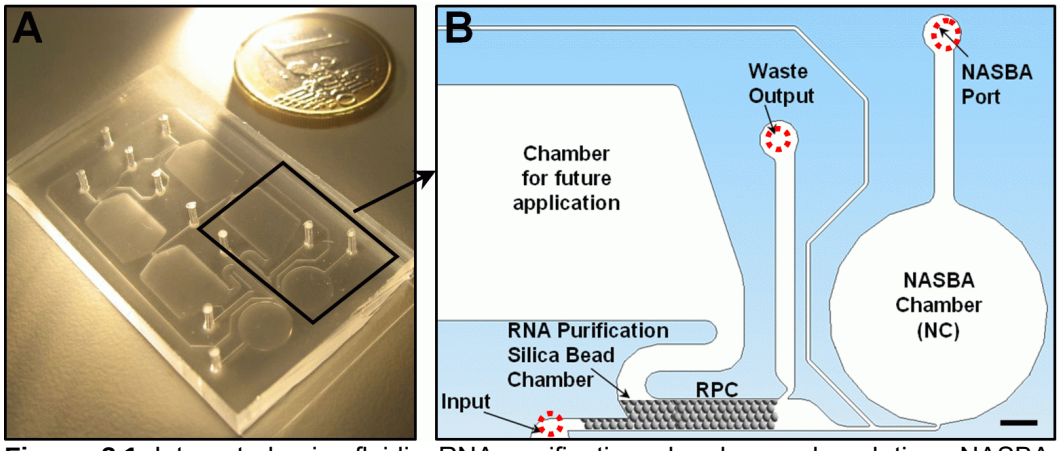

Figure 3.1 Integrated microfluidic RNA purification chamber and real time NASBA device. (**A**) Photograph of the device. The microfluidic architecture is mirrored to allow for 2 separate reactions with the same reagents, but different samples, to incorporate controls. (**B**) Single device architecture showing the distinct functional microfluidic modules: RNA purification chamber (RPC) and real time NASBA chamber. The remaining channels and chambers have been included for future integration of on-chip lysis. All channels and chambers are 80 μm high. Scale bar is 1 mm. Reproduced from REF [1].

3.1.1 Device Design

The integrated microfluidic NASBA chip, Figure 3.1 (for detailed design schematic please see the attached file: "RNA Extraction & Real Time NASBA device.dwg"), is based on microchannels and microchambers, with distinct functional domains: a silica bead-bed RNA purification chamber (RPC, volume 0.25 μL), and a NASBA chamber (NC, volume 2 μL). The remaining channels and chambers have been implemented for the future integration of on-chip chemical lysis. The height of the microchannels and microchambers, 80 μm, was selected because it is easily achievable with SU-8 2100 photoresist. The RNA purification chamber enables capture of RNA present in the sample by selective adsorption in silica, followed by removal of the remaining crude cell lysate, which includes NASBA inhibitors, by washing.

Detection of amplified tmRNA target from NASBA occurs in real time via molecular beacons whose fluorescence is unquenched when hybridised to complementary RNA amplicons. The device is characterized using a fluorescence microscope to measure the change in fluorescence from the NASBA chamber as a function of time. The device is mirrored (Figure 3.1A) to allow for 2 separate reactions with the same reagents but different samples, nominally to implement control reactions. The relatively large number of inlets (7) and outlets (4) is a consequence of this device being designed as a subcomponent of a larger system that is being developed, where a number of the fluidic I/O connections will be replaced with microchannel connections to other components and/or on-chip reagent or waste reservoirs.

3.1.2 Device Microfabrication

PDMS is widely utilized for microfluidic devices due to the ease of fabricating relatively complex structures [2], its general biocompatibility, and the ease of attaching (sealing) it to glass, silicon wafers, or a second PDMS structure. Microfluidic channels were fabricated using standard soft lithography replica moulding techniques [3]. A mould was

created through a single-layer process using negative photoresist, SU8-2100 (Microchem, U.S.A.), which was spun onto a clean silicon wafer using a spinner (P6700 Specialty Coating Systems, Inc., U.S.A.). The resist (5 mL) was spread onto the wafer at 500 rpm for 10 s, and the rotation rate was then ramped at an acceleration of 300 rpm/s to 2,500 rpm, at which rate the sample was spun for 30 s to form an 80 μm layer. The wafer was then soft baked at 65 ºC for 5 min and 95 ºC for 30 min, then UV-exposed for 10 s at 9.5 mW/cm^2 using a Karl-Süss KSM MJB-55W mask aligner. The wafer was post-exposure baked for 5 min at 65 ºC and 12 min at 95 ºC, allowed to cool to room temperature, developed in Microposit EC Solvent (Chestech Ltd., UK) developer for 4 min, and finally blown dry with nitrogen. PDMS (Sylgard 184, Dow Corning) was prepared according to the instructions of the manufacturer, degassed in a vacuum chamber for 30 min, then poured on the SU8 mould and cured in a 60 ºC oven for 10 h. The PDMS was then carefully peeled off the mould. Fluid inlets and outlets were punched with a 1 mm outer diameter flat-tip needle for tube connections. Both a 25 x 50 x 0.4 mm glass cover slide (VWR International Inc., U.S.A.) and the PDMS structures were treated with UV ozone (PSD-UV, Novascan Technologies, Inc., Iowa, U.S.A.) for 10 min before bonding for 10 h at 90 ºC.

3.1.3 Silica Bead Loading and Immobilization

Beads for RNA purification were immobilized within the RPC by loading 3 μL of a 68% (bead: deionised H_2O volume) solution of 10-µm plain silica beads (PSi-10.0, G. Kisker Gbr., Germany) into the input port (IP) (Figure 3.2 A), with all other ports on the chip sealed except for the waste output (WO). The bead solution was left to dry at room temperature for 3 hr, which packs the beads into the extraction chamber. After the beads dried in place, they were immobilised via bonding to the PDMS walls of the extraction chamber using UV ozone treatment: the chip was treated with ozone for 10 min to activate the PDMS, then left to bond overnight at room temperature (Figure 3.2 B). Finally, a bead-washing step with deionised H_2O (dH_2O) was performed (Figure 3.2 C) to remove unbound beads and leave a layer of silica beads bonded to the walls of the RPC. To simplify device fabrication and the on-chip operation, beads for RNA

purification were immobilised within the RNA purification chamber (RPC). Beads can be positioned precisely into the RPC by loading a limited volume of 3 µL of a 68% (bead: deionised H_2O volume) solution of 10-µm plain silica beads (PSi-10.0, G. Kisker Gbr., Germany) into the input port (IP), with all other ports on the chip sealed except for the waste output (WO). This dense solution of beads is left to dry at room temperature for 3 hr. This packs the dry silica beads into the extraction chamber.

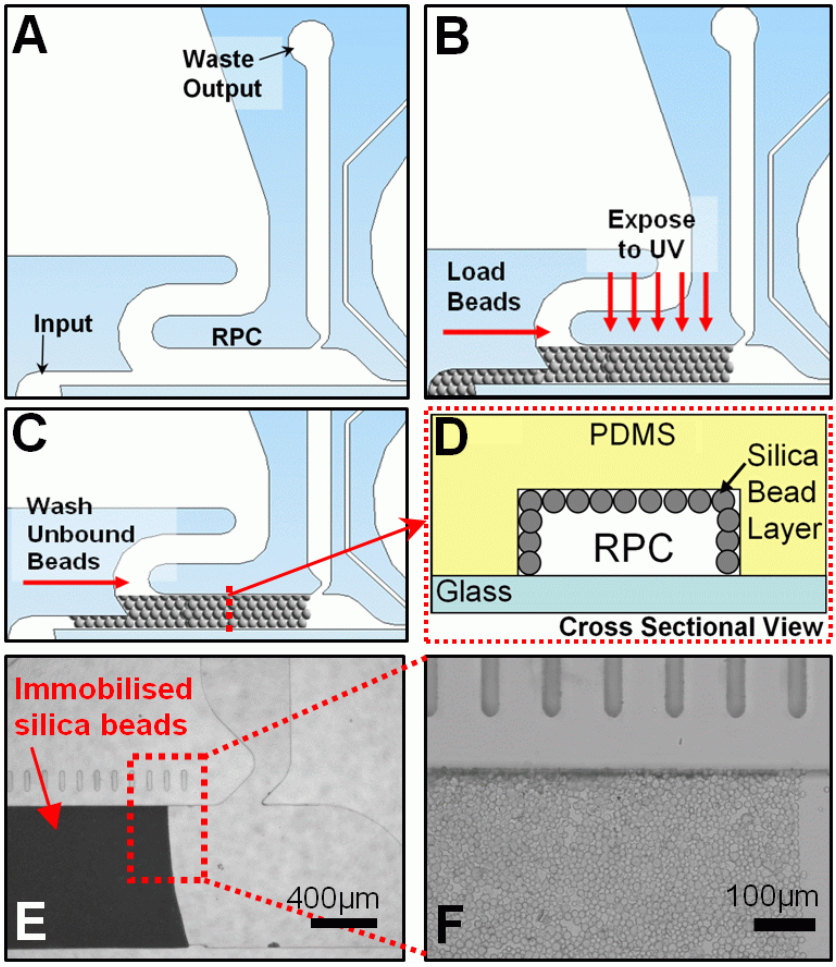

Figure 3.2 Method for silica bead immobilisation on PDMS surface. (A) Before loading the beads, all ports are sealed except for the *Input* and *Waste Output*. (B) 3 *µ*L of plain silica bead solution flows into the input, left to dry, and exposed to UV-ozone for bonding. (C) Unbound beads are washed away with dH_2O, leaving a (D) layer of silica beads bonded to the walls of the RPC (see Supporting Information). (E-F) Bright-field micrographs of the immobilised 10 *µ*m silica beads on the PDMS walls of the RNA purification chamber. Reproduced from REF [1].

After the beads dried in place, similar to conventional PDMS glass bonding, the silica beads are immobilised via bonding to the PDMS walls of the extraction chamber by

using UV ozone treatment. The chip with the packed dried silica beads was treated with ozone for 10 min to activate the PDMS, then left to bond overnight at room temperature. Finally, a bead-washing step with deionised H_2O (dH_2O) is performed to remove unbound beads and leave a layer of silica beads bonded to the PDMS walls of the RPC.

To demonstrate that the beads were immobilized on the surface of the PDMS within the RPC chamber a new PDMS-PDMS chip was fabricated instead of the reported PDMS-glass. The immobilization strategy followed was exactly the same except that 10 µm green-fluorescent silica beads were used. The microfluidic chip was then cut across the RPC chamber to generate a cross-sectional view of the bonded bead and imaged with a fluorescent microscope, as shown in Figure 3.2.1

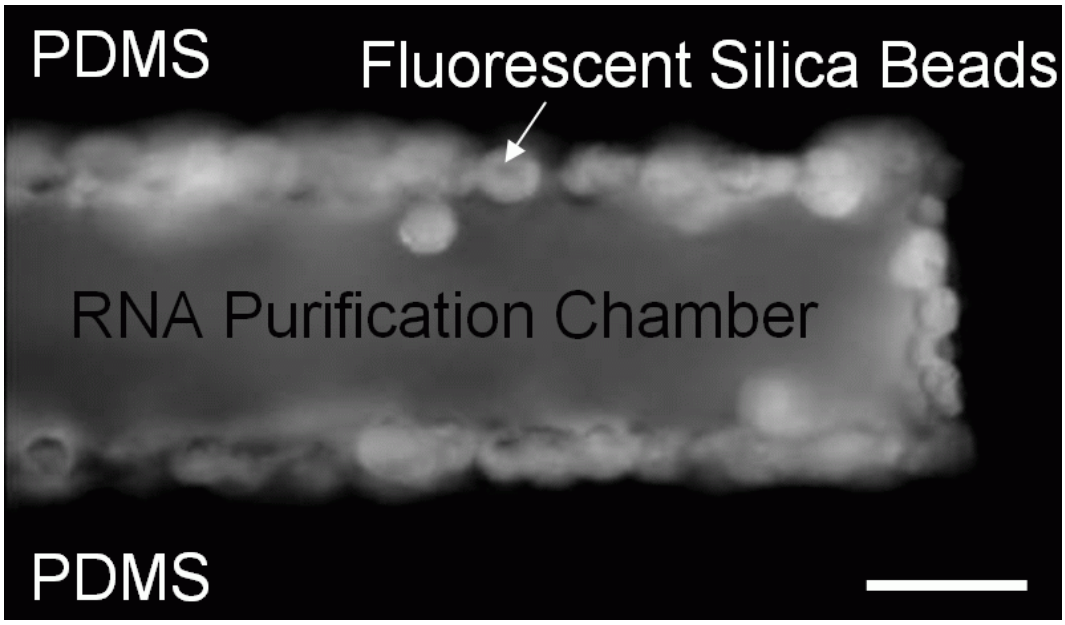

Figure 3.2.1 Fluorescent image of a cross section of the RPC chamber showing a layer of immobilized green fluorescent silica beads on the PDMS walls. Please note that in this case the entire device is made of PDMS, for ease of cutting the bottom glass cover was replaced with a flat PDMS layer. Scale bar 30 *µ*m. Reproduced from REF [1].

3.1.4 E.Coli Culture and Lysis

The *E. coli* strain XL-1 blue was cultured overnight at 37 °C with 250 rpm shaking (Gallenkamp orbital shaker, AGB Scientific Ltd., Ireland) in LB medium (Lysogeny broth,

also known as Luria broth) containing Tryptone (10 g/L, Lab M Ltd., UK), yeast extract (5 g/L, Lab M Ltd., UK) and NaCl (10 g/L, Sigma-Aldrich Ireland Ltd., Ireland) made in-house and autoclaved at 121 °C for 20 min. The cell density was measured as optical density at 600 nm (OD_{600}) on a spectrophotometer (UV-160A, Shimadzu). The number of cells per mL was calculated from a standard curve based on plate counts.

Cell lysis was performed off chip using MicroLYSIS PLUS buffer (Microzone Ltd., UK) according to the manufacturer's recommendations. An overnight culture of *E. coli* (OD_{600} of 1.36) with a cell density of 3.4×10^8 colony forming units (CFU)/mL (based on plate counts) was centrifuged at 10,000 rpm for 5 min, producing a pellet volume of 5 μL, and mixed with 40 μL of lysis buffer. Temperature cycling was then performed between 65 °C and 96 °C for a total of 23.5 min (65 °C for 15 min, 96 °C for 2 min, 65 °C for 4 min, 96 °C for 1 min, 65 °C for 1 min, 96 °C for 30 s) by transferring tubes between two heating blocks. This crude cell lysate was either used directly for nucleic acid amplification or for RNA purification. For experiments where pure RNA was required for off-chip controls, a commercial RNA purification kit (RNeasy Mini Kit, Qiagen, U.K.) was used according to the manufacturer's recommendations. Cell lysate samples were stored at -15 °C until required.

3.1.5 On-Chip RNA Purification

The on-chip RNA purification protocol was adapted from previously reported techniques; [4-6] the on-chip protocol is described in the integrated microfluidic device operation section below. To obtain elution profiles, RNA was eluted by flowing dH_2O through the silica bead chamber and collecting in sequential 5 μL fractions. 1 μL of each fraction was used for RNA quantification with the Quanti-iT® RNA Assay Kit (Molecular Probes) according to the manufacturer's protocol. The fluorescence was read on an Infinite™ 200 reader (Tecan, Switzerland).

3.1.6 Real Time NASBA

All reagents required to perform the NASBA were supplied as part of a NucliSens Basic Kit (bioMérieux, UK), except primers and molecular beacon probes, which were supplied by MWG Biotech (Germany). The NASBA mix was prepared according to the recommendations of manufacturer; the final concentration of each primer was 5 μM, and 5 μM for the molecular beacon probe (FAM fluorophore, BHQ1 quencher; detection at 530 nm). Both primers and the molecular beacon probe were designed for the specific detection of *E. coli* based on the RiboSEQ platform [1].

5'-AATTCTAATACGACTCACTATAGGGAGATAGTCGCAAACGACGAA-3' was used as the forward primer, 5'-CTACATCCTCGGTACTACA-3' as the reverse primer, and 5'-FAM-CCAGCTAGCCTGATTAAGTTTTAAGCTGG-BHQ1-3' as the molecular beacon probe. These primers and probes were used for both on-chip and off-chip experiments. To allow comparison with on-chip results, off-chip real time NASBA was performed using a LightCycler 480 Real time PCR System (Roche Applied Science, U.S.A.); the reagent mixture, without enzymes, was mixed with the RNA template and heated on a block heater at 65 ºC for 5 min and at 41 ºC for 5 min. Next, the enzymes were added, the NASBA mixture was heated for 5 min at 41 °C, loaded into a 96-well plate, and placed in the LightCycler system. The fluorescence (530 nm) was measured every minute for 90 min. For each on-chip NASBA experiment, an *E. coli* tmRNA-positive control and a no-template negative control were amplified off-chip at 41 °C in the LightCycler in 20 μL volumes to verify NASBA reaction mixture performance.

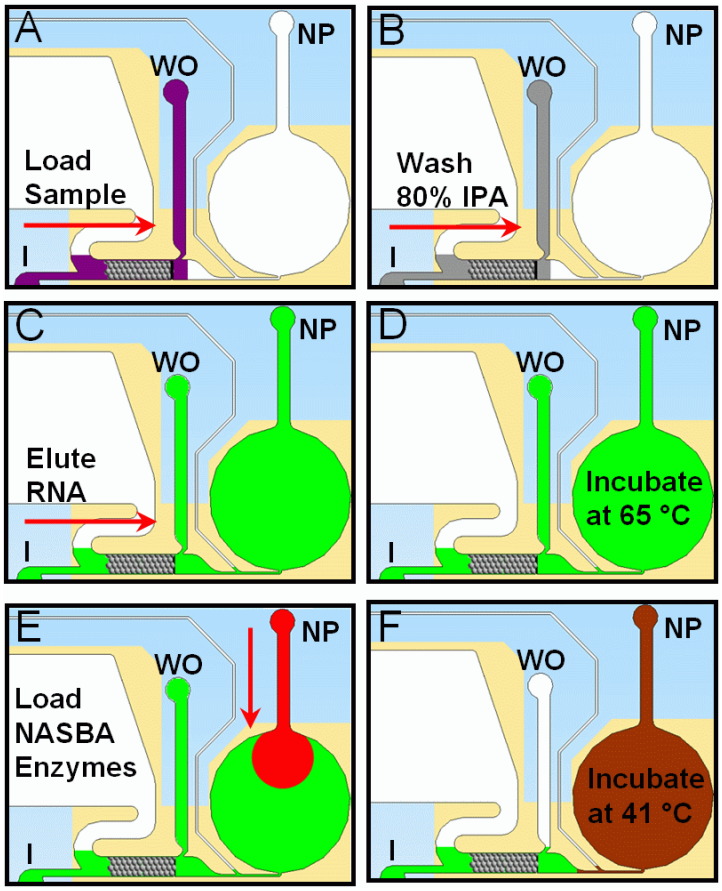

Figure 3.3 Representation of integrated microfluidic NASBA operation; all ports except for I, WO, and NP are sealed. (A) Sample mixture is pumped through the RNA purification chamber. (B) Washing solution is pumped through the purification chamber to remove unbound substances. (C) Bound RNA is eluted with primer-containing solution. (D) The mixture is heated to 65 ºC for 5 min. (E) NASBA enzymes are added through the NP port. (F) The fluids are mixed and incubated at 41 ºC to drive the amplification process. Reproduced from REF [1].

3.1.7 Integrated Microfluidic Device Operation

The RNA purification and NASBA chambers were characterised in this work; therefore, a simple connection scheme was used, in which a syringe pump (Pump 11 Pico Plus, Harvard Apparatus U.S.A.) was connected to the I port (Figure 3.3A) through a 250 *µ*L tube coil (1/32" inside diameter silicone platinum-cured tubing, 95802-01, Cole Parmer, U.S.A.). The opening and closing functions were accomplished manually using adhesive tape (from Roche LightCycler 480 plates kit, Fannin Healthcare, Ireland) to seal and open ports as required. Prior to use of the device for RNA purification and amplification, the NASBA chamber was filled with 1 *µ*g/*µ*L bovine serum albumin (BSA)

solution (Sigma Aldrich, U.S.A.) and the entire device was soaked in dH_2O for at least 12 hr at room temperature. Before operation of the device, the BSA solution was rinsed from the NASBA chamber with approximately 1 mL of dH_2O. The entire device was filled with dH_2O and all ports except for I and WO were sealed. The I port was connected to the syringe pump with the 250 μL tube coil preloaded with the necessary reagents. Between each reagent plug in the tube coil, a 5 μL air spacer was injected [7]. The WO port was connected to waste. Before each experiment, the purification chamber silica beads were conditioned for RNA capture by flowing 100 µL of 6 M GuHCl (Sigma Aldrich) for 20 min at 5 μL/min. Pre-mixed sample solution (10 – 40 μL of the RNA-containing sample mixed with 90 μL of 6 M GuHCl) was then pumped through the extraction chamber (Figure 3.3A) at 5 μL/min. After the RNA bound to the beads (20 min), other substances (cellular debris, proteins, etc.) were washed away by flowing through 100 μL of 80% isopropanol alcohol (IPA) at 17 μL/min (Figure 3.3B). After washing left-over IPA is removed and dried with the 5 μL air spacer. Next, the NP port was opened and the WO port sealed so that the bead-bound RNA sample could be eluted from the beads by pumping through approximately 11 μL of the NASBA reagent mixture (Figure 3.3C). All ports were sealed and the mixture was heated to 65 ºC for 5 min (Figure 3.3D) on a peltier device heating system (PE120, Linkam Scientific Instruments Ltd. UK) to denature secondary and tertiary RNA structures that could hinder subsequent annealing of primers during NASBA. By opening the I and NP ports and connecting the previously described syringe pump, 2 μL of NASBA enzyme mixture were slowly added to the NASBA chamber through the NP port as shown in Figure 3.3E. The enzymes were mixed with the reagent mixture by manually applying 40 2-Hz pressure pulses on the surface of the PDMS over the centre of the NASBA chamber (Figure 3.3F).

Next, all ports on the chip were sealed and the chip was mounted on an inverted fluorescence microscope (Olympus IX81) fitted with an incubation chamber (Solent Scientific, UK) and incubated at 41ºC for 90 min (a heated microscope stage can serve the same purpose as the incubator). During the incubation time, the NASBA chamber

was irradiated once per minute with a 492 nm excitation beam (excitation filter BP492/18 with a xenon light source, CellR MT20, Olympus) for 230 ms; 530 nm fluorescent light was sampled through a filter cube (U-MF2, Olympus) with a CCD sensor (Hamamatsu C4742-80-12AG). As the microscope field of view with a 4x objective covers about 1/5 of the NASBA chamber area, 5 images of the chamber (centre, top, bottom, left, and right side) were obtained for each minute of incubation. Real time NASBA curves were calculated from the average fluorescence as a function of time from the sets of acquired images. To avoid contamination, each reaction was performed in a previously unused device.

3.2 iNASBA array device

The integrated NASBA array (*i*NASBA array) device demonstrates the merging of cellular and molecular functionalities into a single chip enabling from sample-in to experiment and answer-out capabilities is presented. The *i*NASBA array monolithically integrates microfluidic dynamic cell culture, cell stimulation, cell labelling, lysis, and real time NASBA based RNA analysis. By multiplexing this integrated functionality in an array, the device can be used for high content screening, gene expression profiling, and bioanalytical diagnostics. Furthermore, the microfluidic implementation of these procedures has the potential for enhancing assay reproducibility and obtaining more quantitative results [8] relative to the classical analytical procedures.

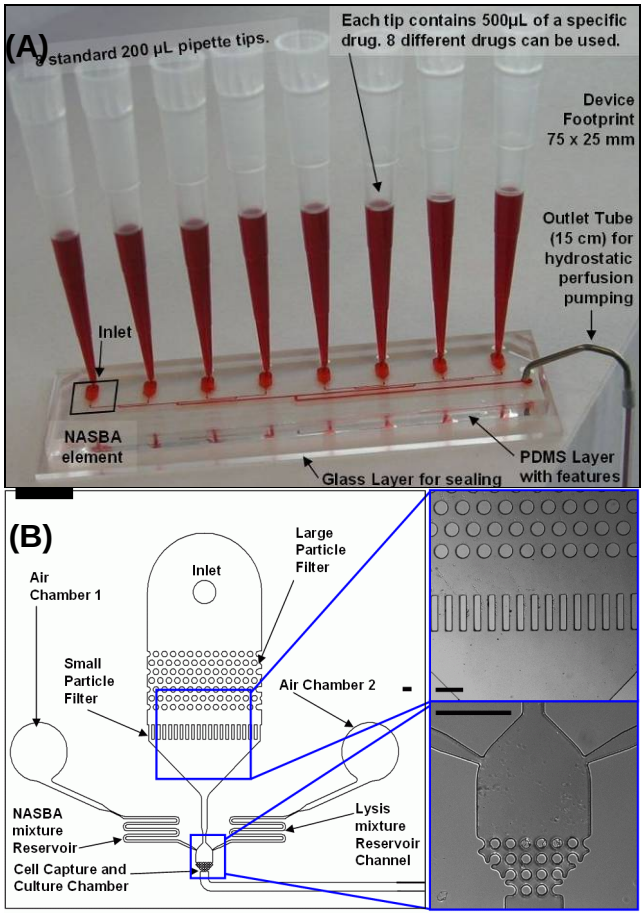

Figure 3.4 Integrated and multiplexed microfluidic NASBA array (*i*NASBA array) **(A)** Photograph of a row of 8 chambers with hydrostatic perfusion pipette tips filled with red food dye (scale-bar: 9 mm). **(B)** Design of each microfluidic NASBA element; scale-bars are equal to 200 µm.

3.2.1 Device Design

A completely integrated and multiplexed device is shown in Figure 3.4A (for detailed design schematic please see the attached file: "iNASBA array device.dwg"). Eight identical NASBA element modules are multiplexed with the same distribution as a 96 well plate, which enables sample loading to be done with a standard 8-channel pipette. Each NASBA module (Figure 3.4B) consists of: a cell retention and culture reservoir (~ 4 nL) for capturing the cell from the flow, culturing, lysis, and finally for performing real time NASBA; large and small particle filters for filtering debris from the culture media and prevent clogging in the cell capture and culture reservoir; lysis and NASBA mixture reservoir channels (~ 8 nL each) for storing and injecting the lysis and NASBA mixtures; chambers 1 & 2 containing the air volume which, when placed on top of localised

heating electrodes, expands and pumps out the fluid through the lysis and NASBA mixture reservoir channels. All microchannels and microchambers exhibit a height of 40 μm, which was selected so that cancer cells which have an approximate diameter range of 5-20 μm can easily flow through the system. Additionally, the 40 μm height is readily achieved with SU8 surface micromachining.

Cell trapping is done using a sieve structure composed by a set of pillars at the end of the culture chamber (Figure 3.4B) with a 5 μm inter-pillar spacing. The device is made of two layers (Figure 3.4A). The top PDMS layer accommodates the fluidic structures which are sealed by a glass slide attached to the bottom. During the cell culture phase the entire device is placed in a standard incubator were, if required, the partial CO_2 pressure can be controlled.

During the real time NASBA analysis phase, the device is mounted on a standard automated temperature controlled fluorescence microscope stage and the change in fluorescence intensity of each NASBA chamber is measured as a function of time. To simplify the operation the device is designed in such a way that the fluidic resistivity of all the inlets is equal and low enough so that the pressure generated by a standard pipette is sufficient to drive fluids into the device. This enables all fluid loading of the device to be done directly by a standard pipette. Furthermore, when the filled pipette tips are left plugged into the inlets, they function as gravity driven pumps (Figure 3.4A) which are used for cell loading and the perfusion of culture media, drugs and labelling dyes. Each row of 8 culture chambers is connected to a common outlet which is connected through a flexible tube (Figure 3.4A) to a waste container. By varying the height and diameter of the outlet tube the perfusion flow velocity can be controlled.

3.2.2 Operation

All fluid loading into the device is done by connecting a standard pipette directly in the inlet. Before starting the experiments localised heating electrodes are placed under the air chamber 1 and 2 of all the NASBA elements. Next, the lysis and NASBA mixtures are

loaded. Initially the device is empty and air filled, then the real time NASBA mixture is flown into the inlet (Figure 3.5). This fills the device including the lysis and NASBA reservoirs with real time NASBA mixture. The lysis mixture is injected into the device and the excess NASBA mixture flushed out. The NASBA mixture in the lysis reservoir is replaced with lysis mixture by activating the heating electrodes under the air chamber 2. This causes the air in the chamber to expand, push out and empty the reservoir channel. Then the heating electrodes are turned off and the lysis mixture allowed to enter the lysis mixture reservoir channel.

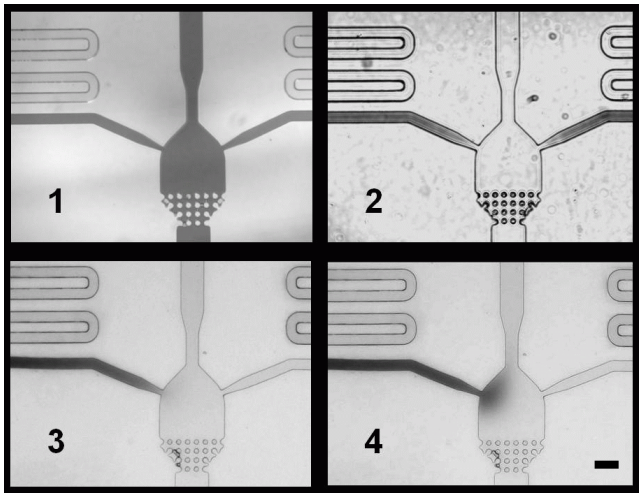

Figure 3.5 Micrographs of reagent loading and injection tests with food dye. Firstly the NASBA mixture (dark dye) is filled (**1**), through the main inlet. By flushing with water (**2)** and activating the heating electrode in the air chamber 2, the NASBA mixture that has entered the lysis reservoir is removed (**3**). Then lysis mixture can be filled. Finally the NASBA mixture is injected and mixed into the culture chamber by activating the heating electrode under the air chamber 1 **(4)**. (Scale-bar:100 μm)

The pipette tip that is used to flow in the lysis mixture is left plugged into the inlet (as in Figure 3.4A), emptied and filled up with media from the top. This establishes a gravity driven flow of culture media which is left to run for 10 minutes. Any left over lysis or real time NASBA mixture in the cell culture chamber is flushed away with the gravity driven flow of culture media. At this stage approximately 500 cells in 5 μL are loaded by gently pipetting them into the bottom of the plugged in tip. The gravity driven flow will gently take the cells into the cell capture and culture chamber. Any cell stimulating drugs or cell staining dyes can be loaded directly into the plugged in pipette tip and the gravity driven flow will perfuse them over the cells. After culturing and drug stimulation the lysis mixture is released by activating the heating electrode under the air chamber 2. Finally

the real time NASBA mixture (Figure 3.5-4) is precisely released and diffusion mixed (Figure 4.5) into the culture chamber by activating the heating electrode under air chamber 1 for 15 s. The whole device is then heated for 5 minutes on a hot plate at 55 °C and then placed on a 41 °C thermally controlled fluorescence microscope stage and the change in fluorescence from each NASBA chamber is measured as a function of time. During the loading process a large portion of the NASBA mixture is flown into the device outlet and only a small part (approximately 2 nL) is loaded into the NASBA mixture reservoir. Considering the total chamber volume of ~200 nL, which is 100 time less than the total NASBA mixture volume used in the conventional off-chip case (app. 20 μL). Furthermore due to the small cross sectional area of the reservoir channels diffusion loss of the reservoir contents is kept to a minimal.

3.2.3 Fabrication

The top layer with the microfluidic channels was fabricated using standard soft lithography replica moulding technique [3]. A mould was created through a single-layer process using negative photoresist, SU8-3050 (Microchem U.S.A.) and the manufacturer recommended protocol (with a spin rate of 2000 RPM) to create 40 µm high features on a clean silicon wafer. PDMS (Sylgard 184, Dow Corning) was prepared according to the manufacturer's instructions and used to inversely replicate the mould. PDMS was used because of its biocompatibility [2] and its ease of bonding to glass. Fluid inlets and outlets were punched with a 1 mm outer diameter flat-tip needle for tube connections.

A 75x25x1 mm^3 glass slide (VWR International Inc., U.S.A.) and the PDMS structures were treated with UV ozone (PSD-UV, Novascan Technologies, Inc., Iowa, US.) for 10 minutes before bonding for 2 h at 90 ºC. Then 0.01 % poly-L-lysine (Sigma Aldrich, Ireland) solution was flown into the device and left at room temperature for 2 hours to coat the device. Any uncoated poly-L-lysine was flushed away by deionised water (dH_2O). Finally, for the localised heating electrodes, a 2 micron high electrode feature layer was developed on a continuous gold coated glass slide (Part. No. 820.003 Lebow

Company, CA, U.S.A.) using Microposit S1818 photoresist (Chestech Ltd., UK) and the manufacturers instructions. The exposed gold and chrome layers were etched away with gold etchant solution and chromium etchant solution (Sigma Aldrich, Ireland) in less than 40 sec. The Microposit S1818 photoresist left on the electrodes was washed away with 70% Propanol-2 solution (Sigma Aldrich, Ireland).

3.3 iCell array device

The design of a multiplexed integrated cell based assay system (*iCell array*) with several readout capabilities such as real time Nucleic Acid Sequence-Based Amplification (NASBA) and immuno-fluorescent (IF) protein expression detection is presented. The microfluidic system is capable of performing 512 dynamically configurable integrated cell based assays coupled with real time NASBA and IF analysis (see Figure 3.6, for detailed design schematic please see the attached file: “iCell array device.dwg”). It has been designed for simple, efficient and shear stress free loading of cells and reagents that can be done with existing laboratory tools such as standard multichannel pipettes or pipetting robots. The device has an onboard gravity driven flow control system making it independent of cumbersome syringe pumps or other active macro-scale flow control components such as pressure sources and solenoid valves. This allows the device to be self contained, mobile and directly used in standard laboratory cell culture incubation chambers and microscope systems.

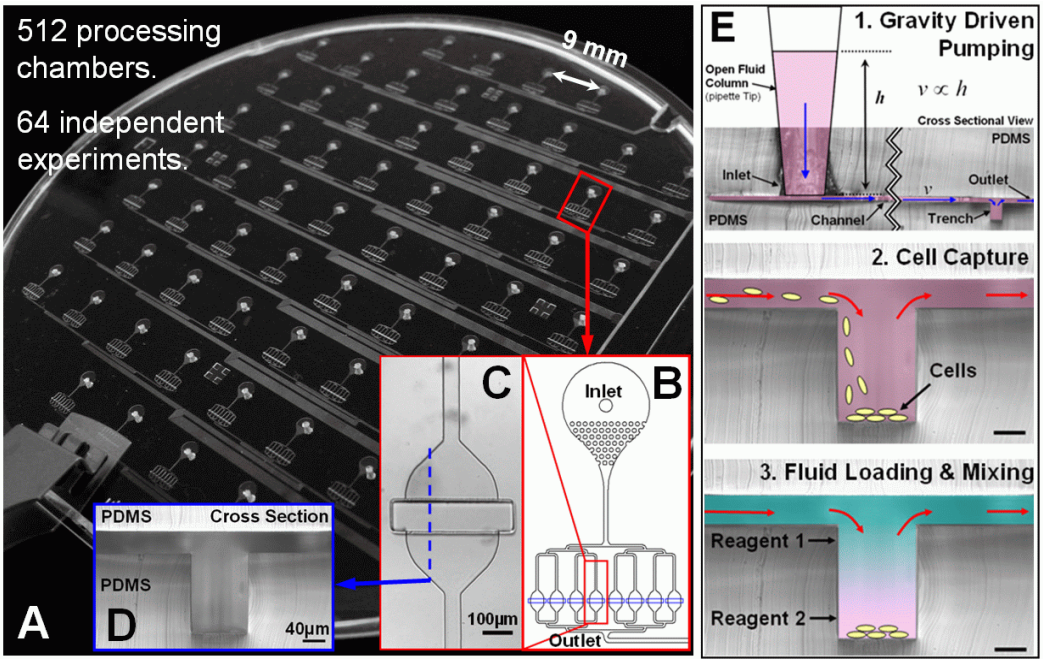

Figure 3.6 *iCell array* (A) consists of 64 processing modules (B) that can perform 64 independent simultaneous integrated assays. For statistical replication purposes each module consists of 8 parallel and equally distributed (C) processing chambers that contain a central trench structure (D). Each processing chamber can execute integrate any sequence basic unit operations (E) The function of each processing chamber depends on the sequence and timing of each gravity driven unit operation and the input fluid.

3.3.1 Fabrication

The microfluidic device was fabricated using standard soft lithography replica moulding techniques [3]. A mould was created through a double-layer process (Figure 3.7) first using negative photoresist, SU8-3050 (Microchem U.S.A.) and then SU8-2150 (Microchem U.S.A.) both layers were deposited onto a clean silicon wafer using a spin coater (P6700 Specialty Coating Systems, Inc., U.S.A.).

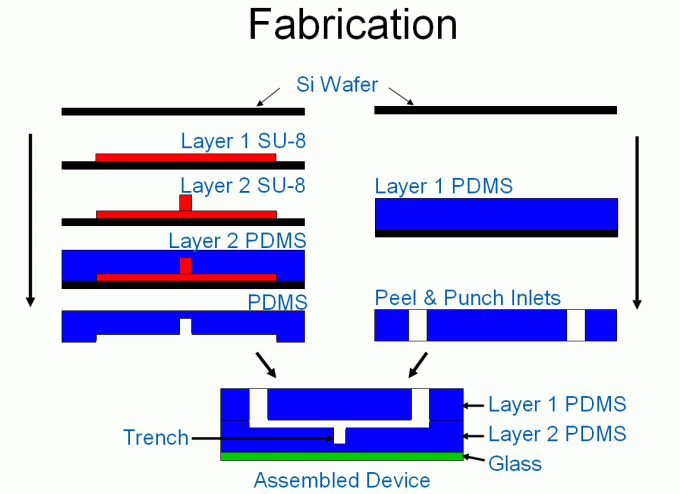

Figure 3.7. The fabrication process of a *iCell* array has been optimized to simplify alignment and complexity. It consists of 2 layers of PDMS (a fluidic layer and a lid/inlet layer) and support glass layer.

The first layer photo resist (5 mL) was spread onto the wafer at 500 RPM for 10 s, and the rotation rate was ramped at an acceleration of 350 RPM/s to 4000 RPM, at which rate the sample was spun for 30 s to form a 40 μm layer. The wafer was soft baked at 95 ºC for 15 min followed by UV-exposure for 30 s at 9.5 mW/cm^2 using a Karl-Süss KSM MJB-55W mask aligner. The wafer was post-exposure baked for 1 min at 65 ºC and 62 min at 95 ºC, allowed to cool to room temperature, developed in Microposit EC Solvent (Chestech Ltd., UK) developer and sonicated (Branson 5510, Kell-Storm, USA) for 4 min, and blown dry with nitrogen. The second layer photo resist (5 mL) SU8-3025 (Microchem U.S.A.) was spread onto the patterned wafer at 500 RPM for 10 s, and the rotation rate was then ramped at an acceleration of 350 RPM/s to 4,000 RPM, at which rate the sample was spun for 3 s. The wafer was then soft baked at 95 ºC for 10 min. Then another layer of photo resist (5 mL) SU8-2150 (Microchem U.S.A.) was spread onto the wafer at 500 RPM for 5 s, and the rotation rate was then ramped at an acceleration of 200 RPM/s to 1,500 RPM, at which rate the sample was spun for 30 s to form a 250 μm layer. The wafer was then soft baked at 65 ºC for 6 min. and then at 105 ºC for 15 min, then aligned and UV-exposed for 70 s at 9.5 mW/cm^2. The wafer was post-exposure baked for 6 min at 65 ºC and 12 min at 95 ºC, allowed to cool to room temperature, developed in Microposit EC Solvent (Chestech Ltd., UK) developer for 12 min, and blown dry with nitrogen. The two layer SU-8 mould was coated with

perfluoro-silane in a vacuum chamber for reducing the PDMS adhesion. PDMS prepolymer (Sylgard 184, Dow Corning) was prepared at 10:1 (w/w) ratio, degassed in a vacuum chamber for 30 min, then spin coated (500 RPM for 30 sec) on the SU8 mould and cured in a 100 ºC oven for 5 min. producing an ~500 μm thick fluidic layer. The PDMS was then carefully peeled off the mould. As the upper seal a second non patterned wafer was also coated with a 2 mm thick layer of PDMS pre-polymer and cured at 80 ºC for 4 hrs. Fluid inlets and outlets were punched into the 2 mm thick layer upper layer. A flat-tip needle was used for making the inlets (1.3 mm OD) and outlet (3 mm OD) holes. The device was assembled by firstly placing the fluidic layer (with the fluidic structures exposed on the upper side) on a 500 μm thick 4 inch glass wafer for support. The assembly was treated with O_2 plasma (PDC-002 Harrick Scientific Corp. USA) for 2 min. after which the upper PDMS layer (containing the inlets and outlets) was manually aligned and bonded at 60 ºC for 2 hrs. The entire device was degassed overnight for removing bubbles that may form between the glass and PDMS.

3.3.2 Device Loading and Flow Control

Firstly the device is primed with PBS, which is done by placing the empty chip into a vacuum desiccator and degassing it for 10 min. This will remove any bubbles formed during the initial fluid loading process (movie SM1). Then a 1000-μL Eppendorf pipette loaded with 100 μL of PBS is inserted into each inlet that will be used during the experiment. Using the pipette the PBS solution is driven into the device until a droplet is formed in the outlet, after which the pipette tip is released form the pipette and left inserted into the device inlet. This forms the fluid column that will drive the fluid flow. The height of the fluid column and thus the device flow velocity can be regulated (Figure 5.6A) by inserting or removing fluid from the top of the pipette tip with a second long tip pipette (0.5 mm round tip Corning® gel-loading tips, Sigma Aldrich, USA). Cells or other particles are loaded by firstly establishing a flow with a fluid column height and then using the long tip pipette to inject the cells at the bottom of the fluid column. For general eukaryotic cells (MCF7, HeLa, etc.) experiments, ~2000 cells in 10 μL of culture media were loaded into each processing module. Cell numbers were quantified using a

hemocytometer (BS.748 Hawksley, UK) according to the manufacturer's instructions. Any additional or non-loaded cells can be removed from the inlet by extracting them from the bottom of the fluid column with long tip pipette (0.5 mm round tip Corning® gel-loading tips, Sigma Aldrich, USA). The PBS fluid column is then replaced with culture medium.

3.3.3 Device Coating for Adherent Cell Culture

To prepare the device for adherent cell culture and stimulation experiments the processing chambers are coated with a poly-L-lysine layer by allowing the 1% poly-L-lysine solution (Sigma Aldrich, USA) to flow continuously for 2 hrs at room temperature. Then the poly-L-lysine is replaced with 300 μL of PBS (Sigma Aldrich, USA) and left to rinse the device for 2 hrs. The remaining PBS is replaced with 300 μL of cell culture medium.

3.3.4 Cell Culture

MCF7, HeLa, 59M and U266 cells were cultured on and off chip using a CO_2 independent medium supplemented with 10% bovine serum albumine, L-Glutamine and penicillin/streptomycin. In the on-chip cell culture and stimulation experiments the entire device was incubated at 37 ºC in an inverted fluorescence microscope (Olympus IX81) fitted with an incubation chamber (Solent Scientific, UK).

3.3.5 Cell Staining and Drugs

Cells were stained on-chip by flowing over them a PBS solution containing fluorescent staining agents. For live cell staining 4 μL/mL of Calcine AM (Sigma Aldrich, USA) was used while for dead cells 4 μL/mL of propidium iodide (Sigma Aldrich, USA) nuclear stain was used. Both stains were dissolved together in PBS and 300 μL loaded into each fluidic column. After 20 minutes fluorescent images were acquired of each processing chamber. In cell stimulation experiments the drug or stimulating agent is dissolved in the cell culture medium according to the required concentration. Cells would receive the stimulation drug or agent after a 24 hrs drug free cell culture period.

3.3.6 Cell Lysis

For the *E. coli* experiments cell lysis was performed off chip using MicroLYSIS PLUS buffer (Microzone Ltd., UK) according to the manufacturer's recommendations. An overnight culture of *E. coli* (OD600 of 1.36) with a cell density of 3.4 x 10^8 colony forming units (CFU)/mL (based on plate counts) was centrifuged at 10,000 rpm for 5 min, producing a pellet volume of 5 µL, and mixed with 40 µL of lysis buffer. Temperature cycling was then performed between 65 °C and 96 °C for a total of 23.5 min (65 °C for 15 min, 96 °C for 2 min, 65 °C for 4 min, 96 °C for 1 min, 65 °C for 1 min, 96 °C for 30 s) by transferring tubes between two heating blocks. This crude cell lysate was either used directly or diluted with PBS to produce required cell concentrations. Cell lysate samples were stored at -15 °C until required. For the on-chip eukaryotic cell lysis experiments MicroLYSIS PLUS buffer was mixed with the NASBA primers (5 μM each primer). The 200μL of lysis mixture was loaded into the fluid column and allowed to flow into the processing chamber for 5 min. after which the flow was stopped and the device mounted on a hot plate at 65 °C for 5 min.

3.3.7 Real Time NASBA

All reagents required to perform the NASBA were supplied as part of a NucliSens Basic Kit (bioMérieux, UK), except primers and molecular beacon probes, which were supplied by Sigma Aldrich (UK). The NASBA mix was prepared according to the manufacturer's recommendations; the final concentration of each primer was 5 μM, and 5 μM for the molecular beacon probe. For the *E. coli* detection the design of both primers and the molecular beacon probe was taken from Dimov et al. 2008 [1]. For the estrogen receptor alpha detection, the primer and the molecular beacon probe designs are described in Verjat et al. [9]. Off-chip real time NASBA was performed using a LightCycler 480 Real Time PCR System (Roche Applied Science, U.S.A.); the reagent mixture, without enzymes, was mixed with the RNA template and heated on a block heater at 65 ºC for 5 min and at 41 ºC for 5 min. Next, the enzymes were added, the NASBA mixture was heated for 5 min at 41 °C, loaded into a 96-well plate, and placed in the LightCycler system. The fluorescence (530 nm) was measured every minute for 90 mins.

For On-Chip experiments the reagent mixture was mixed off chip with the enzyme mixture to produce a master NASBA mixture. This was then flown into the chip for 15 min at ~200 *μ*m/sec. In the case of the *E. coli* detection experiments the reagent mixture contained varying concentrations of *E. coli* lysate (for the negative control RNA free water replaced the *E. coli* lysate). After that the device is mounted on a thermally controlled inverted fluorescent microscope and the green and red fluorescence imaged every minute in every processing chamber. Real time NASBA curves were calculated from the average fluorescence as a function of time from the sets of acquired images.

3.3.8 Cell Fixing, Permeabilization and Immuno-fluorescent staining

Cells captured within the chip were fixed with 4% paraformaldehyde for 25 min at 100 μm/s flow rate. After washing once briefly with PBS-T (Dulbelcco's PBS containing 0.01% Triton X-100), the cells were treated with 0.05% Triton X-100 in PBS for 10 min for permeabilization at 200 μm/s flow rate. The cells were washed once briefly with PBS-T, followed by blocking in PBS-T containing 5% fetal bovine serum (FBS) for 30 min at room temperature and a flow rate of 200 μm/s. The cells were then incubated for 1 hour at room temperature with anti-ERα antibodies (F10, Santa Cruz, CA, USA) diluted at 1:50 in PBS-T containing 1% FBS at 200 μm/s flow rate.. The cells were washed with PBS-T, for 20 min at 600 μm/s flow rate. Then the cells were incubated for 15 min at room temperature with Alexa Fluor 488 fluorescent dye-conjugated secondary antibodies (Molecular Probes Inc., Eugene, OR, USA) (1:200) in PBST containing 1% FBS at 200 μm/s flow rate. The cells were washed with PBS-T for 1 hr at 600 μm/s flow rate, before staining with Propidium Iodide. Immunofluorescent staining(s) were observed under Olympus IX81 Fluorescence Microscope with Optronics MagnaFire digital camera (Microscope Image Centre, UVM).

3.3.9 Device Read Out

For readout the device is mounted on a thermally controlled inverted fluorescent microscope. In our case an Olympus IX81 fitted with an incubation chamber Solent

Scientific (UK) was used. All acquisitions (bright field, and fluorescent) were done with a CCD sensor (Hamamatsu C4742-80-12AG) and through the 10x objective. For green fluorescence imaging an excitation filter BP492/18 with a xenon light source, CellR MT20 (Olympus) and a U-MF2 filter cube (Olympus) was used. For red fluorescence imaging an excitation filter BP540/10 with the previously mentioned xenon light source and a U-MW1GA3 filter cube (Olympus) were used. When scanning multiple processing chambers a programmed motorized stage was used to position and focus the objective over each processing chamber. The image analysis and motorized stage programming was done using the ImageJ and the Cell R software packages (Olympus).

3.3.10 Computational Fluid Dynamics

The flow patterns are calculated by means of two-dimensional Navier-Stokes equations of the total continuity, energy and momentum.

$$0 = \nabla u \qquad \text{(eq. 2.1)}$$

$$\rho \frac{\partial u}{\partial t} + \rho u \cdot \nabla u = \nabla \cdot [-\rho I + \eta \nabla u] + F \qquad \text{(eq. 2.2)}$$

where *u* is the velocity of the mixture flow, ρ is the flow density, *I* is the inertia force, μ is the dynamic viscosity, and *F* is the external body force. To estimate particle trapping efficiency in this trench system, the Kahn and Richardson force (eq. 2.14) for particle tracing was calculated. Mass transfer and component mixing are estimated from mass transfer equation (eq. 2.10). Simulations focused on the key factors of particle capture and species mixing within the trench geometry. In order to predict the key design parameters simulation focused on the effects of the geometrical parameters, flow velocity, particle size, particle trapping efficiency and the mixing of fluid components (see Table 3.1). The pressure boundary condition was used for the inlet and the outlet. In the computational analysis, 50 particles were tracked and the boundary conditions were estimated as listed in Table 3.2. The trench simulation was performed in a two-dimensional tri-angular grid consisting of 1,168 cells for estimation of trapping efficiency

and 4,905 cells for estimating the mixing effects using a commercial computational fluid dynamics (CFD) code, COMSOL ver 3.4 (COMCOL LAB, Stockholm, Sweden) and CFD-ACE V2008.3 (ESI-Group, Huntsville, AL, USA), respectively. The semi-implicit pressure linked equation (SIMPLE) algorithm was applied to solve the momentum equation. The calculation for each case took about 5 min of running time on a Intel Xeon E5420 @ 2.50 GHz.

Table 3.1. Simulation Parameters

Parameter	Values
Trench height	0.25, 2.5, 6.25, 12.5, 25
Trench length	0.25, 2.5, 6.25, 12.5, 25
Velocity	9.0×10^{-2}, 1.8×10^{-3}, 9.0×10^{-3}, 9.0×10^{-4}, 9.0×10^{-5}
Particle diameter, D_p/H_0 at D = 1.9×10^5,	2.5×10^{-3}, 7.25×10^{-3}, 2.5×10^{-2}, 7.25×10^{-2}, 2.5×10^{-1},
Particle density, D	1.9×10^2, 1.9×10^3, 1.9×10^4, 1.9×10^5, 1.9×10^6,

Tn is the time to complete species replacement within the trench. It is defined as the time that it takes for a new added species to reach a stable final concentration in the trench and is calculated as the difference in the time between the added species normalized average concentration of 1 x 10^{-4} and 0.99 at a given constant flow rate of the added species. Thus *Tn* depends amongst other things on the flow velocity of the added species, the diffusion coefficient of the added species, the trench geometry and the inlet and outlet flow path lengths.

Table 3.2. Boundary Condition

Boundary	Condition	Value
Inlet	Pressure boundary, P_{in}	Normal 0.04, 0.4, 4, 20, 40 Pa
Outlet	Pressure boundary, P_{out}	0
Wall	No slip	-

3.4 References

[1] I. K. Dimov, J. L. Garcia-Cordero, J. O'Grady, C. R. Poulsen, C. Viguier, L. Kent, P. Daly, B. Lincoln, M. Maher, R. O'Kennedy, T. J. Smith, A. J. Ricco, and L. P. Lee, "Integrated microfluidic tmRNA purification and real-time NASBA device for molecular diagnostics," *Lab on a Chip*, vol. 8, pp. 2071-2078, 2008.

[2] S. K. Sia and G. M. Whitesides, "Microfluidic devices fabricated in Poly(dimethylsiloxane) for biological studies," *ELECTROPHORESIS*, vol. 24, pp. 3563-3576, 2003.

[3] G. M. W. Younan Xia, "Soft Lithography," *Angewandte Chemie International Edition*, vol. 37, pp. 550-575, 1998.

[4] M. C. Breadmore, K. A. Wolfe, I. G. Arcibal, W. K. Leung, D. Dickson, B. C. Giordano, M. E. Power, J. P. Ferrance, S. H. Feldman, P. M. Norris, and J. P. Landers, "Microchip-Based Purification of DNA from Biological Samples," *Anal. Chem.*, vol. 75, pp. 1880-1886, 2003.

[5] C. J. Easley, J. M. Karlinsey, J. M. Bienvenue, L. A. Legendre, M. G. Roper, S. H. Feldman, M. A. Hughes, E. L. Hewlett, T. J. Merkel, J. P. Ferrance, and J. P. Landers, "A fully integrated microfluidic genetic analysis system with sample-inâ€“answer-out capability," *Proceedings of the National Academy of Sciences*, vol. 103, pp. 19272-19277, 2006.

[6] B. C. P. Cremonesi, G. Malferrari, I. Biunno, C. Vimercati, P. Moroni, S. Morandi, M. Luzzana, "Technical Note: Improved Method for Rapid DNA Extraction of Mastitis Pathogens Directly from Milk," *J. Dairy Sci.* , vol. 89, pp. 163–169, 2006.

[7] V. Linder, S. K. Sia, and G. M. Whitesides, "Reagent-Loaded Cartridges for Valveless and Automated Fluid Delivery in Microfluidic Devices," *Anal. Chem.*, vol. 77, pp. 64-71, 2005.

[8] S. Nagrath, L. V. Sequist, S. Maheswaran, D. W. Bell, D. Irimia, L. Ulkus, M. R. Smith, E. L. Kwak, S. Digumarthy, A. Muzikansky, P. Ryan, U. J. Balis, R. G. Tompkins, D. A. Haber, and M. Toner, "Isolation of rare circulating tumour cells in cancer patients by microchip technology," *Nature*, vol. 450, pp. 1235-1239, 2007.

[9] T. Verjat, E. Cerrato, M. Jacobs, P. Leissner, and B. Mougin, "Multiparametric duplex real-time nucleic acid sequence-based amplification assay for mRNA profiling.," *BioTechniques* pp. 476-481, 2004.

Chapter 4: Integrated Microfluidic Device for RNA Extraction and Real Time NASBA

A characterization is presented of the first integrated microfluidic tmRNA purification and nucleic acid sequence-based amplification (NASBA) device incorporating real time detection. The real time amplification and detection step produces pathogen-specific response in less than 3 min from the chip-purified RNA from 100 lysed bacteria. On-chip RNA purification uses a new silica bead immobilization method. On-chip amplification uses custom-designed high-selectivity primers and real time detection uses molecular beacon fluorescent probe technology; both are integrated on-chip with NASBA. Present in all bacteria, tmRNA (10Sa RNA) includes organism-specific identification sequences, exhibits unusually high stability relative to mRNA, and has high copy number per organism; the latter two factors improve the limit of detection, accelerate time-to-positive response, and suit this approach ideally to the detection of small numbers of bacteria. Device efficacy was demonstrated by integrated on-chip purification, amplification, and real time detection of 100 *E. coli* bacteria in 100 μL of crude lysate in under 30 min for the entire process.

4.1 Characterization of the NASBA Chamber

The NASBA chamber (see Section 3.1 for device and experimental details) is the central sensing unit in the integrated device. It was characterized initially by extracting and purifying total RNA from *E. coli* off chip, then preparing serial dilutions of the total RNA and loading into multiple devices. The template RNA dilutions were mixed on-chip with the NASBA mix (enzymes, primers, molecular beacons, etc.) as described in Section 3.1, then pumped to the NASBA chamber. All experiments were performed in triplicate and included a negative control where the RNA template solution was replaced with sterile RNA-free water (Molecular Biology Grade Water, Sigma Aldrich, U.S.A.).

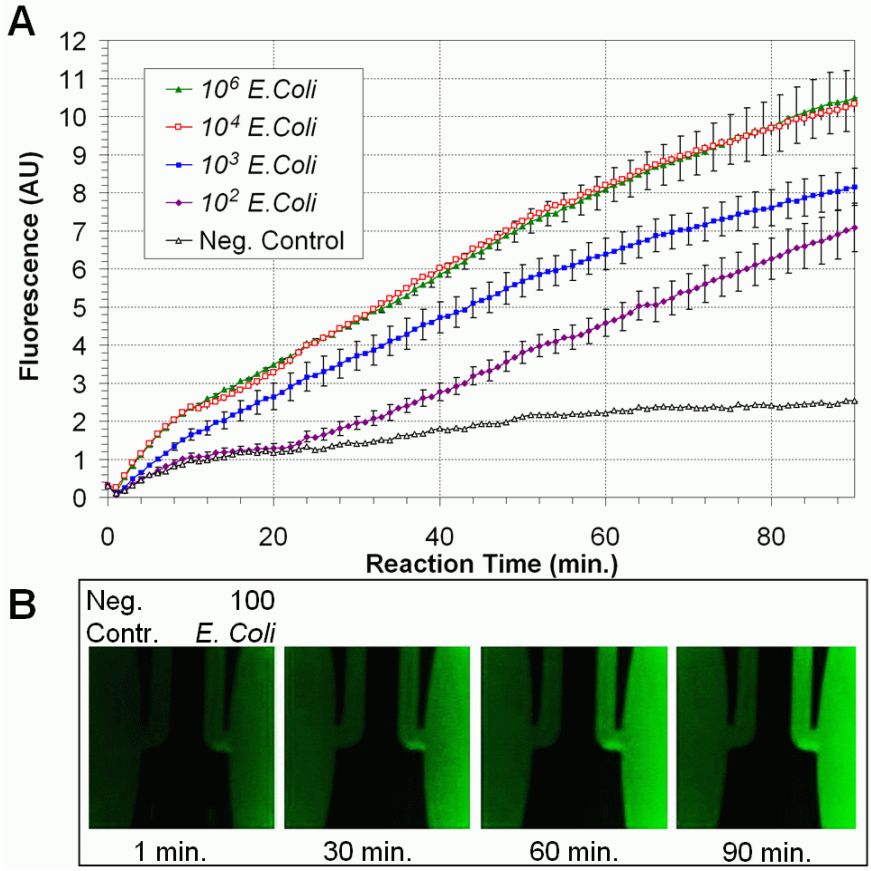

Figure 4.1. Characterization of real time NASBA reaction for off-chip-purified *E. coli* RNA template. (**A**) Fluorescence intensities in arbitrary units (AU) were plotted over the course of the NASBA reaction. Experiments were performed in triplicate with different numbers of template molecules from total RNA extractions (ranging from 10^2 to 10^6 *E. coli* cells, as indicated). (**B**) Time-lapse images showing the fluorescence increase of the integrated NASBA chamber entrance loaded with total RNA equivalent to 100 *E. coli* (right of each frame) and the negative control (left of each frame). Reproduced from REF [1].

Figure 4.1A shows a clear relationship between the rate of fluorescence increase and the input template RNA concentration. Error bars, the standard deviations of the triplicate measurements, show that the results are reproducible (average variation of ± 6%). Similar results were obtained from positive control experiments performed on the Roche LightCycler 480. The NASBA chamber has an approximate volume of 2 μL, one tenth of the standard 20 μL NASBA reaction volume. The data suggest that the BSA-treated and water-soaked PDMS chambers support an efficient real time NASBA reaction, notwithstanding its greater bio-chemical complexity relative to PCR: NASBA involves 3 enzymes, PCR only one.

4.2 Characterization of RNA Purification

RNA loading, washing, and elution procedures were performed as described in Section 3.1.5. In order to characterize the RNA purification module, RNA was purified from the crude lysate of 10^7 *E. coli* cells and a total RNA elution profile was obtained by collecting consecutive 5 *μ*L aliquots of the eluted solution and measuring the RNA concentration.

While 1 *μ*L of each 5 *μ*L aliquot was used for RNA quantification with the Quanti-iT® RNA Assay Kit, RNA from another 2.5 *μ*L aliquot was amplified by real time NASBA using the Roche LightCycler 480 and the end-point amplicon fluorescence recorded. The experiments were conducted on two different devices, and are summarized in Figure 4.2.

As expected, the results show the amount of RNA is highest in the first elution fraction and decreases as elution continues. The end-point amplicon fluorescence, however, is highest in the 3rd elution fraction (between the 10th and 15th *μ*L). The 5 *μ*L air spacers that separated the reagents did not cause any problems or bubble formation as they passed through the RPC, because the injected air plugs only passed through straight channels and a soft 90° turn geometry (from I to WO). Additionally the bead immobilisation method creates a layer of silica beads (see Figure 3.2.1 in Section 3.1) which leaves plenty of space for debris and air to pass through without leaving bubbles or clogging. Since there is a trade-off between clogging probability and capture efficiency, the height of the purification chamber during manufacture can be adjusted to fine tune the free-flow space to minimise clogging and maximise capture efficiency. Although it was neither required nor used in our application, another advantage of the bead immobilisation method is that it allows the sample solution to flow back and forth over the same beads, increasing capture efficiency; immobilized beads' extraction efficiency can be between 10^2- to 10^3-fold greater than non-immobilised beads [2].

Since most inhibitors (including IPA) are washed away, there is a possibility that the elution time for the RNA fragments is size dependent; thus, our target fragments (363-

nucleotide tmRNA molecules) mostly elute in the 3rd elution fraction. Similar elution results and differences in amplicon and eluted RNA peaks were reported in a similar microfluidic device [3]. For the integrated operation of chips, the 3rd eluted fraction was used for downstream on-chip real time NASBA.

To evaluate the integration of on-chip RNA purification with real time NASBA, crude lysates of *E. coli* cells (Figure 4.3) were prepared. Three *E. coli* lysates from 10^2, 10^5, and 10^8 CFU were prepared together with a negative control (dH_2O) as previously described. RNA from the samples was purified and amplified using 4 separate microfluidic chips, one for each sample. Real time NASBA results, Figure 4.3, show successful on-chip integrated RNA purification and real time NASBA. The time taken for positive samples to reach above background fluorescence during real time NASBA amplification is known as the time-to-positivity or TTP and can be related to the initial amount of target RNA present in the sample. The lysate from 100 *E. coli* cells was readily detected with a TTP of less than 3 minutes, suggesting a limit of detection significantly below 100 cells. Note that since RiboSEQ targets are used, each *E. coli* contains approximately 500-1,000 copies[4] of tmRNA target fragment, so detection of < 100 cells is not surprising. This high copy number, along with the relatively high stability of tm-RNA, also increases the detection robustness, a critical factor in complex sample matrices such as blood. The difference in end-point fluorescence displayed in Figures 4.1A and 4.3 most likely results from differences caused by the change in the purification capacity between the two experiments; also, the method used to purify RNA is different for the two experiments. These factors may influence the kinetics of the NASBA reaction and consequently the endpoint fluorescence. Furthermore, the negative control fluorescence in the off-chip purification process (Figure 4.1A) is higher (2 AU) than on the on-chip purification (Figure 4.3). Since the procedures were similar, the lower negative control fluorescence in the on-chip purification may be due to reduced contamination. In the on-chip procedure, there are no sample pipetting or sample transfer steps after the purification. Fluorophore bleaching can occur during the real

time NASBA reaction; to reduce this effect, the exposure time was limited to 230 ms for the data shown in Figure 4.3.

The TTP for samples of crude *E. coli* lysate (Figure 4.3) demonstrates that the various cell numbers can be distinguished from the negative control in as little as 3 min, which, to the best of our knowledge, is more rapid than any previous report of on-chip amplification and detection from as few as 100 cells [5]. With this approach, the total time from "sample to answer" can be less than 30 min. Table 4.1 shows the comparison of on-chip and conventional "off-chip" RNA purification and real time NASBA. Compared to the conventional off-chip method, on-chip NASBA requires approximately 10 times less volume, and the resultant discrimination is approximately 10 times faster (3 min on-chip, 15 – 25 min off chip; see Supporting Information). Relative to conventional, off-chip procedures, on-chip integration reduces the direct pipetting steps from 11 to 2 and the sample-transfer steps from 3 to 1, reducing significantly the likelihood of sample contamination.

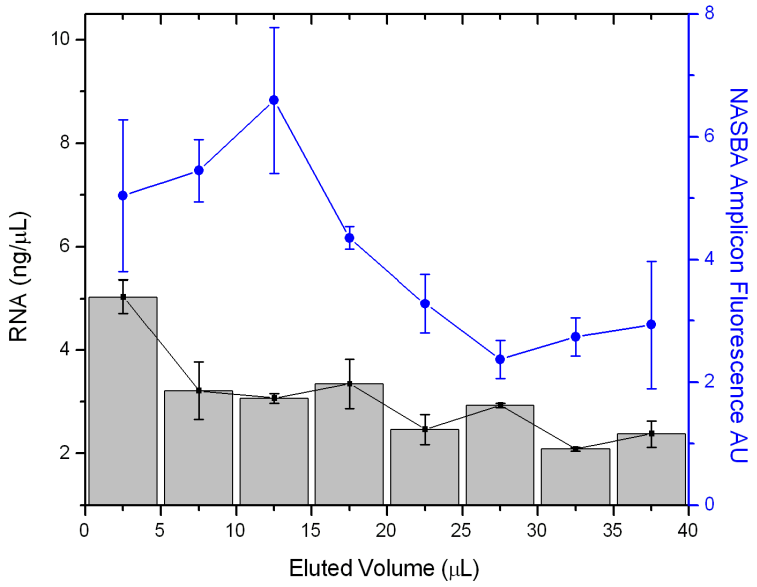

Figure 4.2. Elution profile (grey bars with standard error variations) of total RNA extracted from crude lysate of approximately 10^7 *E. coli* shows total RNA concentration in each 5 *μ*L elution fraction. Blue data points with the standard error bars (right y-axis) show end-point NASBA amplicon fluorescence after a 90-min off chip real time NASBA amplification of 2.5 *μ*L of each eluted fraction. Reproduced from REF [1].

4.3 Integrated RNA Extraction and Real Time NASBA Operation

To evaluate the integration of on-chip RNA purification with real time NASBA, crude lysates of *E. coli* cells (Figure 4.3) were prepared. Three *E. coli* lysates from 10^2, 10^5, and 10^8 CFU were prepared together with a negative control (dH_2O) as previously described. RNA from the samples was purified and amplified using 4 separate microfluidic chips, one for each sample. Real time NASBA results, Figure 4.3, show successful on-chip integrated RNA purification and real time NASBA. The time taken for positive samples to reach above background fluorescence during real time NASBA amplification is known as the time-to-positivity or TTP and can be related to the initial amount of target RNA present in the sample. The lysate from 100 *E. coli* cells was readily detected with a TTP of < 3 minutes, suggesting a limit of detection significantly below 100 cells. Note that since RiboSEQ targets are used, each *E. coli* contains approximately 500-1,000 copies[4] of tmRNA target fragment, so detection of < 100 cells is not surprising. This high copy number, along with the relatively high stability of tmRNA, also increases the detection robustness, a critical factor in complex sample matrices such as blood. The difference in end-point fluorescence displayed in Figures 4.1A and 4.3 most likely results from differences caused by the change in the purification capacity between the two experiments; also, the method used to purify RNA is different in each case. These factors may influence the kinetics of the NASBA reaction and consequently the endpoint fluorescence. Furthermore, the negative control fluorescence in the off-chip purification process (Figure 4.1A) is higher (2 AU) than on the on-chip purification (Figure 4.3). Since the procedures were similar, the lower negative control fluorescence in the on-chip purification may be due to reduced contamination. In the on-chip procedure, there are no sample pipetting or sample transfer steps after the purification. Fluorophore bleaching can occur during the real time NASBA reaction; to reduce this effect, the exposure time was limited to 230 ms for the data shown in Figure 4.3.

	RNA Purification and real time NASBA	
	On-chip	*Conventional*
Total Reagent Volume Used	**213 μL**	**2,450 μL**
NASBA Volume	**2 μL**	**20 μL**
Time to Positive	**3 min**	**25 min**

Table 4.1. Comparison of on-chip and conventional "off-chip" RNA purification and real time NASBA. Reproduced from REF [1].

The TTP for samples of crude *E. coli* lysate (Figure 4.3) demonstrates that the various cell numbers can be distinguished from the negative control in as little as 3 min, which, to the best of our knowledge, is more rapid than any previous report of on-chip amplification and detection from as few as 100 cells [5]. With this approach, the total time from "sample to answer" can be less than 30 min. Table 3.1 shows the comparison of on-chip and conventional "off-chip" RNA purification and real time NASBA. Compared to the conventional off-chip method, on-chip NASBA requires approximately 10 times less volume, and the resultant discrimination is approximately 10 times faster (3 min on-chip, 15 – 25 min off chip; see Figure 4.4). Relative to conventional, off-chip procedures, on-chip integration reduces the direct pipetting steps from 11 to 2 and the sample-transfer steps from 3 to 1, reducing significantly the likelihood of sample contamination.

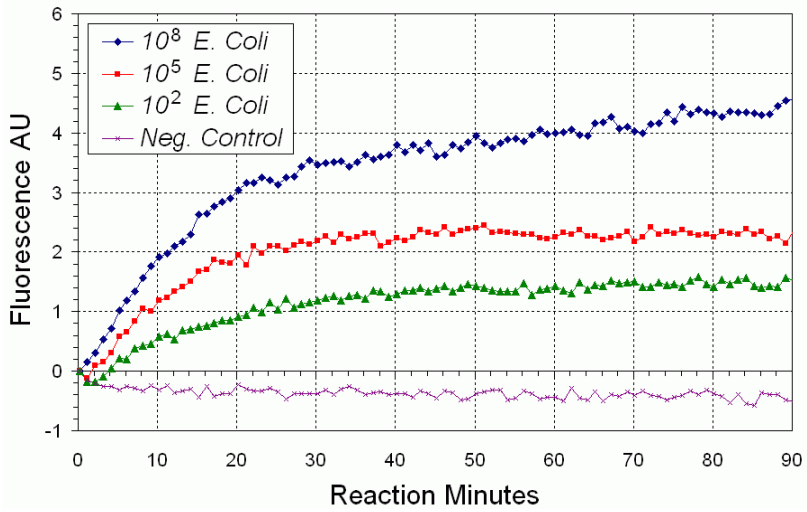

Figure 4.3. On-chip RNA purification and real time NASBA results. On-chip analysis starts by loading crude cell lysate from *E. coli*, followed by RNA purification, then by NASBA with real time detection. Each different sample was run on a on a fresh device. Reproduced from REF [1].

4.4 Conclusion

In this work, the first monolithic microfluidic platform that incorporates tmRNA purification, NASBA-based amplification, and real time fluorescence detection was demonstrated. A unique new method of silica bead immobilisation simplifies device fabrication, effective sample purification, concentration, and operation. The PDMS-based microfluidic device uses a NASBA reaction volume of 2 μL, one tenth of conventional NASBA reaction volumes. Result discrimination can be achieved within the first 3 min after NASBA is initiated, approximately one tenth of the time required in the off-chip NASBA reaction. Direct sample manipulation and pipetting steps are reduced from 11 in the conventional case to 2 in the on-chip case. The fundamental components were characterised and their integrated operation demonstrated with real time detection of crude *E. coli* bacteria lysates from as few as 100 cells in a time of less than 30 min from sample loading to answer. The design is not limited to microbial identification applications: it can be adapted for use as a general RNA purification, amplification, and detection platform for point-of-care molecular diagnostics and clinical applications.

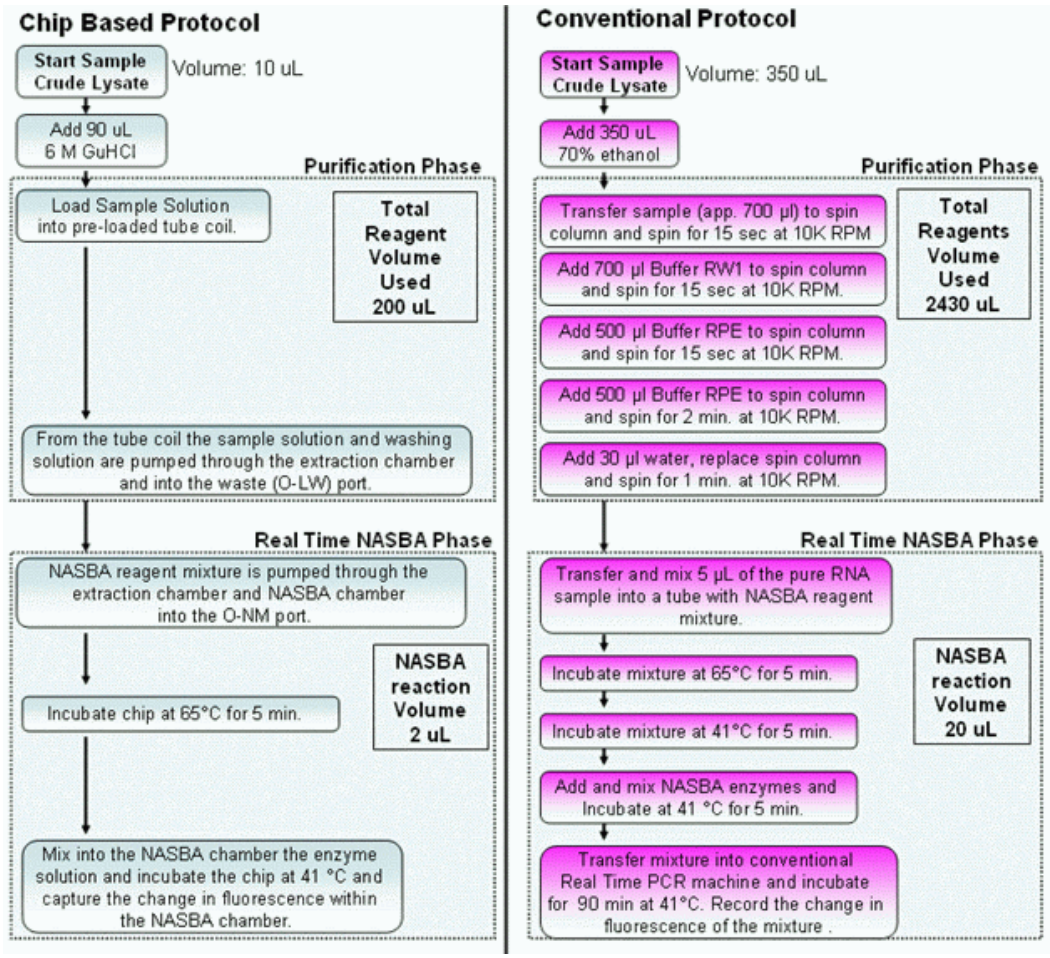

Figure 4.4. Microfluidic RNA purification and Real Time NASBA protocol versus conventional RNA purification and Real Time NASBA protocol. In the microfluidic case approx. ten time less volume is used, results are obtained in approximately one tenth of the time and direct pipetting steps are reduced from 11 to 2. Reproduced from REF [1].

4.5 References

[1] I. K. Dimov, J. L. Garcia-Cordero, J. O'Grady, C. R. Poulsen, C. Viguier, L. Kent, P. Daly, B. Lincoln, M. Maher, R. O'Kennedy, T. J. Smith, A. J. Ricco, and L. P. Lee, "Integrated microfluidic tmRNA purification and real-time NASBA device for molecular diagnostics," *Lab on a Chip*, vol. 8, pp. 2071-2078, 2008.

[2] Y.-C. Chung, M.-S. Jan, Y.-C. Lin, J.-H. Lin, W.-C. Cheng, and C.-Y. Fan, "Microfluidic chip for high efficiency DNA extraction," *Lab on a Chip*, vol. 4, pp. 141-147, 2004.

[3] L. A. Legendre, J. M. Bienvenue, M. G. Roper, J. P. Ferrance, and J. P. Landers, "A Simple, Valveless Microfluidic Sample Preparation Device for Extraction and Amplification of DNA from Nanoliter-Volume Samples," *Anal. Chem.*, vol. 78, pp. 1444-1451, 2006.

[4] B. Glynn, K. Lacey, J. Reilly, T. Barry, T. J. Smith, and M. Maher, "Quantification of Bacterial tmRNA using in vitro Transcribed RNA Standards and Two-Step qRT-PCR " *Research Journal of Biological Sciences* vol. 2, pp. 564-570, 2007.

[5] L. Chen, A. Manz, and P. J. R. Day, "Total nucleic acid analysis integrated on microfluidic devices," *Lab on a Chip*, vol. 7, pp. 1413-1423, 2007.

Chapter 5: *i*NASBA - Integrated NASBA Array For Quantitative Nucleic Acid Testing

Characterisation of the integrated Nucleic Acid Sequence-Based Amplification (*i*NASBA) array is presented. Since NASBA is an isothermal amplification method for nucleic acids, it does not require a thermo-cycler. The amplification conditions for NASBA are constant and the optimization for each new assay is simpler than in the case of PCR. Moreover, NASBA is as sensitive as RT-PCR and allows selective amplification of single-stranded RNA in a background of comparable genomic dsDNA. The *i*NASBA array includes microfluidic dynamic cell culture, cell stimulation, cell labelling, lysis, and real time NASBA based RNA analysis on a single chip. By multiplexing this integrated functionality the device can be used for high content screening, gene expression profiling, and diagnostics. Compared to conventional laboratory analysis, the *i*NASBA array may enable diagnostics for bacteria, viruses, and cancer markers at reduced costs, contamination and sample volumes.

5.1 Hydrostatic Flow

First the hydrostatic flow was charcterised (see Section 3.2 for device and experimental details). The outlet from the row of 8 chambers was connected to a flexible tube (silicone platinum-cured tubing, Cole Parmer, U.S.A.) with several internal diameters and heights. The device and tubes were filled with dH_2O and left to flow until a droplet was formed at the waste container. The time and droplet volume were measured for each tube height and diameter.

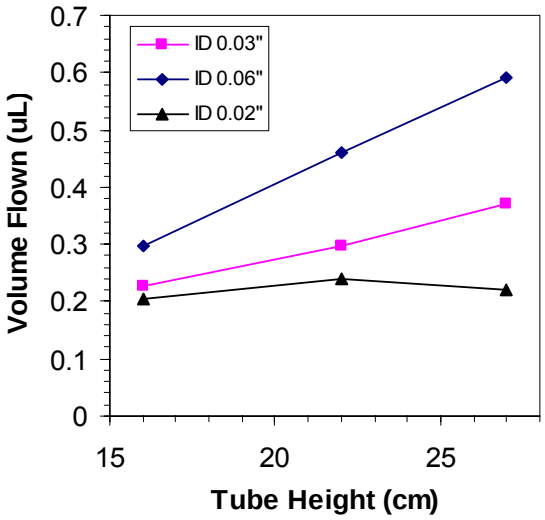

Figure 5.1 Hydrostatic flow characterization through each culture chamber for different outlet tube inner diameters (0.02”-0.06”).

The results (Figure 5.1) show that gravity flow can replace the entire volume of fluid in the culture chamber once per second in the slowest case (see Figure 3.4 in Section 3.2 i.e. approximatley 4 nL per second).

5.2 Cell capture and Dynamic culture

Then cell capture and dynamic culture experiments were done by loading the cells, capturing them and then leaving the media perfusion at 0.2 nL/min (as explained in Section 3.2) for 24 hours. The entire device was placed in a 37 °C temperature controlled incubation chamber (Solent Scientific, UK). HeLa and 59M cells were tested, the culture media used was Dulbecco modified Eagle medium (DMEM) supplemented with 2 mM glutamine, 10% fetal bovine serum (FBS), penicillin, and streptomycin. After the 24 hrs culture period cell viability was checked by using Calcine AM (4 mg/mL in PBS), that stains live cells with green fluorescence, and Propidium iodide (4 mg/mL in PBS) that stains dead cells with red fluorescence (Sigma Aldrich, Ireland) and injecting 100 μL of the 2 dyes into the bottom of the plugged in pipette and allowing the gravity driven flow to perfuse the dye over the cells. Fifteen minutes after the dye injection, the red and green fluorescence in the culture chamber was checked using an inverted

fluorescence microscope (Olympus IX81). The results (Figure 5.2) show that the two cell types can retain viability after a 24-h culture.

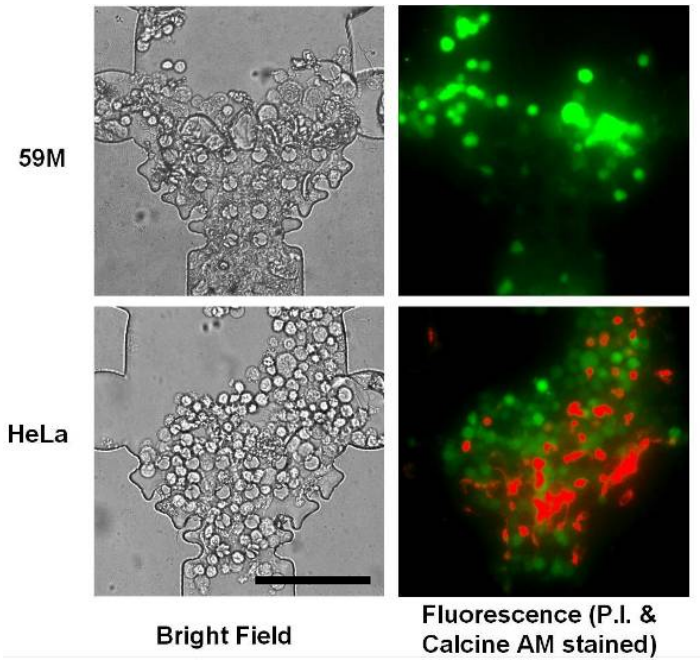

Figure 5.2. Cell culture for 24 hours demonstrating that several cell types can retain viability after being cultured with gravity driven perfusion flow, scale-bar: 150 µm.

5.3 In chamber injection and mixing

For RNA profiling the lysis and real time NASBA mixtures have to be injected into the culture chamber. This was tested with concentrated red food dye. The whole device was mounted on an inverted microscope (Olympus IX81) and the red dye was loaded only into the NASBA mixture reservoir (as explained in Section 3.2) and then the rest of the device was loaded with dH_2O. For injection, the heating electrode under air chamber 1 was activated with ~ 1.5 V and 10 mA for 15 seconds. This injected ~ 1 nL of dye into the cell capture and culture chamber (Figure 5.3). The results from Figure 5.3 show that the food dye, diffusion mixed, within 4 minutes.

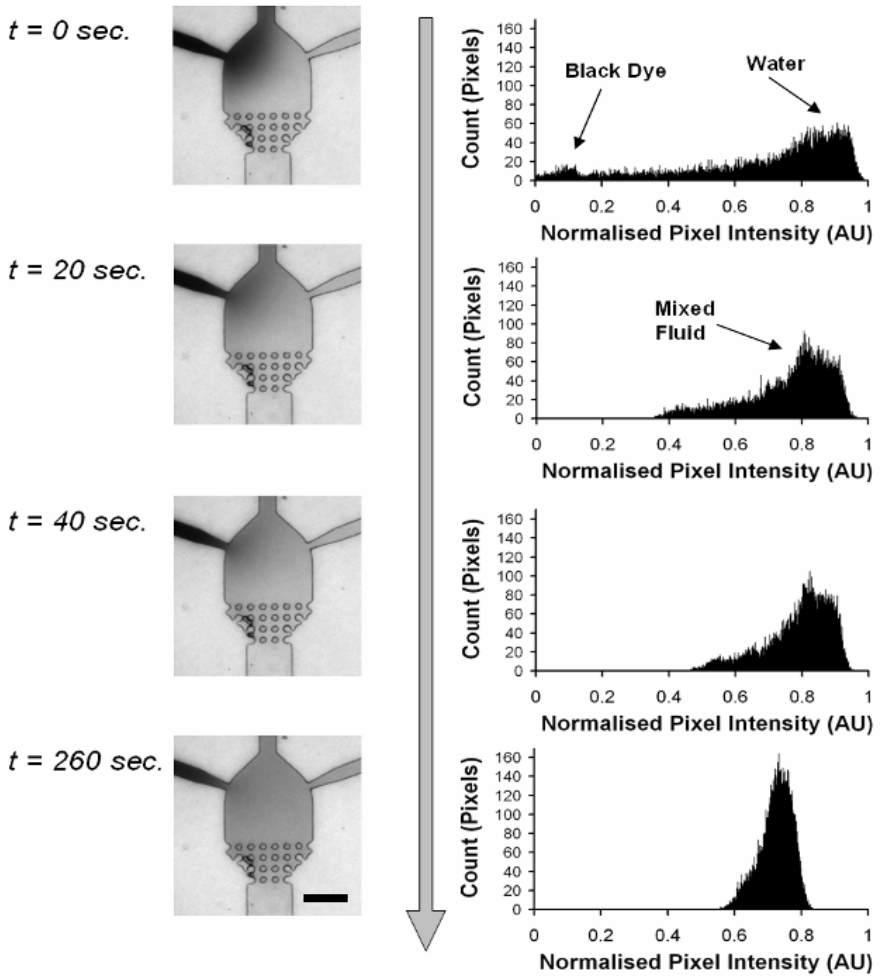

Figure 5.3. In chamber mixing characterization; time lapse micrographs and 2D-histograms of the culture chamber grey scale intensity distribution during the diffusion mixing of the fluids, scale-bar: 150 µm.

5.4 Real Time NASBA in culture chamber

After demonstrating the injection and mixing process, the on-chip real time NASBA was tested. This was done by injecting a pre-mixed real time NASBA mixture. Four mixtures (3 positive controls and a negative control) were injected into all the 8 culture chambers. All reagents required to perform the NASBA amplification were supplied as part of the NucliSens Basic Kit (bioMérieux, UK), except primers and molecular beacon probes, which were supplied by MWG Biotech (Germany). The NASBA mix was prepared according to the manufacturer's recommendations; the final concentration of each

primer was 5 μM, and 5 μM for the molecular beacon probe (FAM fluorophore, BHQ1 quencher; detection at 530 nm).

Both primers and the molecular beacon probe were designed for the specific detection of *E.coli* based on the RiboSEQ platform [1]. The positive controls contained crude *E.Coli* lysate (using the MicroLYSIS PLUS buffer, Microzone Ltd., UK) from approx. 10^7, 10^5 and 10^3 *E.Coli*/mL while the negative controls had the lysate volume replaced with RNA-free water (Molecular Biology Grade Water, Sigma Aldrich, U.S.A.). The device was incubated at 41ºC in a thermally controlled inverted fluorescent microscope (Olympus IX81 with a Solent Scientific, UK, incubation chamber).

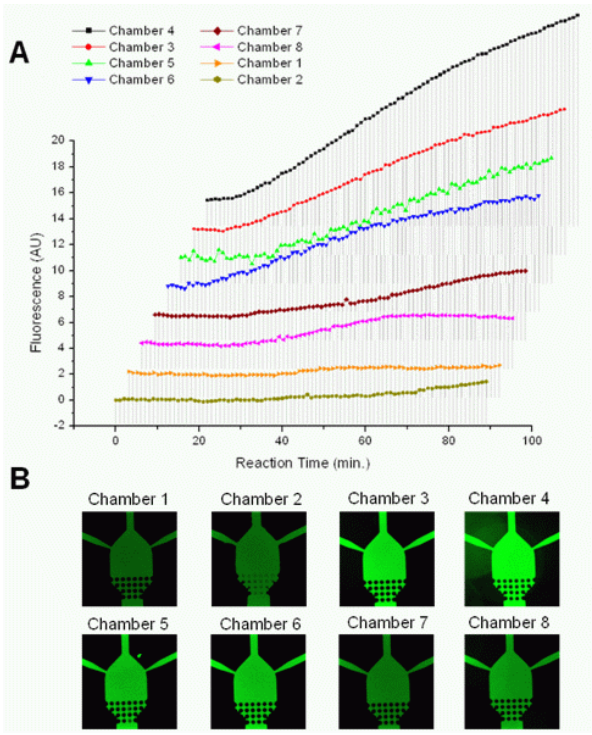

Figure 5.4. Eight parallel on-chip microfluidic real time molecular beacon based NASBA reactions. **(A)** Fluorescence intensity plots in arbitrary units for each chamber over the course of the NASBA reactions. Each real time NASBA chamber was loaded with NASBA mixture and the following samples: Chamber 1 & 2-RNA free water (Neg. Control); Chamber 3 & 4-Lysate with approx. 10^7 *E.Coli*/mL; Chamber 5 & 6-Lysate with approx. 10^5 *E.Coli*/mL; Chamber 7 & 8-Lysate with approx. 10^3 *E.Coli*/mL **(B)** fluorescence in each NASBA chamber after 90 min.

Every minute during the incubation each NASBA chamber was excited with a 492-nm beam (excitation filter BP492/18 with a xenon light source, CellR MT20, Olympus) for

190 ms and the 530 nm fluorescent light was sampled through a filter cube (U-MF2, Olympus) with a CCD sensor (Hamamatsu C4742-80-12AG). The change in the average fluorescence of each chamber was plotted over time (Figure 5.4) and shows that 8 parallel real time NASBA reactions were successfully performed in the 4 nL cell culture chambers.

5.5 Discussion

By utilizing gravity driven passive pumping 8 individually addressable culture media reservoir and pumping units can be densely integrated. By varying the height of the outlet tube the flow velocity in the culture chambers can be adjusted. The opened pipette tips allow for an easy, gentle and independent insertion of cells for loading the device, quick insertion of the stimulation drugs and labelling dyes.

5.6 Conclusions

An integrated NASBA array was designed and fabricated. Proof of concept experiments have shown that each critical part of the device (Figure 5.1-5.4) can be successfully implemented. These results demonstrate for the first time that cellular and molecular functions can be integrated onto a single device providing a potential tool of important value for high content screening, gene expression profiling, and diagnostics. Compared to conventional laboratory analysis, the iNASBA array could enable diagnostics of bacteria, viruses, and cancer markers with lower cost, less contamination, and smaller sample volumes. Even though the iNASBA array device has demonstrated the integration of cellular and molecular functions it still requires improvements in the design to achieve efficient shear-stress free cell loading and culturing. In the current implementation cell capture is done through size based exclusion where cells with a diameter of 5 *μm* or more are capture between the pillar gaps in the cell culture chamber. The problem with this type of cell capture is that it has low capture efficiency as most of the cells pass through the capture structures and into the outlet because most of the flow lines generally go around and pillars. Furthermore since PDMS is an

elastomer the pillars are flexible so the cells can squeeze thorough them. This is evident in Figure 5.2, where cells are squeezed between the pillars. A further disadvantage of the pillar design is that, as cells are captured they are effectively blocking the flow. This has important implications in the system flow control and the shear stress perceived by the cells. As a result a novel cell capture design will be presented in the following chapter that addresses most of these issues.

5.7 Acknowledgements

The author would like to thank Claus R. Poulsen, Sharon O'Toole, John O'Leary and Marek Radomski for providing the cancer cells and Justin O'Grady, Majella Maher and Terry J. Smith for providing the NASBA probes and primers. This work was supported by the Science Foundation Ireland under Grant No. 05/CE3/B754.

5.8 References

[1] I. K. Dimov, J. L. Garcia-Cordero, J. O'Grady, C. R. Poulsen, C. Viguier, L. Kent, P. Daly, B. Lincoln, M. Maher, R. O'Kennedy, T. J. Smith, A. J. Ricco, and L. P. Lee, "Integrated microfluidic tmRNA purification and real-time NASBA device for molecular diagnostics," *Lab on a Chip*, vol. 8, pp. 2071-2078, 2008.

Chapter 6: *i*Cell Array for Quantitative Cell Based Science

Characterisation of the *iCell array*, is presented. This technology can perform completely integrated cell based assays with bio-analytical read-out protocols such as immunofluorescent imaging and NASBA based real time nucleic acid amplification. The *iCell array* enables parallel and configurable on-chip integration of complex procedures such as highly efficient capture of adherent and non adherent cells, perfusion cell culture, cytotoxicity assays, drug treatment, gene expression analysis, protein immunoassays and real time optical analysis. With on-board gravity driven flow control the device is simple and economical to operate with dilute samples (down to 5 cells per reaction), low reagent volumes (50 nL per reaction), highly efficient cell capture (~100% capture rates) and single cell protein and gene expression sensitivity. In the current design *iCell array* can process up to 512 10-nL reactions in a single chip and up to 64 different user-defined integrated assays can be done simultaneously. To the best of my knowledge this is the first demonstration of a versatile fully integrated microfluidic array platform for dynamic cell studies that can be universally and economically used from routine applications in a biology laboratory to high content screenings.

6.1 Characterisation of the iCell array operation

The microfluidic *iCell array* (Figure 3.6 see Section 3.3 for device and experimental details) integrates a wide range of unit operations such as cell capture, filtering, reagent loading, mixing and controlling in a simple and configurable manner. This allows a seamless and flexible 'on-chip' integration of complex cell based or particle based assays together with bright field or fluorescent microscopic monitoring and real time detection of nucleic acid amplification or protein expression. The key to achieving this level of integration and flexibility lies in the ability to dynamically configure and execute a sequence of basic unit operations that are required in a complete assay, including experimental and analytical procedures. Assays are performed in the basic processing chamber structure (Figure 3.6C-D). This structure consists of a chamber with a trench.

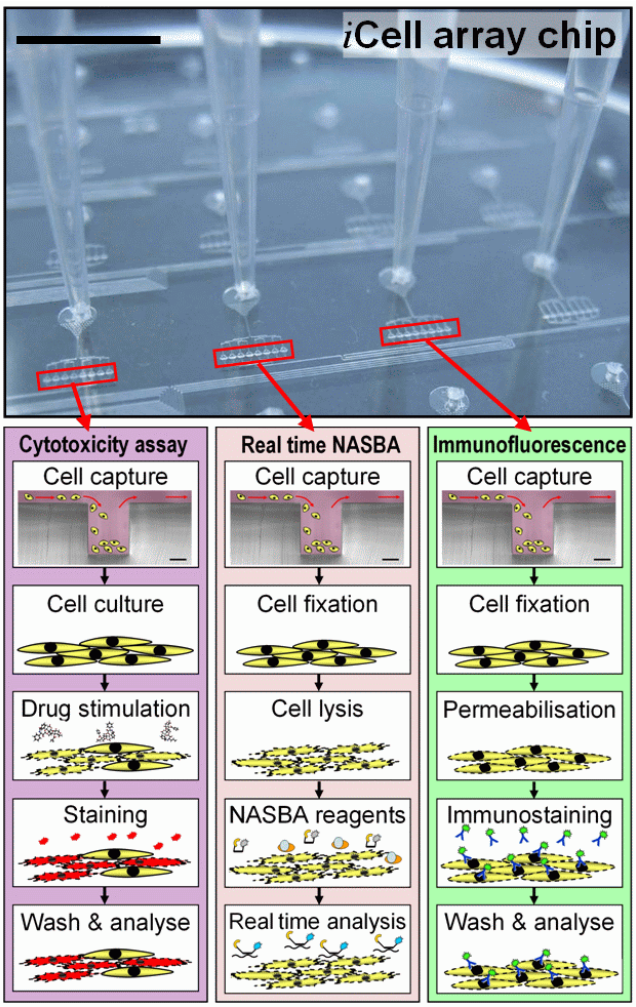

Figure 5.1. Photograph of the multiplexed integrated cell based assay system (*iCell array*) with fluid columns in 4 of the 64 processing modules. The integrated function of each processing module can be flexibly selected by the user and depends entirely on the sequence and timing of the fluid inputs. The basic steps required for three different cell based assays are illustrated. This versatility allows the user to combine cell stimulation and gene and protein expression analysis on a single microfluidic platform, Scale-bar: 9 mm.

The key characteristic of the trench structure is that it allows the capture of cells and particles through gravitational sedimentation. In addition, a controlled flow over the top of the trench allows successive, diffusion driven loading, mixing and replacement of fluids within the trench. The required flow control is achieved by setting the height of a fluid column that generates the pumping hydrostatic pressure at the inlet (Figure 3.6 E). The fluid column is open on the top which allows for easy insertion of cells and the replacement of the fluid being loaded into the device. The operation paradigm of this

device is different to the more established “connection of specialized blocks” paradigm used in electronic integrated circuits and high density fluidic circuits (e.g. as in fluidic devices shown by Quake, et al. [1]). Instead, the device operates by using a single multipurpose structure that can retain cells or particles and delay the diffusion of molecules of interest in the same space where different reactions are sequentially performed. This approach has several advantages, firstly higher assay sensitivities are achieved because the molecules of interest do not have to be transported and thus they interact with less surface area, reducing the loss of target “molecules”. Second the purpose or function of the structure is completely determined by the fluid flown into it and its previous contents, thus by selecting the sequence of input fluids the multipurpose structure can be “programmed” to perform a variety of complex assays. In addition the simplicity of the multipurpose structure and its operation allows it to be easily multiplexed into an array that can perform a large number of simultaneous integrated assays.

6.1.1 Characterisation of Basic Unit Operations

To demonstrate the effectiveness of the novel design and operation the two basic unit operations (Figure 3.6 E); 1. Cell capture and 2. Fluid loading and diffusive mixing are characterized. Computational fluid dynamics was used to predict the effect of the main design parameters on the performance of the principal unit operations (see Section 3.3.10). These unit operations are cell capture and fluid loading and mixing. Cell capture allows the loading and retention of cells or particles in the processing chamber, through the gravitational sedimentation and capture of particles that are denser than the medium. The particle trajectories were calculated by solving the force balance equation for each particle (see Section 2.3).

The particle capture efficiency within the processing chamber trench was evaluated for different inlet velocities, trench geometries and particles sizes. From the calculations it (Figure 5.2A-C) can be seen that a 100 % particle capture efficiencies can be achieved as long as the operational range of the fluid inlet velocity is kept below 100μm/s and the ratio of the channel to trench depth (h_1/h_0) is over 5. As was shown by Manbachi et al.

2008 [2] once the particles reach the bottom of the processing chamber trench, they are shielded from shear stress, this is because the magnitude of the fluid velocity at the bottom of the trench is at least 3 orders of magnitude less (Figure 5.5) as compared to the top of the trench in chambers with a channel to trench depth (h_1/h_0) ratio over 5. This result also means that once cells or particles reach the bottom of the trench they are effectively captured. This was confirmed in experiments with 1.5-μm silica beads and input flow speeds of 20 μm/s close to 100% of the beads were captured within the chamber (see Figure 5.5, and movie SM2). Experiments with adherent cells (HeLa, MCF7) and non-adherent cells (plasma cells U266, macrophage J774) also demonstrated very high capture and retention efficiencies (see movie SM8). The number of loaded cells in each processing chamber can be controlled by the loading time (Figure 5.6B-C) and the density of the cell suspension at the inlet. In addition, the successful capture and retention of bacterial cells (*E. coli)* at the bottom of the trench was also demonstrated, however; the capture efficiency of *E. coli* was low due to the small difference in density between bacterial cells and the aqueous medium (see Figure 5.7 and movies SM3 and SM4).

Species loading and mixing within the processing chamber and the trench geometries was predicted by calculating the transient convection and diffusion mass transport model (**eq. 2.10**) in a transient incompressible Navier-Stokes fluid velocity field (**eq. 2.4**) within the trench geometry.

The calculations (Figure 5.2D-E) demonstrate that the average concentration of a species within the trench can be completely controlled by the fluid flow over the trench. The removal of the initial species by a new species is simply done by flowing the new species over the trench, and allowing for the new species to diffuse into the trench while the initial one diffuses out of the trench. This can be repeated in a cyclical manner to produce a sequential exposure of the cells in the trench to different species (Figure 5.2D). If an intermediate mixture level is required within the trench such that a fraction of the mixture in the trench should correspond to the new species and the rest to the initial

contents then that result can be achieved by stopping the flow at a time *ts* < *Tn* (*Tn* is the time to complete species replacement within the trench, see Section 3.3.10) as shown in Figure 5.2E-F. Once the flow has been stopped the 2 species mix through diffusion and the concentration within the trench is homogenised (Figure 5.2E-F).

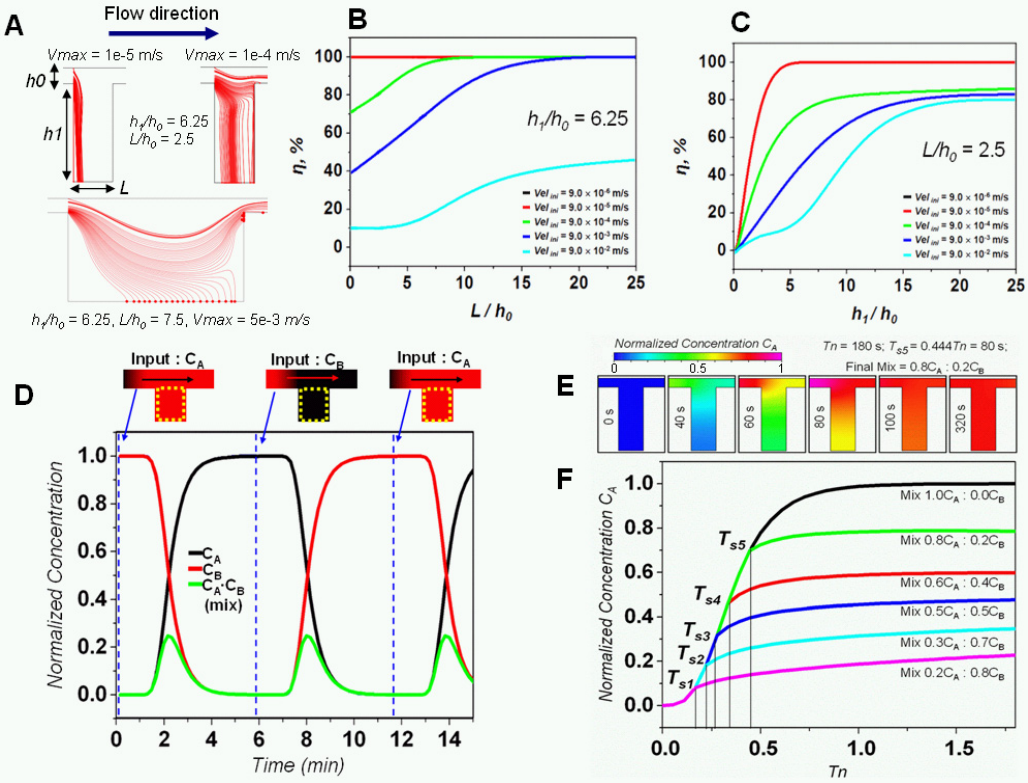

Figure 5.2. Predicting the effect of the main design parameters on the performance of the basic unit operation using computational fluid dynamics. (A) Particle trajectories for different inlet velocities and trench geometries (B) Trench length and inlet velocity effect on the particle capture efficiency η (C) Trench depth and inlet velocity effect on the particle capture efficiency η (D) sequential loading (inlet velocity 10^{-4} m/s) of species C_A (D ~ 10^{-10} m^2/s) into a trench structure h_1/h_0=6.25, L/h_0=2.5 with species C_B. (E) Time lapse of the C_A concentration within the trench during the creation of a $0.8C_A$: $0.2C_B$ mixture, flow is stopped at *Ts*= 80s or at *Tn*=0.444. Within 40 s the C_A concentration (D ~ 10^{-10} m^2/s) homogenizes and stabilizes within the trench (F) Creation of several mixture ratios of the initial species C_B and the new added species C_A in the trench structure, the mixture ratio is controlled by the flow stopping time T_S which is less than the refreshment time *Tn*.

Species form within the trench can diffuse out and into the surrounding channel but the reduced micron scaled dimensions if the channel delay that process, such that average the concentration within the trench can be kept constant within a ± 10% variation for

over 150 min (Figure 5.3) sufficient for most enzymatic reactions such as PCR or

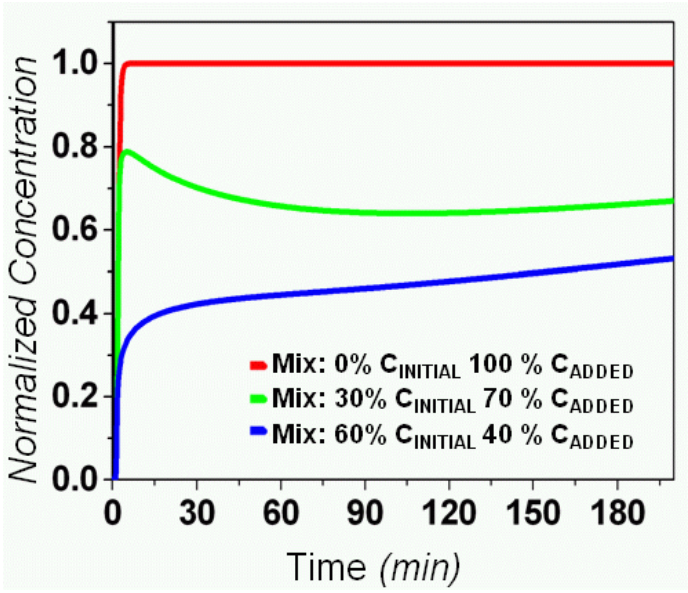

Figure 5.3. Mixtures can be maintained within the trench for long periods of time without the need for active valves. If the flow is stopped at a time ts < *Tn* then a mixture is created and maintained as shown in the figure. For variation of ± 10% the mixture can be stable for over 150 min. Simulation parameters: diffusion coefficient D=5.9 x 10^{-9} m^2/s geometry h_1/h_0 = 6.25, L/h_0 = 2.5. For proteins or bigger bio-molecules, D is usually 2 orders of magnitude smaller (D ~ 10^{-11} m^2/s) so mixtures are more and last for longer times.

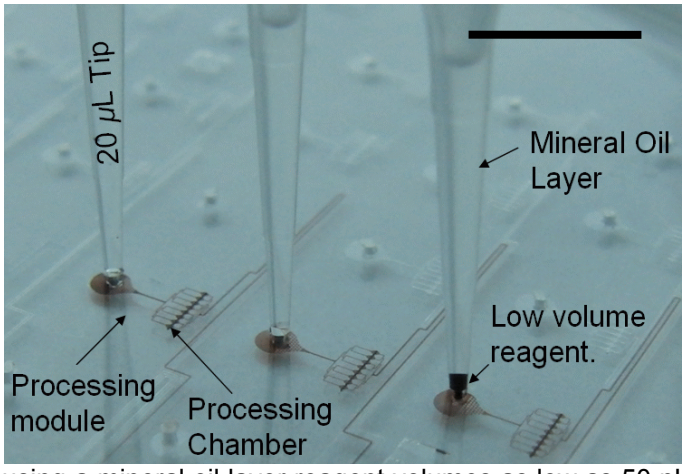

Figure 5.4. By using a mineral oil layer reagent volumes as low as 50 nL can be loaded into the processing chamber. This reduces the reagents costs and allows the device to be used in applications where sample or reagent volumes are extremely limited, scale-bar: 9 mm .

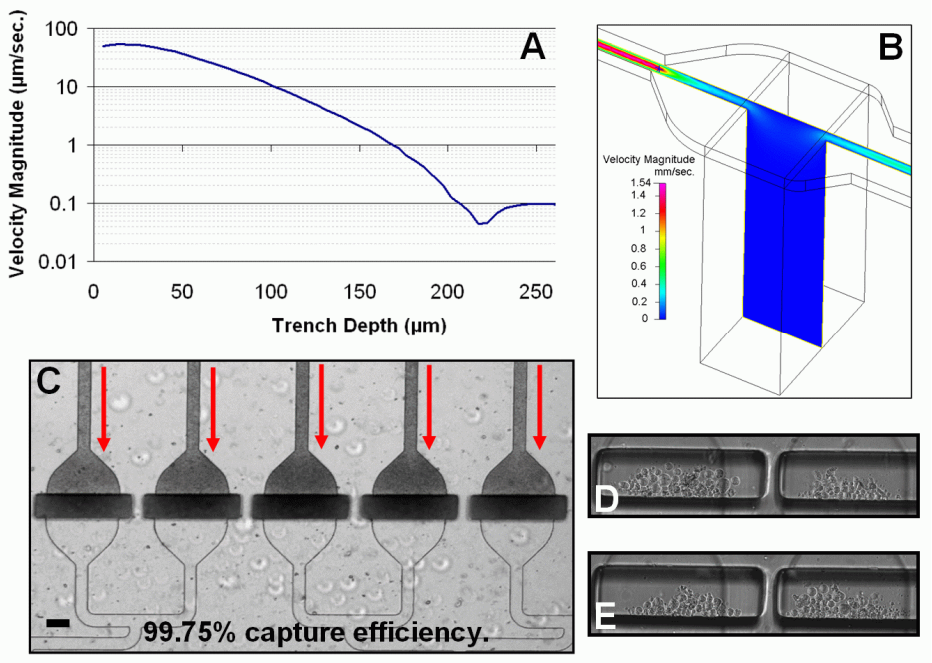

Figure 5.5. (A-B) CFD simulation results of the flow velocity magnitudes in the processing chamber and trench. Cell capture is achieved due to the flow velocity magnitude in the trench being approximately 3 orders of magnitude lower the flow above it. So particles that enter the low flow velocity region are effectively captured. Experiments with 1 µm silica beads (C) demonstrate the capture efficiency of the structure. See support movie SM2 (D-E) Cancer (HeLa) cells are also efficiently captured in the processing chamber, scale-bar: 100 µm.

NASBA [3]. This is a similar strategy to the one used by Du et al. 2009 [4] to maintain stable gradients within microfluidic channels for several hours. Experimental results with a fluorescent dye confirmed that when a new solution is flown into the processing chamber it gradually mixes with and finally replaces the previous contents of the chamber (Figure 5.8) and that the time to complete species replacement within the trench *Tn* is dependent on the flow velocity over the trench.

Gravity driven fluid control is accomplished by inserting a standard pipette tip into a primed device inlet and then loading it with the input fluid (Figure 5.6A), the flow velocity is regulated by the height of the fluid column. By using standard 200 *µ*L pipette tips, velocities of more than 600 *µ*m/sec can be generated at the inlet of the processing chamber. The hydrostatic pressure head of small inlet volumes can be increased by stacking a second (immiscible and inert) liquid such as mineral oil on top. This allows volumes as low as 50 nL to be readily driven into each processing chamber (Figure 5.4).

This method makes the device ideal for applications where sample or reagent volumes are very scarce or expensive.

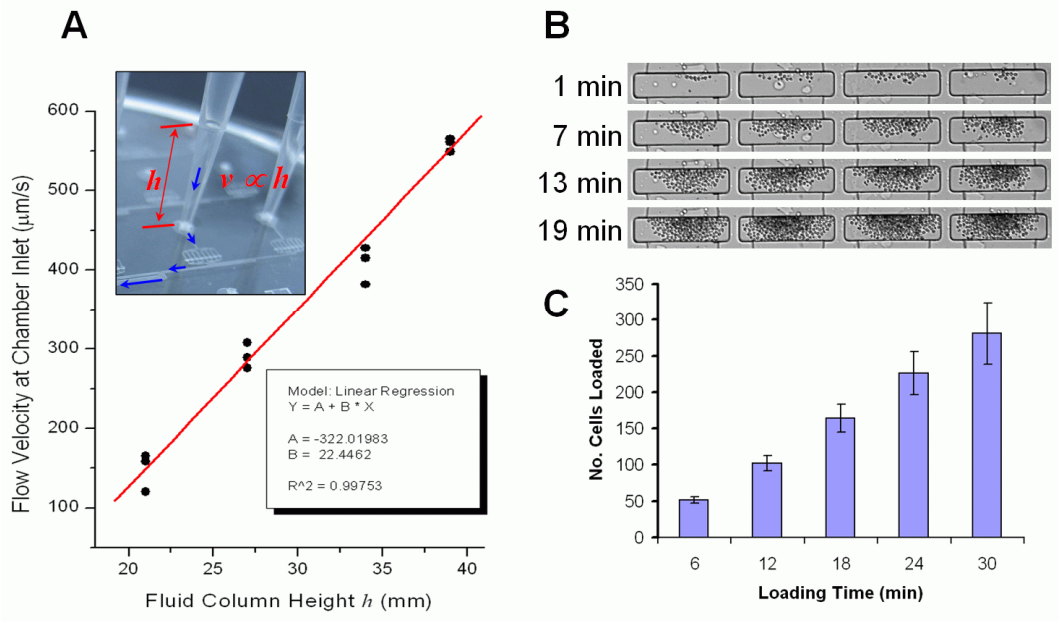

Figure 5.6. Unit operations: (A) Gravity driven fluid control that depends on the height of the fluid column. The height of the fluid column can be regulated by controlling the amount of fluid inserted into the tip. (B-C) Cell capture is accomplished by allowing cells in the flow to sediment to the bottom of the central trench structure. Flow velocities at the bottom of the trench structure are 3 orders of magnitude lower than in the rest of the device allowing the cells to be effectively retained. Due to the high capture efficiency the number of loaded cells in the trenches can be controlled with the cell loading time.

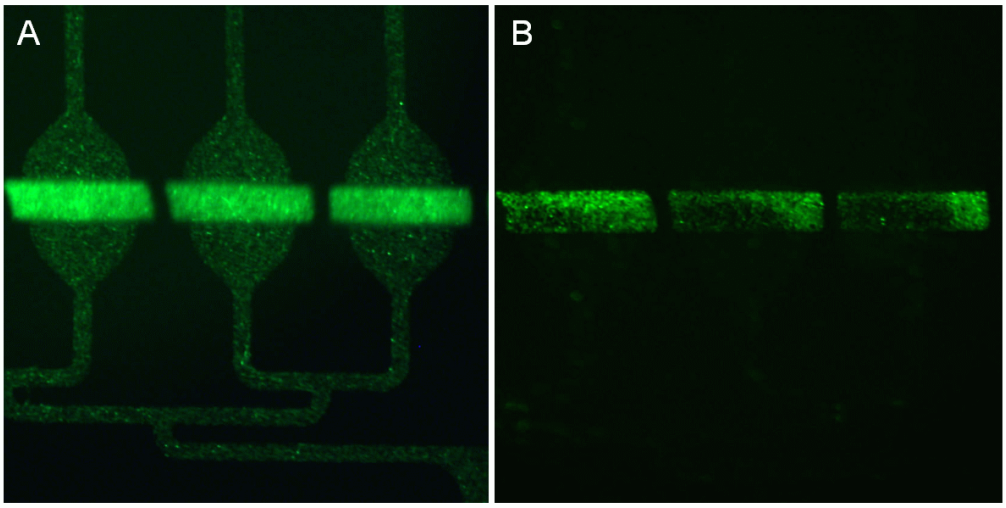

Figure 5.7. GFP *E. Coli* were captured with the processing chamber allowing bacterial cell based assays to also be done with the *iCell* array. (A) Initially the device is loaded with the bacterial solution, (B) After which a washing solution is flown in to rinse out any non captured bacteria. Due to the low flow field at the bottom of the processing chamber trench, the bacteria present there will be effectively captured and not washed away. Due to the very low density of the *E. Coli* bacteria, the capture efficiency is much lower than that of denser particles or cells such as cancer cells.

6.1.2 Complex Integrated Assays

The basic unit operations can be dynamically and seamlessly combined into sequences that perform more complex integrated assays. The key characteristic of the trench structure is the ability to efficiently capture cells through sedimentation and the mere diffusive loading, mixing and replacement of liquids through a controlled flow over the top of the trench. As shown in Figure 5.1 a wide range of cell-based assay can be performed in parallel on the same platform. Figure 5.1 illustrates the combination of individual operation units required for a cytotoxicity assay, real time gene expression analysis (NASBA) and immuno-fluorescent protein analysis. Priming of the chip, loading with the cell suspension and cell capture are common unit operations for all three assays. The user has now the option to grow the cells within the chip by continuously perfusing the cells with fresh medium or to perform molecular analysis assays directly on the captured cells. Cells can be stimulated with drugs and fixed, permeabilized or lysed for the consecutive analysis. In this study several assays were implemented on-chip including, a tmRNA based *E. coli* diagnostics assay, Paclitaxel cytotoxicity assay, gene expression analysis on mRNA level of the Estrogene receptor alpha (ESR1 - is associated with breast cancer) and the protein expression analysis of the ESR1 nuclear receptors. In order to further demonstrate the versatile potential of the chip, a drug treatment study for the down regulation of ESR1 nuclear protein was performed.

The initial steps for on-chip experiments are often shared by a number of different cell-based assays (Figure 5.1). The priming of the chip and cell capture is usually followed by a sequential combinations of unit operations such as cell culture, fluorescent staining and lysis (Figure 5.8). On-chip cell culture showed quick adoption of cells to the new microenvironment and exponential cell growth until reaching of confluence in three days. Cells were cultured under continuous perfusion with a constant feed of nutrients with fresh medium and constant removal of cell growth by-products with the out going feed.

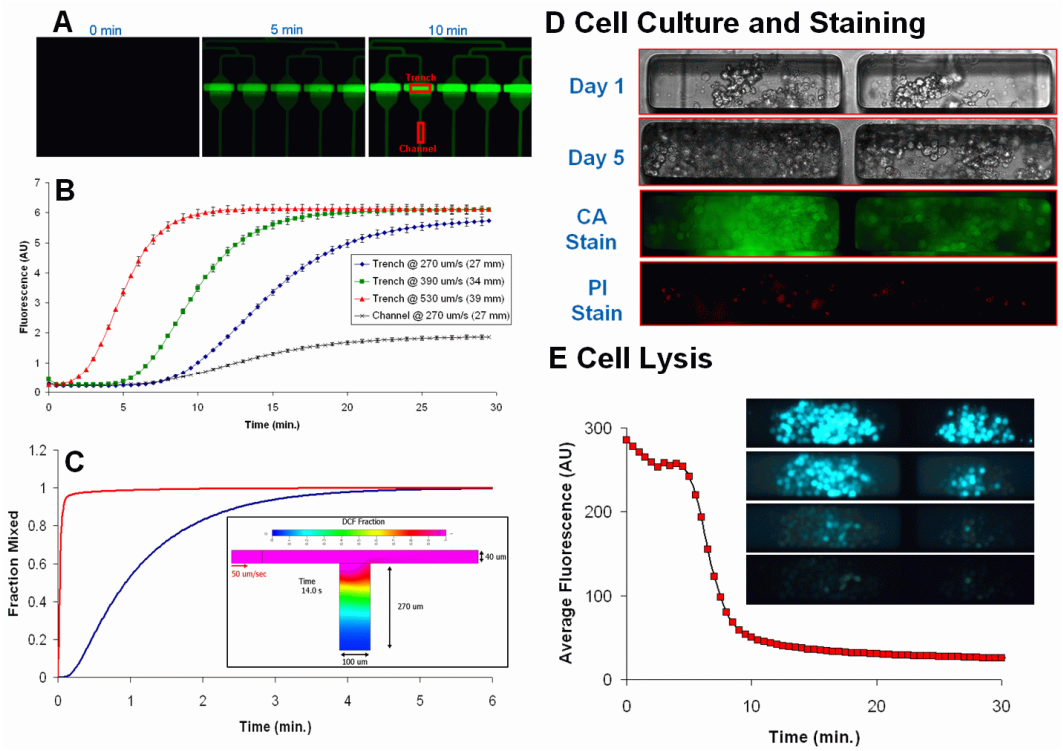

Figure 5.8. Fluid loading and mixing unit operation is achieved due to the slow diffusion mixing of the input fluid with the previous contents of trench. (A) Experiments with fluorescent dye (DCF) mixing with water. (B) Dependence of the mixing speed on the input flow velocity. (C) Simulations demonstration the mixing of DCF with water within the trench. The fluid loading and mixing unit operation enables the execution of some basic cell based assay procedures such as cell culture and staining (D) and cell lysis (E).

Moreover, cells captured in the trench structure are protected from the shear stress of the flowing medium due to minimal velocities in the bottom of the trench. Trapped cells were exposed to CA staining and Propidium iodide showing cell viability after five days of cell culture (Figure 5.8D). Finally, fluorescently stained cells were lysed using a commercial buffer compatible with nucleic acid amplification for 30 min and the efficiency of the cell lysis was monitored in real time by fluorescent microscopy. Figure 5.8E demonstrates the cell lysis process which initiates within five minutes and it is almost complete within less than ten minutes from the loading of the lysis reagent.

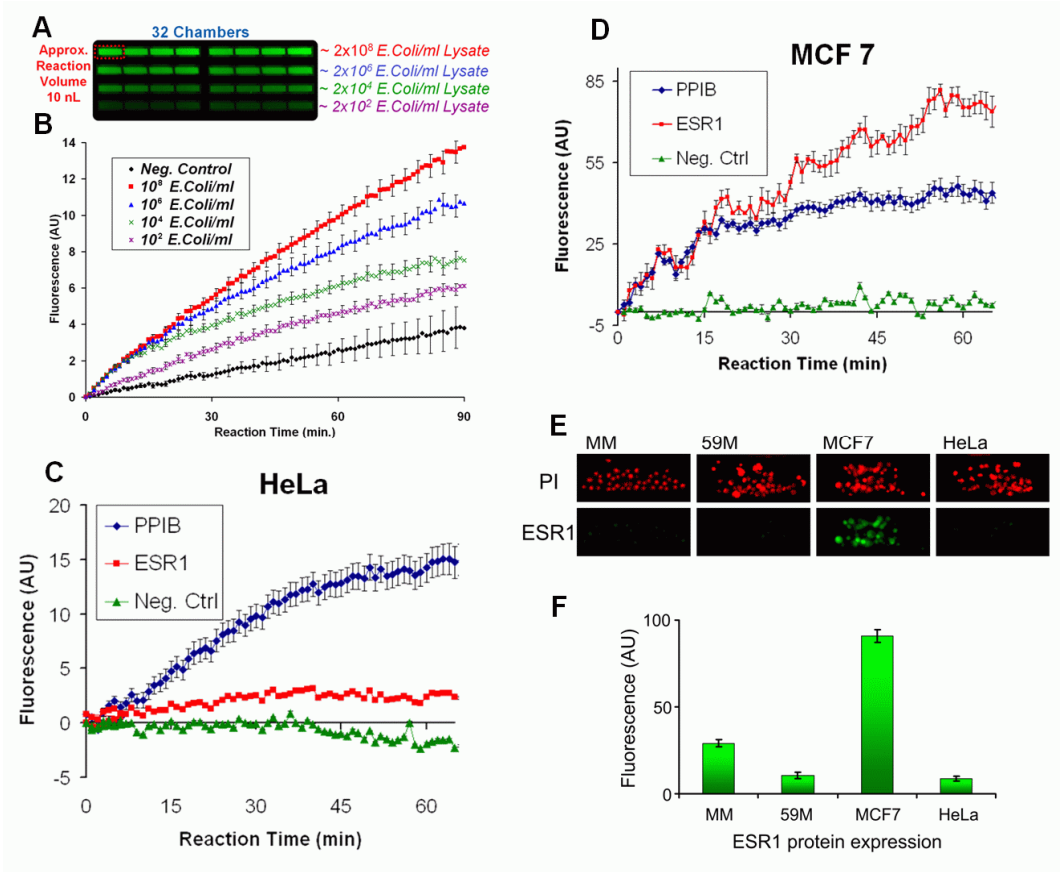

Figure 5.9. *iCell array* real time NASBA (A) End-time fluorescence within the processing chambers after the (B) real time NASBA *E. coli* diagnostic assay. This further demonstrates that rapid and sensitive NASBA can be performed within the *iCell array* chip. (C-F) Oncogene: Estrogen Receptor Alpha (ESR1) integrated single-chip cell based assays. Multiplexed real time NASBA assays detects the expression of the ESR1 gene in comparison to the house keeping gene PPIB in (C) HeLa and (D) MCF7 cells. As expected the ESR1 gene is highly expressed in the MCF7 cells. (E) This was further verified with a ESR1 nuclear receptor protein detection immuno-fluorescent assay. U266 (MM), 59M, MCF7 and HeLa cells on-chip, fixed, permeabilized and nuclear stained using Propidium iodide (PI) and anti-ESR1 (green) antibody. (F) MCF7 cells show specific nuclear staining for ESR1. All standard error bars are based on the eight replicates (n=8) in each processing module.

Nucleic acid analysis based amplification of RNA and real time detection can be readily performed within the device. Real time NASBA is used for the nucleic acid detection on-chip. Compared to other in-vitro amplification methods such polymerase chain reaction (PCR) [5], strand-displacement amplification (SDA) [6] or rolling-circle amplification (RCA) [7], NASBA has the unique characteristic that it can, in a single step, amplify RNA sequences. Furthermore NASBA has the unique ability to specifically amplify RNA in a background of DNA of comparable sequence [8], this reduces the requirements on

sample purification. Also since NASBA operates at 41 ºC, much lower than the 95 ºC required in PCR cycling, there are fewer problems with on-chip the sample drying or thermal displacement, eliminating the need for valves or other active components for containing the contents of the reaction chamber. It also reduces the thermal design requirements of the chip and makes the chip operation simpler.

Here NASBA is demonstrated (Figure 5.9) by performing an on-chip *E. coli* diagnostic assay. Based on custom designed RiboSEQ targeting primers [9] and molecular beacons the device was able to detect down to 10 *E. Coli* cells in 100 *μ*L within 7 minutes (Figure 5.9B), giving a sensitivity of approximately a single target copy. Note that each *E. coli* contains approximately 500-1,000 copies [10] of the tmRNA RiboSEQ target fragments resulting in approximately a single target copy within a 10 nL volume. tm-RNA also has a relatively high stability compared to mRNA which also increases the detection robustness. This sensitivity is also reinforced by the larger depth of trench geometry of the processing chamber that insures that more fluorescent signal is collected in a single exposure. This is also clearly evident in Figure 5.8A-B where at constant fluorophore concentration and excitation, the intensity of the fluorescent signal collected from the trench area is 8 fold higher then one from the inlet channel.

Next, NASBA is performed on eukaryotic cells captured in the *iCell array*. Since estrogen receptor alpha (ESR1) is a major oncogene in breast cancer [11], ESR1 positive MCF7 breast cancer cells were used to demonstrate multiplexed, real time NASBA-based gene expression analysis. Furthermore this analysis was complemented with an ESR1 protein detection based on immuno-fluorescent staining. With primers and molecular beacons specific to ESR1 and to the house keeping gene PPIB [12] the device is capable of performing an integrated real time NASBA protocol (Figure 5.9C-D) from as few as ten cells. Due to the versatility of the *iCell arra*y an immuno-staining assay on-chip was used to detect the expression of ESR1 protein. Since gene level expression of ESR1 was shown in MCF7 cells using NASBA and its absence in HeLa cells, the same model cells were used for immunostaining. ESR1

protein is known to be localized in the nucleus of MCF7 cells [13] and absent in HeLa cells [14]. Additionally other cell lines were used; the ovarian cancer cell line 59M and non-adherent plasma cells U-266 (MM) to investigate the protein analysis. The cells were captured, fixed, permeabilized and immunostained on the chip (Figure 5.9E-F). The anti-ESR1 antibody staining showed a specific nuclear staining in MCF7 cells and much lower staining signals in HeLa, 59M and U-266 cells.

These can be further combined into a complete drug study experimental protocols, this was demonstrated (Figure 5.10) with a cytotoxicity analysis of the anti-cancer drug Paclitaxel [15] on HeLa cells and a study of the down regulation effects of the As_2O_3 drug on ESR1 in breast cancer cells MCF7.

Paclitaxel is a well know anti-cancer agent that reduces the growth and proliferation of cancer cells. To perform the dynamic cytotoxicity experiments 64 processing chambers were loaded with approximately 50 HeLa cells and cultured for one day after which the cells were stimulated with eight different concentrations of Paclitaxel raging from 0 μM (control) up to 100 μM for 48 hours. Cell viability was quantified through Propidium iodide and Calcine AM fluorescent staining of all the cells. As expected the fluorescent imaging revealed (Figure 5.10A-B) that as the drug concentration is increased and so does the number of dead cells in relation to the number of live cells.

The effects As_2O_3 on ESR1 expression were studied by loading 128 processing chambers with ESR1 positive MCF7 cells and as a negative control ESR1 negative HeLa cells. The MCF7 cells were stimulated for 48 hrs with seven different concentrations of As_2O_3 and the ESR1 protein quantified with nuclear immuno-fluorescent staining. As in previous reports [16] the results show (Figure 5.10C) that As_2O_3 has a strong effect in down-regulating the expression of ESR1 in MCF7 cells.

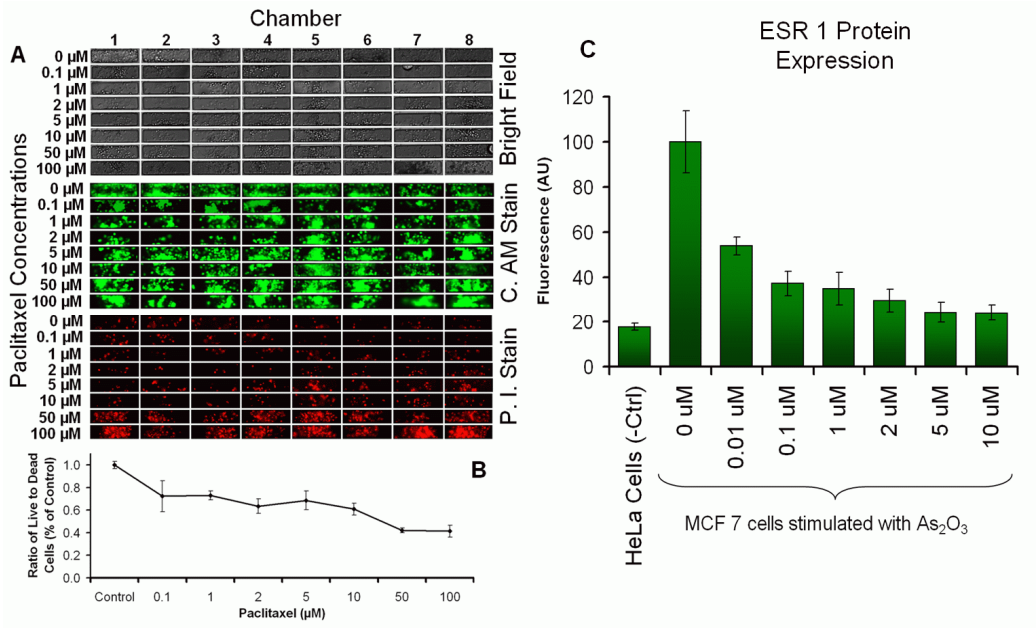

Figure 5.10. Complete drug study experimental protocol execution on the *iCell array. (*A) HeLa based cytotoxicity assay validating the effect of Paclitaxel, a well know anti-cancer agent that (B) reduces the growth and proliferation of cancer cells. (C) Study of the down regulation effects of the As_2O_3 drug on ESR1 in breast cancer cells MCF7. In a fully integrated on-chip assay the effects of arsenite on the protein expression of ESR1 in MCF7 cells were studied by loading 128 processing chambers with MCF7 and HeLa cells and stimulating the cells with several concentrations of As_2O_3 over a period of 72 hrs, after which the protein expression was analysed on-chip with immuno-fluorescent nuclear staining and detection. All standard error bars are based on the eight replicates (*n*=8) in each processing module.

6.2 Discussion

The *iCell* array is compatible with standard existing laboratory infrastructure. The inlet distribution is the same as that of standard 96 well plate so cells and reagents can be loaded using multichannel pipettes and/or pipetting robots (Figure 5.11). Additionally in contrast to standard microfluidic devices that use syringe pumps, reagent replacement or refilling is done in a simple and bubble free manner; this way cells are loaded efficiently and with very low shear stress into the device. The trench structure captures and isolates cells from the direct flow which also enables the capturing and processing of bacterial cells (Figure 5.7 and movies SM3, SM4). Furthermore the *iCell* array integrates flow control and gravity driven pumping which makes it independent from external pumps or other macroscale active components and allows it to be easily

inserted and used within incubation or environment control chambers and standard fluorescent microscope systems or even some plate readers. In essence the *iCell* array is a nanolitre processing multi-chamber plate that can perform dynamic flow assays with high sensitivity, high level of integration (experiment to answer), and spatial multiplexing without the need for cumbersome, custom made and expensive external active control components such a pumps, pressure sources, solenoid valves, etc. The fabrication process is a simple two layer soft photolithography that does not require precise alignment of multiple layers since only the 1.3 mm inlets have to be aligned to the fluidics layer allowing a large tolerance. Furthermore due to fluidic resistance all the processing modules are fluidically independent so in applications that do not require the use of the complete 512 processing chambers the user can load a subset of modules without having to seal the remaining inlets. This simplifies the *iCell* array operation protocols.

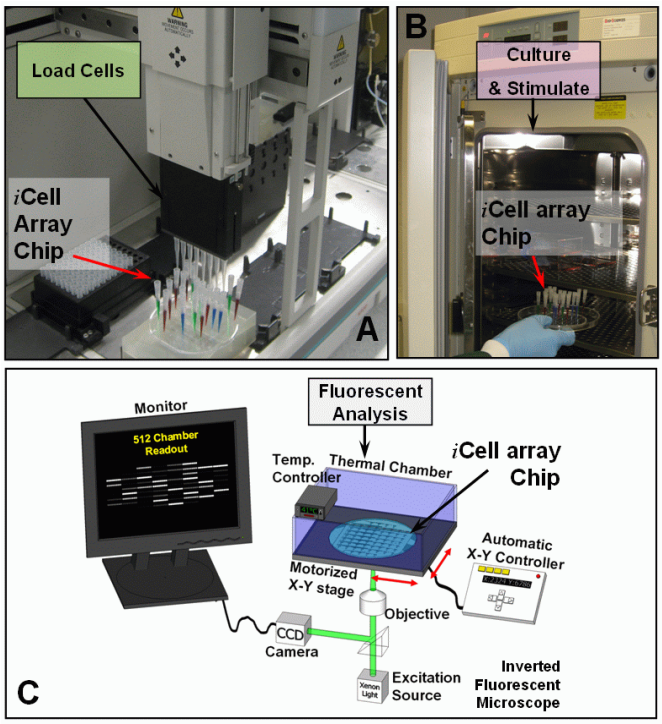

Figure 5.11. With on-chip gravity driven flow control, iCell array is flexible and can be easily integrated into existing infrastructure and workflows such as robotic pipetting systems (A), incubators (B), and fluorescent microscope systems (C).

6.3 Conclusions

This work has demonstrated a novel microfluidic platform, the *iCell array*, that can perform completely integrated complex cell based assays with real time NASBA based nucleic acid amplification and protein expression detection. The technology can combine, in an array format, unit operations such as particle or cell capture, filtering, reagent loading, mixing and controlling in a simple and configurable way. This permits the parallel and versatile on-chip integration of complex procedures such as cell culture, cell stimulation, cell lysis, cell fixing, protein immunoassays, bright field and fluorescent microscopic monitoring, and real time detection of nucleic acid amplification. High assay sensitivity is achieved by trapping and retaining cells or biopolymers of interest in the same space where reactions are sequentially performed. The *iCell array* system does not require any off chip steps providing a true experiment to answer capability. With onboard gravity driven flow control the device is simple and economical to operate, it uses less reagent volumes, and it does not require external macro-scale power sources. This enables the *iCell array* to be directly used with existing laboratory infrastructure such a multichannel pipettes and/or robotic fluid handling systems, incubation or environmental control chambers and microscope systems. In its current design the *iCell array* can process up to 512 10 nL reactions in a single chip and up to 64 different integrated assays can be done simultaneously. To be best of my knowledge this is the first demonstration of a versatile fully integrated microfluidic array platform for dynamic cell studies which can be universally and economically used in any biological laboratory.

6.4 Acknowledgements

The author would like to thank Dr. Arman Rahman for providing the non adherent plasma cells U266. This work was supported by the Science Foundation Ireland under Grant No. 05/CE3/B754.

6.5 Supporting Movies

SM1. *iCell* array processing module priming based on the degassing method.

Movie file: SM1.priming.bubble.removal.avi

SM2. *iCell* array 1 micro particle capture with very high efficiency (**3 movies**).

Movie file: SM2a.1um.silica.bead.capture.avi

Movie file: SM2b.1um.silica.bead.capture.avi

Movie file: SM2c.1um.silica.bead.capture.avi

SM3. *iCell* array GFP *E. Coli* loading.

Movie file: SM3.GFP.EColi.loading.avi

SM4. *iCell* array captured GFP *E. Coli* with washing flow above them.

Movie file: SM4.Captured.GFP.EColi.during.washing.step.avi

SM5. Lysis movie.

Movie file: SM5.Lysis.HeLa.cells.avi

SM6. Real Time NASBA movies showing the increase in fluorescence over time.

Movie file: SM6.Real-time.NASBA.avi

SM7. Mixing simulation.

Movie file: SM7.Mixing.Simulation.mpg

SM8. Cell loading movie of plasma cells U266 with an inlet velocity of ~300 μm/sec.

Movie file: SM8.Cell.loading.movie.avi

6.6 References

[1] J. W. Hong and S. R. Quake, "Integrated nanoliter systems," *Nat Biotech*, vol. 21, pp. 1179-1183, 2003.

[2] A. Manbachi, S. Shrivastava, M. Cioffi, B. G. Chung, M. Moretti, U. Demirci, M. Yliperttula, and A. Khademhosseini, "Microcirculation within grooved substrates regulates cell positioning and cell docking inside microfluidic channels," *Lab on a Chip*, vol. 8, pp. 747-754, 2008.

[3] J. Compton, "Nucleic acid sequence-based amplification.," *Nature*, vol. 350 (6313), pp. 91-92, 1991.

[4] Y. Schaerli, R. C. Wootton, T. Robinson, V. Stein, C. Dunsby, M. A. A. Neil, P. M. W. French, A. J. deMello, C. Abell, and F. Hollfelder, "Continuous-Flow Polymerase Chain Reaction of Single-Copy DNA in Microfluidic Microdroplets," *Analytical Chemistry*, vol. 81, pp. 302-306, 2009.

[5] K. B. Mullis, "The unusual origin of the polymerase chain reaction. ," *Sci. Am.*, pp. 56-65, 1990.

[6] G. T. Walker, M. S. Fraiser, J. L. Schram, M. C. Little, J. G. Nadeau, and D. P. Malinowski, "Strand displacement amplification--an isothermal, in vitro DNA amplification technique," *Nucl. Acids Res.*, vol. 20, pp. 1691-1696, 1992.

[7] A. Fire and S.-Q. Xu, "Rolling replication of short DNA circles," *Proc. Natl. Acad. Sci. U. S. A.* , pp. 4641–4645, 1995.

[8] B. Deiman, P. van Aarle, and P. Sillekens, "Characteristics and applications of nucleic acid sequence-based amplification (NASBA)," *Molecular Biotechnology*, vol. 20, pp. 163-179, 2002.

[9] I. K. Dimov, J. L. Garcia-Cordero, J. O'Grady, C. R. Poulsen, C. Viguier, L. Kent, P. Daly, B. Lincoln, M. Maher, R. O'Kennedy, T. J. Smith, A. J. Ricco, and L. P. Lee, "Integrated microfluidic tmRNA purification and real-time NASBA device for molecular diagnostics," *Lab on a Chip*, vol. 8, pp. 2071-2078, 2008.

[10] B. Glynn, K. Lacey, J. Reilly, T. Barry, T. J. Smith, and M. Maher, "Quantification of Bacterial tmRNA using in vitro Transcribed RNA Standards and Two-Step qRT-PCR " *Research Journal of Biological Sciences* vol. 2, pp. 564-570, 2007.

[11] J. J. Pinzone, H. Stevenson, J. S. Strobl, and P. E. Berg, "Molecular and Cellular Determinants of Estrogen ReceptorExpression," *MOLECULAR AND CELLULAR BIOLOGY*, vol. 24, pp. 4605–4612, 2004.

[12] T. Verjat, E. Cerrato, M. Jacobs, P. Leissner, and B. Mougin, "Multiparametric duplex real-time nucleic acid sequence-based amplification assay for mRNA profiling.," *BioTechniques* pp. 476-481, 2004.

[13] H. Tan, Y. Zhong, and Z. Pan, "Autocrine regulation of cell proliferation by estrogen receptor-alpha in estrogen receptor-alpha-positive breast cancer cell lines," *BMC Cancer*, vol. 9:13, pp. doi:10.1186/1471-2407-9-31, 2009.

[14] A. Tsuji, H. Koshimoto, Y. Sato, M. Hirano, Y. Sei-Iida, S. Kondo, and K. Ishibashi, "Direct Observation of Specific Messenger RNA in a Single Living Cell under a Fluorescence Microscope," *Biophysical Journal*, vol. 78, pp. 3260-3274, 2000.

[15] M. A. Jordan, K. Wendell, S. Gardiner, W. Brent Derry, H. Copp, and L. Wilson, "Mitotic Block Induced in HeLa Cells by Low Concentrations of Paclitaxel (Taxol) Results in Abnormal Mitotic Exit and Apoptotic Cell Death," *Cancer Res*, vol. 56, pp. 816-825, 1996.

[16] A. Stoica, E. Pentecost, and M. B. Martin, "Effects of arsenite on estrogen receptor-alpha expression and activity in MCF-7 breast cancer cells," *Endocrinology*, vol. 141, pp. 3595-3602, 2000.

Chapter 7: Conclusions and Prospects

With the successful demonstration of the iCell array micro-device that can perform cell stimulation followed by protein and genetic analysis on a single substrate a variety of possible applications become apparent. Here several improved schemes for future generations of micro-devices are presented.

7.1 Future Improvements

One of the important advantages of microfluidic systems in cell based assays is that by controlling flow over the cells, precise perturbations of the cellular environment in time and space can be accomplished. The perturbations can be done on adherent and non adherent cells in microfluidic devices. The key to this control ability lies in the diffusive mixing properties of laminar flow created by microfluidics. With laminar flow complex concentration gradients not achievable on a macro-scale can be realized. These gradients allow several conditions to be probed simultaneously while also mirroring conditions found in vivo. Furthermore gradient generation permits many growth conditions to be analyzed in a combinatorial fashion. Diffusion within microfluidic devices is often too slow. Although slow diffusion poses a complication when mixing is desired, slow diffusive mixing creates opportunities for varying the liquid-phase environment over distances comparable to the size of cells. This has enabled demonstrations such as the migration of organelles from one side of a cell to the other when a single endothelial cell was subject to a gradient that varied across the cell. Since gradients are such an important aspect of microfluidic systems an approach is proposed to incorporate any gradient generator to the system described in the previous section. This approach can also be used to incorporate additional functionality such as reagent distribution and metering mechanisms.

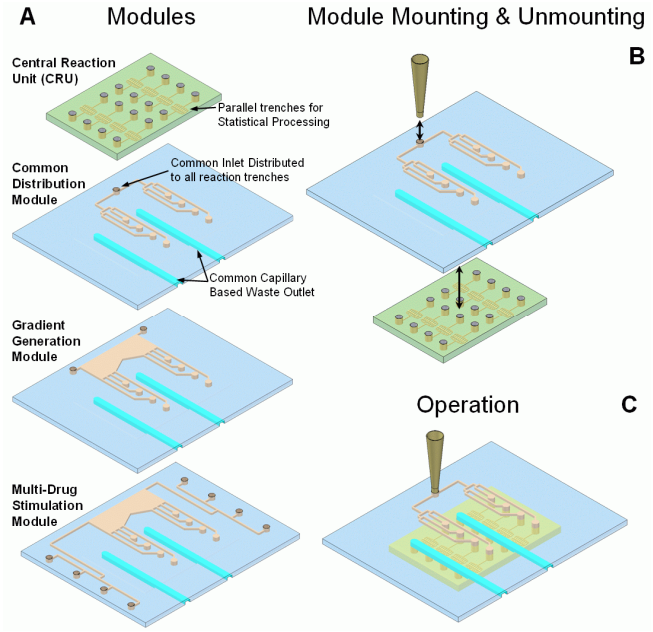

Figure 6.1. Modular approach for implementing further microfluidic functionality without sacrificing versatility. (A) Versatility is maintained by having an array of modules, and each module can implement a different fluidic function; here is a conceptual design of 4 basic modules, although further modules can be developed. The central reaction unit is where the cell a captured and processed. (B) For use the modules can be mounted and later disassembled (when reversible bonding is used). (C) During operation gravity driven flow can be harnessed for perfusion and loading the same way it is currently done.

The approach is based on a modular concept. Each module is a fluidic layer and the modules connect to each other by stacking. The modules are mounted by connecting their inlets and outlets, thus simplifying the alignment requirements. Figure 6.1 demonstrates this.

The reasons in favour of perusing this approach are:

1. The ability of PDMS to reversibly bond to other surfaces made from materials such as glass or polymer.
2. No high pressures are required during the operation of the mounted modules.
3. Versatility is determined by the upper modules so any new application would just require a change of the upper fluidic module.
4. The upper fluidic module also allows the reaction trenches to be closer to each other, thus increasing the reaction density in the central reaction unit (Figure 6.1A).

A further advantage of this approach is that more complex experimental protocols can be implemented in a versatile manner by just sequentially combining the use of several different upper modules and maintaining the lower central reaction unit. This is conceptually shown in Figure 6.2 depending on the required fluidic operation the upper module is changed.

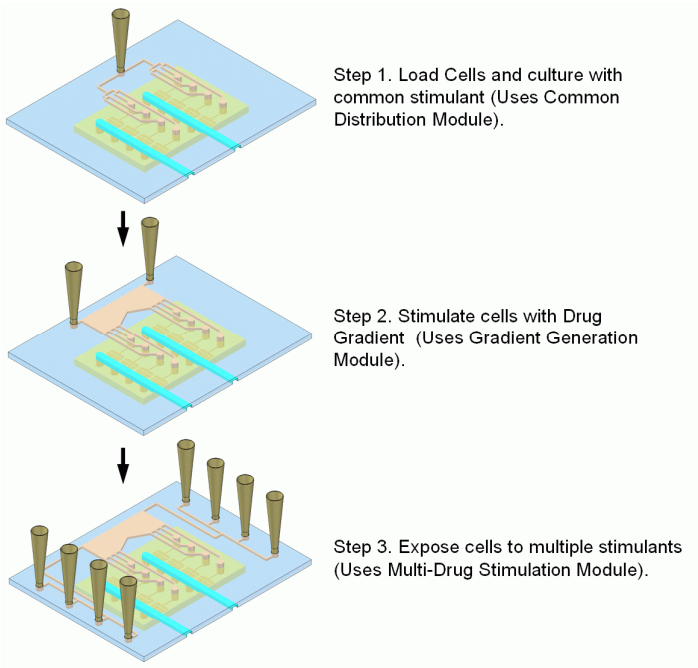

Figure 6.2. Complex experimental protocols can be implemented in a versatile manner by using a sequence of upper fluidic modules and maintaining the same central reaction unit.

By adding thin film tin-doped indium oxide heaters on the base of the cell processing module cell culture and NASBA thermal control can also be miniaturized.

7.2 Further Applications

One of the unique advantages of the trench based cell capture is that the device can also function with non-adherent cells such as *E.Coli* and Macrophages. By loading two or more cell types into a single trench the cell interaction can be studied. As a

demonstration of that the figure (Figure 6.3) below demonstrates the result of combining genetically modified fluorescent *E. Coli* with J774 macrophages. The time lapse images show the activation and phagocytosis of the *E.Coli* bacteria by the macrophages. As time progresses the macrophages scan the surface and phagocytose most of the bacteria, leaving behind a cleaner surface. In this application the device could be used to perform quantitative measurements of the process, for example the cell trajectories can be tracked and statistically analyzed, furthermore the ingestion and digestion parameters can be studied and quantified. The modulation of drugs or other stimulation agents on the response of these processes can also be studied because soluble factors can be dynamically perfused during the interaction of the two non-adherent cells.

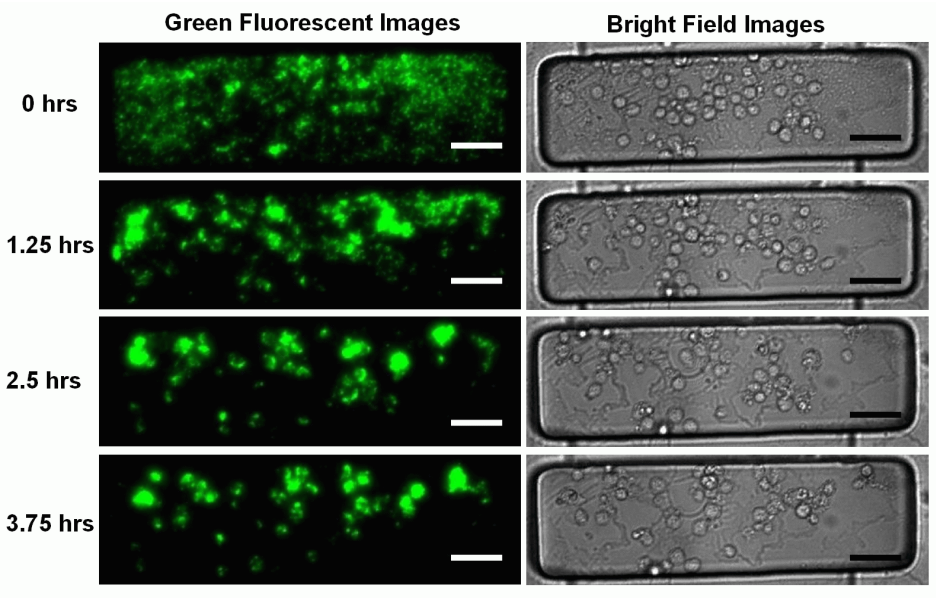

Figure 6.3. Active J774 macrophages captured in the trench are seen taking up green fluorescence protein (GFP) containing *E.Coli* cells in a cooperative manner. The macrophage fluorescence increases as they engulf more *E. Coli*. The total fluorescence is reduced as the macrophages digest the *E. Coli* cells with GFP. Scale bars represent 50 μm.

The trench structure's ability for real time perfusion of soluble factors and bright field and epifluorescent monitoring combined with the micro-scales of the miniaturized device can also enable a novel application that has not been reproduced in the macro-scale. The real time monitoring of cell surface protein expression as it occurs during cell stimulation. The principle that enables this measurement and the initial experimental data are shown

in Figure 6.4. The real time protein expression measurement was achieved by maintaining a very low concentration of fluorescently labelled anti-bodies in the perfusion medium. The fluorescent anti-body in this case was specific to the CD86 costimulatory molecule. During an antigen-dependent inflammatory response macrophage cells are activated and over express costimulatory molecules such as CD80, CD86 and CD40 on their surface which helps induce an effective T cell response. This is one of the key mechanisms and outcomes of activated macrophages that makes them behave as antigen presenting cells (APCs) and activates the adaptive immune system. During the real time monitoring of surface protein expression J774 macrophages were activated with LPS (200 ng/ml) in the positive control case, while in the negative control no LPS was present in the culture medium. As the stimulated macrophages began to express the CD86 proteins on the cell surface, the fluorescent CD86 anti-bodies generated a fluorescent signal from the cell surface. As the free solution antibodies are being consumed and bound on the cell surface, new ones replace them through the continuous perfusion. This maintains a constant supply of in solution antibodies and enables the real time monitoring of the CD86 protein expression on the surface of the macrophage cells. Furthermore the micro-scale dimensions of the device keep the background fluorescence generated by the in solution antibody to a minimum, lowering the LOD to physiologically relevant levels. This measurement technique can be further enhanced by simultaneously using several anti-bodies with different fluorophore labels to generate simultaneous real time multiple surface protein readout with single cell resolution. This novel measurement can be very relevant to fundamental studies in systems and cell biology research and it also has the potential to be a very relevant diagnostic tool.

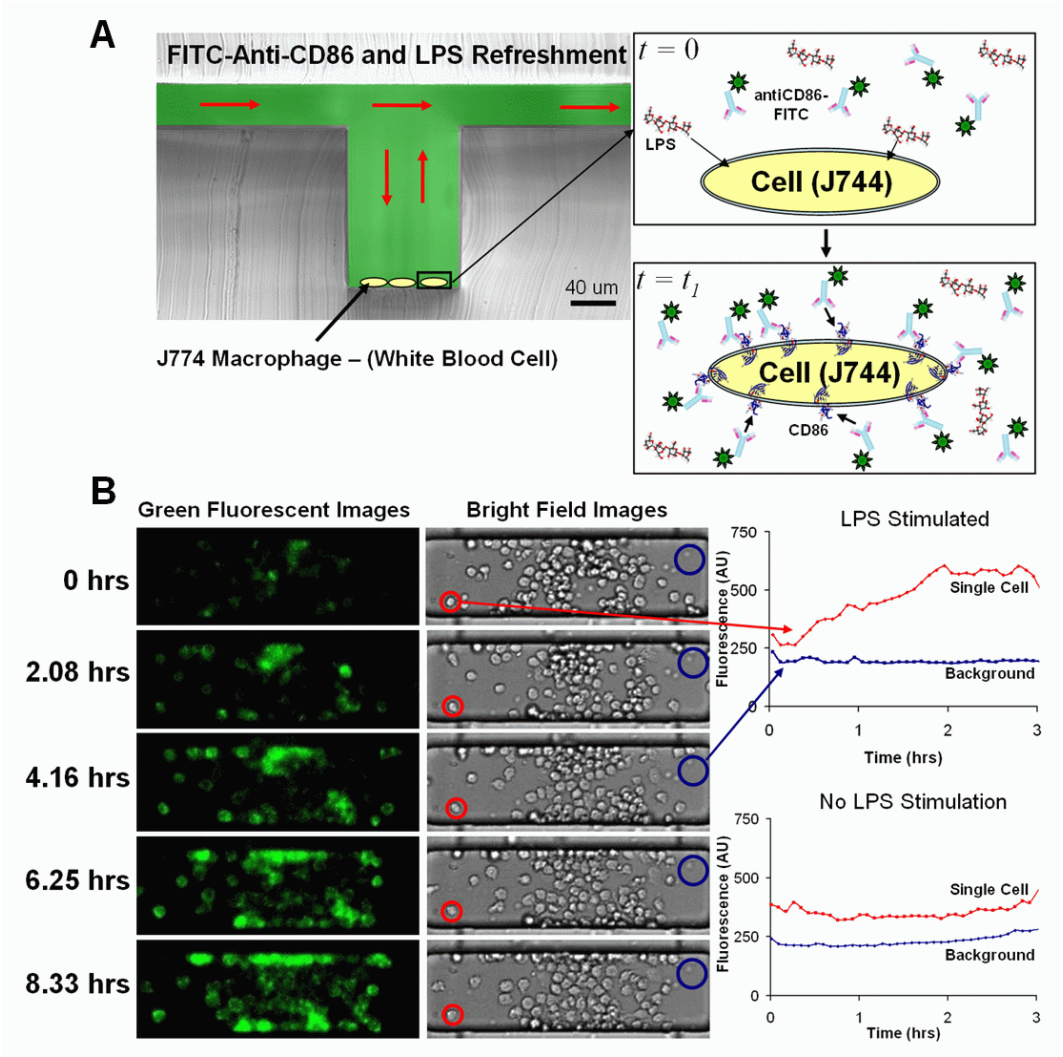

Figure 6.4. Real time monitoring of cell surface protein expression. (A) Measurement principle as demonstrated by CD86 protein measured in real time on the surface of J774 macrophage cells during an LPS stimulation. (B) Time lapse images of J774 cell being stimulated with LPS (200 ng/ml) and real time kinetic quantification of single cell CD86 surface concentration of stimulated and non-stimulated cells.

7.3 Summary of Results

Fundamental components and mechanisms necessary for highly integrated and parallel cell-based bio-analytical micro-devices were developed and demonstrated. Furthermore the complexity of the components and mechanisms was kept to a minimum making them highly up-scalable and economical to use.

Critical issues were addressed in this work by first demonstrating an integrated microfluidic tmRNA purification and real time nucleic-acid-sequence-based-amplification (NASBA) device. The integrated device produced a pathogen-specific response in less than 3 min from the chip-purified RNA. Further enhancements produced a novel integrated NASBA array and then a more versatile *i*Cell array.

The versatility of the *i*Cell array is based on the novel combination of hydrodynamics and cell sedimentation within micro-trench structures and gravity driven sequential perfusion and diffusion mechanisms. This led to the development of a novel microfluidic technology that can completely integrate cell based assays with bio-analytical read-out. The highly scalable *i*Cell array mechanisms enable the configurable on-chip integration of conventional procedures such as adherent and non-adherent cell-culture, cell-stimulation, cell-lysis, cell-fixing, protein-immunoassays, bright field and fluorescent microscopic monitoring, and real time detection of nucleic acid amplification. Furthermore the micro-scale characteristics of the technology enabled unique and novel stimulations, operation and protein read-out procedures that can not be effectively implemented in the macro-scale.

With on-board gravity driven flow control the device is simple and economical to operate with dilute samples (down to 5 cells per reaction), low reagent volumes (50 nL per reaction), highly efficient cell capture (approximately 100% capture rates) and single cell protein and gene expression sensitivity. The key results from this work demonstrate a novel technology for versatile, fully integrated microfluidic array platforms.

By multiplexing this integrated functionality, the device can be used from routine applications in a biology laboratory to high content screenings. Thus this technology can be instrumental in helping fulfil the promise of microfluidics to change significantly the way modern biology is performed.